

**SNOWMELT RUNOFF ANALYSIS AND IMPACT
ASSESSMENT OF TEMPERATURE CHANGE IN THE
UPPER PUNATSHANG CHU BASIN, BHUTAN**



**A Thesis Submitted in Partial Fulfillment of the Requirements for the
Degree of Master of Science in Geoinformatics**

Suranaree University of Technology

Academic Year 2014

การวิเคราะห์ปริมาณน้ำท่าจากการละลายของหิมะและการประเมินผลกระทบ
การเปลี่ยนแปลงอุณหภูมิในลุ่มน้ำภูานางซุดอนบน ประเทศภูฏาน



นายฉิกมิ เทนชิน

วิทยานิพนธ์นี้เป็นส่วนหนึ่งของการศึกษาตามหลักสูตรปริญญาวิทยาศาสตรมหาบัณฑิต

สาขาวิชาภูมิสารสนเทศ

มหาวิทยาลัยเทคโนโลยีสุรินทร์

ปีการศึกษา 2557

**SNOWMELT RUNOFF ANALYSIS AND IMPACT ASSESSMENT
OF TEMPERATURE CHANGE IN THE UPPER PUNATSHANG
CHU BASIN, BHUTAN**

Suranaree University of Technology has approved this thesis submitted in partial fulfillment of the requirements for the Degree of Master of Science in Geoinformatics.

Thesis Examining Committee

(Asst. Prof. Dr. Songkot Dasananda)

Chairperson

(Assoc. Prof. Dr. Suwit Ongsomwang)

Member (Thesis Advisor)

(Assoc. Prof. Dr. Chatchai Jothiyangkoon)

Member

(Asst. Prof. Dr. Sunya Sarapirome)

Member

(Prof. Dr. Sukit Limpijumnong)

Vice Rector for Academic Affairs
and Innovation

(Assoc. Prof. Dr. Prapun Manyum)

Dean of Institute of Science

จิกมี เทนซิน : การวิเคราะห์ปริมาณน้ำท่าจากการละลายของหิมะและการประเมินผล
กระทบการเปลี่ยนแปลงอุณหภูมิในลุ่มน้ำภูานางชุตอนบน ประเทศภูฏาน
(SNOWMELT RUNOFF ANALYSIS AND IMPACT ASSESSMENT OF
TEMPERATURE CHANGE IN THE UPPER PUNATSANG CHU BASIN)
อาจารย์ที่ปรึกษา : รองศาสตราจารย์ ดร.สุวิทย์ อ่องสมหวัง, 129 หน้า

การประเมินผลและติดตามการละลายของหิมะและธารน้ำแข็งในพื้นที่ของประเทศภูฏาน
สามารถดำเนินการได้ยากลำบาก เนื่องจากสภาพพื้นที่ไม่เอื้ออำนวยและสูงชัน ฉะนั้น การประยุกต์
แบบจำลอง Snowmelt Runoff Model (SRM) และข้อมูลการรับรู้จากระยะไกลจึงเป็นทางเลือกที่
เหมาะสมสำหรับการได้มาของสารสนเทศที่สมบูรณ์เพื่อใช้ปรับปรุงรูปแบบการจัดการและการ
ตัดสินใจทางด้านทรัพยากรน้ำ วัตถุประสงค์หลักของการศึกษาคือ เพื่อประมาณปริมาณน้ำท่าใน
ฤดูกาลหลอมละลายของหิมะและผลกระทบจากการเปลี่ยนแปลงอุณหภูมิสมมติต่อปริมาณน้ำท่า
ในการนี้ ข้อมูลนำเข้าซึ่งประกอบด้วย คุณลักษณะของพื้นที่ลุ่มน้ำ ตัวแปร และพารามิเตอร์ต่างๆ จะ
ถูกประมวลผลด้วยแบบจำลอง ในการประมวลผลจะปฏิบัติการแบบวนซ้ำโดยอาศัยกระบวนการ
การเปรียบเทียบและการทดสอบความสมเหตุสมผล พร้อมกับการประเมินความถูกต้องด้วยวิธีการวัด
แบบมาตรฐาน (NSE, PBIAS และ D_v) ผลลัพธ์ที่ได้รับจะประกอบด้วย ปริมาณน้ำท่าและปริมาณ
น้ำท่าเฉลี่ยพร้อมกับกราฟน้ำท่า (hydrograph) สำหรับฤดูกาลหลอมละลายของหิมะ (เดือนเมษายน
- สิงหาคม) ของปี พ.ศ. 2548-2552 รวมทั้ง การตรวจสอบผลกระทบของการเปลี่ยนแปลงอุณหภูมิที่
มีต่อปริมาณน้ำท่าโดยอาศัยภาพเหตุการณ์สมมุติที่แตกต่างกันสามรูปแบบ คือ (1) เพิ่มขึ้น 1 องศา
เซลเซียส (2) เพิ่มขึ้น 2 องศาเซลเซียส และ (3) เพิ่มขึ้น 3 องศาเซลเซียส

ผลการศึกษา พบว่า ปริมาณน้ำท่าจากแบบจำลองในปีอุทกศาสตร์ พ.ศ. 2548-2552 มี
ปริมาณเท่ากับ 5,713.29, 5,719.19, 5,750.92, 6,516.85 และ 5,400.42 ล้านลูกบาศก์เมตร ตามลำดับ
และในประเมินความถูกต้องจากความสัมพันธ์ของปริมาณน้ำท่าที่ได้จากแบบจำลองกับปริมาณ
น้ำท่าที่ตรวจวัดได้ในแต่ปีอุทกศาสตร์ พ.ศ. 2548-2552 พบว่า พิสัยค่าความถูกต้องจากการวัดด้วย
NSE มีค่าอยู่ระหว่าง 70 ถึง 91 เปอร์เซ็นต์ ค่าสัมบูรณ์ของ PBIAS มีค่าอยู่ระหว่าง 0.36 ถึง 3.04
เปอร์เซ็นต์ และค่า D_v มีค่าพิสัยอยู่ระหว่าง -3.09 ถึง 3.04 เปอร์เซ็นต์

จากกราฟน้ำท่าที่ได้รับ พบว่า แบบจำลอง SRM สามารถจำลองสถานการณ์ปริมาณการ
ไหลของน้ำรายวันได้อย่างสมเหตุสมผล ซึ่งแสดงถึงความสอดคล้องของปริมาณการไหลของ
น้ำรายวันที่ได้จากแบบจำลองและการตรวจวัดจริง ยกเว้นค่ายอดสูงสุดบางตำแหน่ง แต่อย่างไรก็
ตาม พบว่า แบบจำลอง SRM มีข้อจำกัดในการจำลองสถานการณ์น้ำท่าสำหรับช่วงเวลาที่มิสภาพ
ภูมิอากาศแบบผิดปกติ เช่น พายุหมุน พายุ และฝนตกหนัก ในกรณีศึกษาผลกระทบของการ

เปลี่ยนแปลงอุณหภูมิต่อปริมาณน้ำท่า พบว่า การเพิ่มขึ้นของอุณหภูมิเฉลี่ย 1 องศาเซลเซียส จะส่งผลทำให้ปริมาณน้ำท่าเพิ่มขึ้น 14.36 เปอร์เซ็นต์ นอกจากนี้ พบว่า พารามิเตอร์ที่มีความอ่อนไหวในการจำลองสถานการณ์น้ำท่าจากแบบจำลอง SRM ได้แก่ อัตราการเปลี่ยนแปลงของอุณหภูมิ (temperature lapse rate, γ) และ ปัจจัยการเปลี่ยนแปลงอุณหภูมิต่อวันที่ส่งผลต่อการละลายหิมะ (degree day factor, α)

จากการศึกษาสามารถสรุปได้ว่า ผลลัพธ์ที่ได้รับจากแบบจำลอง SRM ในพื้นที่ลุ่มน้ำมีความถูกต้องสูง และนับว่าเป็นเครื่องมือที่มีประสิทธิภาพสำหรับใช้จำลองสถานการณ์ปริมาณน้ำท่าจากการหลอมละลายของหิมะและการศึกษาผลกระทบของการเปลี่ยนแปลงอุณหภูมิต่อปริมาณน้ำท่า ผลลัพธ์ที่ได้รับจากการศึกษาสามารถนำไปใช้เป็นแนวทางสำหรับการจัดการทรัพยากรน้ำ การออกแบบระบบชลศาสตร์ และแผนบรรเทาภัยเพื่อแก้ไขผลกระทบจากการเปลี่ยนแปลงภูมิอากาศได้



JIGME TENZIN : SNOWMELT RUNOFF ANALYSIS AND IMPACT
ASSESSMENT OF TEMPERATURE CHANGE IN THE UPPER
PUNATSANG CHU BASIN, BHUTAN. THESIS ADVISOR :
ASSOC. PROF. SUWIT ONGSOMWANG, Dr. rer. Nat. 129 PP.

SNOWMELT RUNOFF ANALYSIS / SRM MODEL / IMPACT OF
TEMPERATURE CHANGE / PUNATSANG CHU BASIN / BHUTAN

In the area like Bhutan, accessing and monitoring of glacier and snow melt is difficult due to its unfriendly and rugged terrain, thus SRM modeling with remote sensing data offers the potential for furnishing information to improve water resources management and decision making. The main objective of the study is to estimate runoff during snowmelt period and impact of hypothetical temperature change on streamflow. Herewith input data include basin characteristic, variables and parameters to execute the model. The processes are routinely operated by calibration and validation process and accuracy assessment with standard measurement (NSE, PBIAS and D_v). The output include runoff volume and average runoff with hydrograph for a melting season (April- August) of year 2005-2009. Besides, the impact of temperature change on the streamflow are investigated using three different hypothetical scenarios: (1). $T + 1^\circ\text{C}$, (2) $T + 2^\circ\text{C}$ and (3) $T + 3^\circ\text{C}$.

The simulated runoff volume were 5,713.29, 5,719.19, 5,750.92, 6,516.85 and 5,400.42 million m^3 , respectively for hydrological year 2005-2009. The simulated discharge is then correlated with measured discharge for all hydrological years, it was

found that NSE ranging 70 – 91%, |PBIAS| ranging 0.36 to 3.04% and D_v : ranging - 3.09 to 3.04%.

Based on hydrographs and NSE values, it has been observed that the SRM model has simulated the daily flows reasonably well showing generally a good agreement with the daily observed flows except few peaks. However, it was found that SRM model has limitation to model the period when there is occurrence of extreme weather condition like cyclone, storm and heavy rainfall. In case of impact of temperature change on the streamflow, it was observed that with increase in every 1°C of average temperature, runoff increases by 14.36%. In addition, it was observed that temperature lapse rate (γ) and degree day factor (α) are the most sensitive parameters of the SRM simulation.

In conclusion, the results achieved by SRM model for the basin display considerably good agreement and proved to be an efficient tool to simulate snowmelt runoff and study impact of temperature change on streamflow. The output can be used as guideline for water resources management, hydraulic system design and mitigation plan to combat climate change effect.

School of Remote Sensing

Academic Year 2014

Student's Signature _____

Advisor's Signature _____

ACKNOWLEDGEMENTS

I would like to extend my heart felt gratitude to all institutions and people who supported me during the completion of this research, without their help and encouragement, this master thesis would never have happened. I would like to thank especially:

1. Royal Government of Bhutan and Thailand International Cooperation Agency for awarding me a scholarship to pursue my master degree in Geo-informatics.
2. Department of Hydro-Met Services, Ministry of Economic Affairs, Bhutan for furnishing me with meteorological data for my research work.
3. Assoc. Prof. Dr. Suwit Ongsomwang, my advisor, whose encouragement, guidance, motivation, help and support from the initial to final level of my research work. His wisdom, knowledge and commitment for the work always inspired and motivated me throughout the study period.
4. Thesis committee members, Asst. Prof. Dr. Songkot Dasananda, Assoc. Prof. Dr. Suwit Ongsomwang, Assoc. Prof. Dr. Chatchai Jothiyangkoon and Asst. Prof. Dr. Sunya Sarapirome, who supported me with their valuable comments and suggestions during all my thesis work and despite their busy schedule, they always had a time to evaluate my thesis at different levels.
5. My senior colleagues: Dr. Muhammad Bilal, Hong Kong Polytechnic University, Mr. Deo Raj Gurung, ICIMOD, Nepal and Miss. Gunjal Silwal,

Tribhuvan University, Nepal for their valuable insights and sharing their past scientific ideas on the topic promptly with me.

6. All the staff and students of School of Remote Sensing for their help and support during my stay here.

7. My family for their endless love, support and prayers which have always been a source of inspiration and guidance for me.

Jigme Tenzin



CONTENTS

	Page
ABSTRACT IN THAI.....	I
ABSTRACT IN ENGLISH	III
ACKNOWLEDGEMENTS.....	V
CONTENTS.....	VII
LIST OF TABLES.....	XII
LIST OF FIGURES	XIV
LIST OF ABBREVIATIONS.....	XVIII
CHAPTER	
I INTRODUCTION.....	1
1.1 Background and significance of the study.....	1
1.2 Research objectives.....	5
1.3 Scope and limitation of the study.....	5
1.4 Study area.....	6
1.5 Benefits of the study.....	7
II BASIC CONCEPTS AND LITERATURE REVIEWS.....	8
2.1 Snowmelt runoff model (SRM)	8
2.2 Structure of SRM	12
2.3 Data required for executing the model.....	14
2.3.1 Basin characteristics	14

CONTENTS (Continued)

	Page
2.3.1.1 Basin and zone areas	14
2.3.1.2 Area-elevation curve	16
2.3.2 Variables.....	17
2.3.2.1 Temperature.....	17
2.3.2.2 Precipitation.....	18
2.3.2.3 Snow cover area	18
2.3.3 Parameters	23
2.3.3.1 Runoff coefficient of snow and rain (C_S and C_R)	24
2.3.3.2 Degree day factor (α).....	24
2.3.3.3 Temperature lapse rate (γ).....	26
2.3.3.4 Critical temperature (T_{CRIT}).....	27
2.3.3.5 Rainfall contribution area (RCA).....	28
2.3.3.6 Recession coefficient (k).....	29
2.3.3.7 Time lag (L).....	31
2.4 Accuracy assessment.....	34
2.4.1 Accuracy criteria	34
2.4.2 Accuracy criteria in model tests	36
2.5 Literature review	37
III DATA, TOOLS AND RESEARCH METHODOLOGY.....	44
3.1 Data.....	44

CONTENTS (Continued)

	Page
3.1.1 Temperature and precipitation	44
3.1.2 Discharge.....	45
3.1.3 Digital elevation model (DEM).....	45
3.1.4 MODIS snow product	46
3.2 Tools.....	49
3.2.1 WinSRM model	49
3.2.2 ESRI ArcMap	49
3.2.3 MODIS Reprojection Tools (MRT).....	50
3.2.4 MODIS Snow tools	50
3.2.4 MATLAB	51
3.3 Research methodology	51
3.3.1 Input data preparation.....	53
3.3.1.1 Hydro-meteorological data.....	53
3.3.1.2 Basin characteristics	53
3.3.1.3 Snow cover area (SCA) extraction.....	57
3.3.1.4 Initial input parameters.....	59
3.3.2 Runoff simulation during snowmelt period by SRM model	63
3.3.2.1 Model Calibration.....	63
3.3.2.2 Model validation.....	65
3.3.2.3 Data output	65

CONTENTS (Continued)

	Page
3.3.2.3 Data output	65
3.3.3 Impact of temperature change on stream flow	65
IV RESULTS AND DISSCUSSIONS	67
4.1 Snowmelt runoff simulation.....	67
4.1.1 Basin characteristics, variables and parameters for SRM model.....	67
4.1.1.1 Basin characteristics	67
4.1.1.2 Temperature and precipitation.....	70
4.1.1.3 Snow covered area (SCA)	73
4.1.1.4 Local recession coefficient extraction.....	78
4.1.2 SRM runoff simulation under calibration process and its optimum range of local parameters	81
4.1.3 SRM runoff simulation under validation process and its optimum range of local parameters	84
4.1.4 Efficiency of SRM for runoff simulation and their optimum range of local parameters	89
4.1.5 Snowmelt simulation and its contribution to river discharge.....	97
4.2 Impact of temperature change on streamflow.....	99
4.2.1 Impact of temperature change on streamflow based on 2005 simulation data	99

CONTENTS (Continued)

	Page
4.2.2 Impact of temperature change on streamflow based on 2006 simulation data	101
4.2.3 Impact of temperature change on streamflow based on 2007 simulation data	102
4.2.4 Impact of temperature change on streamflow based on 2008 simulation data	104
4.2.5 Impact of temperature change on streamflow based on 2009 simulation data	105
4.2.6 Synthesis of impact of temperature change on streamflow during 2005-2009 simulation data.....	107
4.3 Sensitivity analysis for the SRM simulation.....	110
V CONCLUSIONS AND RECOMMENDATIONS.....	112
5.1 Conclusions.....	112
5.1.1 Snowmelt runoff simulation by SRM model	113
5.1.2 Impact of temperature change on streamflow	114
5.2 Recommendations	115
REFERENCES	117
CURRICULUM VITAE.....	129

LIST OF TABLES

Table		Page
2.1	List of remote sensing data for mapping snow cover area.....	21
2.2	Performance ratings for NSE and PBIAS	36
2.3	Results of model performance in the WMO project (10 years, snowmelt season).....	36
3.1	List of weather stations within the study	45
3.2	Summary of the MODIS snow products.....	48
3.3	Interpretation key for MODIS Snow Product.....	48
4.1	Summary of the hypsometric elevation zones of Upper Punatsang Chu basin	69
4.2	Accumulated percent of SCA of melt season (April- August) for different hydrological year	78
4.3	Recession constant value (x and y) for calculating recession coefficient (k) of year 2005 – 2009	78
4.4	Range of optimum local parameters of calibration period.....	82
4.5	Statistics data of SRM simulated runoff and its accuracy for year 2005.....	83
4.6	Statistics data of SRM simulated runoff and its accuracy for year 2006.....	84
4.7	Range of optimum local parameters for validation period	85
4.8	Statistics data of SRM simulated runoff and its accuracy for year 2007.....	87
4.9	Statistics data of SRM simulated runoff and its accuracy for year 2008.....	87

LIST OF TABLES (Continued)

Table	Page
4.10 Statistics data of SRM simulated runoff and its accuracy for year 2009.....	88
4.11 Details of SRM applications and their results applied by researchers during 1962-1999.....	92
4.12 Contribution of snowmelt to river discharge	97
4.13 Discharge volume change and percent increase of streamflow based on simulation data of 2005.....	100
4.14 Discharge volume change and percent increase of streamflow based on simulation data of 2006.....	102
4.15 Discharge volume change and percent increase of streamflow based on simulation data of 2007.....	103
4.16 Discharge volume change and percent increase of streamflow based on simulation data of 2008.....	105
4.17 Discharge volume change and percent increase of streamflow based on simulation data of 2009.....	106
4.18 Comparison of average streamflow, percent increase and average percent increase of streamflow under the hypothetical scenarios of year 2005-2009.	108
4.19 Sensitivity analysis result for the SRM simulation year 2007	110

LIST OF FIGURES

Figure		Page
1.1	Map depicting the study area extent	7
2.1	The structure of the SRM.....	14
2.2	Elevation zone and areas of the South Fork of Rio Grande Basin, Colorado, USA.....	15
2.3	Determination of the zonal mean hypsometric elevation using area-elevation curve for the South Fork of the Rio Grande basin.	16
2.4	Depletion curves of the snow coverage for 5 elevation zones of the basin Felsberg, derived from the Landsat imagery shown in Figure 7. A: 560-1100 m (amsl), B: 1100-1600 m (amsl). C: 1600-2100 m (amsl). D: 2100-2600 m (amsl)., E: 2600-3600 m (amsl).	20
2.5	Sequence of snow cover maps from Landsat 5- MSS, Upper Rhine River at Felsberg, 3250 km ² , 560-3614 masl. Black is snow free, gray is cloud covered and white is snow covered areas.	22
2.6	Spectral reflectance curves of typical cloud and snow.	23
2.7	The diagram depicts the role of critical temperature to distinguish the precipitation to be rain or snow.	28

LIST OF FIGURES (Continued)

Figure	Page
2.8 Recession flow plot Q_n vs. Q_{n+1} for the Dischma basin in Switzerland. Either the slope envelope line or the dashed medium line is used to determine k-values for computing the constants x and y in the Equation 2.10.....	30
2.9 Snowmelt hydrographs illustrating the conversion of computed runoff amounts for 24-hours periods to calendar day periods. The various time lags (bold lines) are taken into account by proportions of the daily inputs, I.	32
3.1 Example of MOD10A2 and MYD10A2 snow products.....	49
3.2 Workflow diagram of research methodology.	52
3.3 Profile view of a sink before and after running fill.....	54
3.4 Profile view of a peak before and after running fill.....	54
3.5 The coding of the direction of flow.	55
3.6 Determining the accumulation flow.....	56
3.7 Steps involved in combining the MODIS snow product and applying could removal algorithm.	59
3.8 Time lag graph of Upper Punatshang Chu basin.	62
4.1 Hypsometric elevation zones of Upper Punatshang Chu basin, Bhutan.....	68
4.2 Hypsometric curve of Upper Punatshang Chu basin.	69
4.3 Average temperature and rainfall trend for year 2005.....	69
4.4 Average temperature and rainfall trend for year 2006.....	71
4.5 Average temperature and rainfall trend for year 2007.....	71

LIST OF FIGURES (Continued)

Figure	Page
4.6 Average temperature and rainfall trend for year 2008.....	72
4.7 Average temperature and rainfall trend for year 2009.....	72
4.8 Schematic diagram of Model builder for zonal SCA extraction.....	74
4.9 Zonal snow cover depletion curve for year 2005.....	75
4.10 Zonal snow cover depletion curve for year 2006.....	75
4.11 Zonal snow cover depletion curve for year 2007.....	76
4.12 Zonal snow cover depletion curve for year 2008.....	76
4.13 Zonal snow cover depletion curve for year 2009.....	77
4.14 Recession graph of 2005.....	79
4.15 Recession graph of 2006.....	79
4.16 Recession graph of 2007.....	80
4.17 Recession graph of 2008.....	80
4.18 Recession graph of 2009.....	81
4.19 Comparison of measured and computed hydrograph of year 2005.	82
4.20 Comparison of measured and computed hydrograph of year 2006.	83
4.21 Comparison of measured and computed hydrograph of year 2007.	85
4.22 Comparison of measured and computed hydrograph of year 2008.	86
4.23 Comparison of measured and computed hydrograph of year 2009.	86
4.24 Superimposed data of measured and calculated runoff and rainfall of May 2009.....	89
4.25 Relationship between snowmelt depth and average snow covered area.....	98

LIST OF FIGURES (Continued)

Figure	Page
4.25 Relationship between snowmelt depth and average snow covered area.....	98
4.26 Comparison of simulated streamflow in each scenario based on simulation data of 2005.....	100
4.27 Comparison of simulated streamflow in each scenario based on simulation data of 2006.....	101
4.28 Comparison of simulated streamflow in each scenario based on simulation data of 2007.....	103
4.29 Comparison of simulated streamflow in each scenario based on simulation data of 2008.....	104
4.30 Comparison of simulated streamflow in each scenario based on simulation data of 2009.....	106

LIST OF ABBREVIATIONS

APHRODITE	=	Asian Precipitation –Highly-Resolved Observation Data Integration Toward Evaluation of Water Resources
ASTER	=	Advanced Spaceborne Thermal Emission and Reflection Radiometer
DEM	=	Digital Elevation Model
DOE	=	Design of experiment
ESRI	=	Environmental Systems Research Institute
GAWSER	=	Guelph All-Weather Storm-Event Runoff
GLOF	=	Glacier Lake Outburst Flood
HBV	=	Hydrologiska Byråns Vattenbalansavdelning
HDF–EOS	=	Hierarchical Data Format- Earth Observation System
HEC-	=	Hydrologic Engineering Center
ICIMOD	=	International Centre for Integrated Mountain Development
IPCC	=	Intercontinental Panel on Climate Change
LST	=	Land surface temperature
MCMC	=	Monte Carlo Markov Chain
MENRIS	=	Mountain Environment and Natural Resources Information System Division
MODIS	=	Moderate Resolution Imaging Spectroradiometer

LIST OF ABBREVIATIONS (Continued)

MoEA	=	Ministry of Economic Affairs
MRT	=	MODIS Reprojection Tools
MW	=	Megawatt
NASA	=	National Aeronautics and Space Administration
NDSI	=	Normalized Difference Snow Index
NDVI	=	Normalized Difference Vegetation Index
NSE	=	Nash-Sutcliffe Efficiency
NWSRFS	=	National Weather Service River Forecast System
PBIAS	=	Percent Bias
PRMS	=	Precipitation Runoff Modeling System
SCA	=	Snow cover area
SCDC	=	Snow cover depletion curve
SCE –UA	=	Shuffled Complex Evolution – University of Arizona
SFA	=	Snow free area
SRM	=	Snowmelt Runoff Model
SRTM	=	Shuttle Radar Topographic Mission
SSARR	=	Streamflow Simulation and Reservoir Regulation
SWIR	=	shortwave infrared wavelength
TRMM	=	Tropical Rainfall Measuring Mission
VNIR	=	Visible/Near Infrared
WMO	=	World Meteorological Organization

CHAPTER I

INTRODUCTION

1.1 Background and significance of the study

Precipitation can be in many different forms, such as rain, freezing rain, hail, sleet, and snow. Snow is composed of small particles of ice in the form of granular material. It is a soft structure, unless packed by external pressure and, snow is one of the source of water as it acts as natural reservoir for many water supply systems (Haq, 2008).

Snow is an important environment parameter, not only influencing the Earth's radiation balance but also playing a significant role in river discharge. Snowmelt and snow cover area (SCA) has been the major source of runoff and groundwater recharge in middle and higher latitudes areas (Jain, Goswami, and Saraf, 2010). The process of converting snow and ice into water, known as snowmelt, needs input of energy (heat). Hence, snowmelt is linked to the flow and storage of energy into and through the snowpack (USACE, US Army Corps. of Engineers, 1998). Therefore, estimation of snowmelt runoff is very important for regulating the flow from the reservoirs, estimating flood flow for the design of hydraulic structures and for other water resource development activities in the Himalayan region.

Singh and Jain (2003) affirmed that the snowpack depletes either fully or partially during the forthcoming summer season depending up the climatic conditions. Attributing to the climatic condition, there is change in areal extent of SCA and snow

free area (SFA) over the time, and the contribution from the rain and snow to the stream flow varies with season. However, the precipitation like rain dominates the lower altitude part of the basins (<2000 m amsl.) and, rain and snow in middle and higher altitude region of the basins (about >2000 m amsl.) with change in altitude. With increase in altitude of the basin, the rain contribution to stream flow reduces and the snowmelt contribution increases, therefore, runoff is dominated by the snowmelt runoff above 3,000 m (amsl.) altitude (Singh and Jain, 2003).

Owing to the above statement, modeling the stream flow from a basin is based on transformation of incoming precipitation to outgoing stream flow by considering losses to the atmosphere, temporary storage, lag and attenuation as water is routed by fast and slow pathways above and below the ground. In most parts of the world, the seasonal short-term variation in stream flow reflects the variation in rainfall. However, in higher altitude and latitude regions where snowfall is predominated, runoff depends on the heat supplied to snowmelt rather than just the timing of precipitation. Hence, to understand the hydrological behavior and simulate the stream flow in such area, it is very important to model the snowmelt runoff (Jain, Lohani, and Singh, 2012).

In line with research on “climate change by Liu and Rasul (2007), the Himalayan Mountains, and ICIMOD” clearly mentioned that according to IPCC (2007) the climate change is a major concern in the Himalayas because of potential impacts on the economy, ecology, and environment of the Himalayas and areas downstream. Bhutan, being part of the eastern Himalaya region is adversely affected by climate change causing the snow and glacier residing on mountains to melt faster in larger extent as compared to other part of the world. This causes change in the hydrological

cycle which may further disturb river runoff, accelerate water-related hazards, and affect agriculture, vegetation, forests, biodiversity and health. The Himalaya region known as the water tower of the world is the source of nine giant river systems in Asia and with increment in rate of shrinkage of glaciers is likely to seriously threaten water availability in the region, particularly during the lean flow seasons when melt water contribution is crucial to sustain the river flow which supports human activities and ecosystem services and downstream. The effect of change in global climate is evidently seen in regions such as the Arctic, Sub-Saharan Africa, Small Island States, and Asian mega deltas. However, the vulnerability of the Himalayas is unclear because of the lack of data and knowledge at the regional level (Liu and Rasul, 2007).

According to Gitay, Saurez, Watson and Dokken (2002), the global mean surface temperature has increased by 0.6°C ($0.4 - 0.8^{\circ}\text{C}$) over the last ten decades. Further, Chettri et al., (2010) substantiated that the Eastern Himalayan region's mean annual temperature is increasing at the rate of $0.01^{\circ}\text{C}/\text{year}$ or more. In line to this, Shrestha and Devkota (2010) concluded that warming is observed and predicted to be more rapid in the high mountain area than lower elevation, with elevation above 4,000 m (amsl) experiencing the highest warming rates.

Tse-ring, Sharma, Chettri, and Shrestha (2010) confirmed that Bhutan is experiencing a warming trend of about 0.5°C by analyzing the surface air temperature from 1985 to 2002. To understand the impact of temperature in snowmelt runoff, many researchers have adopted the method of creating a hypothetical scenarios of temperature increment.

Bhutan has witnessed flash floods and glacier outburst floods devastating acres of agriculture lands and infrastructure properties, destruction to historical monuments

and causing threat to people living downstream in the Punatshang Chu basin in the years 1957, 1960 and 1994. The basin shelters Punakha-Wangdue fertile valley along two major rivers: Pho (Male) Chu and Mo (female) Chu fed by snow and glacier in the upper region of the basin. After the confluence of these two rivers, the main river is called Punatshang Chu which follows to the south entering Indian Territory and joining the Brahmaputra River.

The Punatshang Chu basin is the second largest basin amongst the five basins of Bhutan. Taking advantage of its topographical features - rugged, steep terrain and fast flowing rivers the basin is declared as home to the biggest ongoing hydropower projects: Punatshang Chu Hydropower Project Phase I (1200 MW) and Phase II (1000 MW), thus, from the economic perspectives the hydropower plants have been the major contributor to the economy of the country accounting for the increase in the overall gross domestic product.

With repeated occurrence of natural calamities in the basin, it is deemed necessary to study about the snow and glacier residing in the upper reach of the valley so that the planning and mitigation program can be executed professionally. And with the inception of some major hydropower plants downstream it is very important to study about the influence of snow and glacier on hydro power generation. Therefore, the information on spatio-temporal variation of snow and the snowmelt runoff can be applied practically to build hydraulics infrastructure for the future hydropower project after the completion of this research. Furthermore, it can provide sufficient information on water availability during different seasons advancing in the field of water resource planning and management.

1.2 Research objectives

Based on the basic concept of SRM model and its related literature reviews, the generic objective could be possibly established for daily snowmelt runoff estimation in snowmelt seasons for the study. Therefore, the specific objectives of the research are as follows:

- (1) To estimate runoff from snowmelt to the river during snow melting period;
- (2) To assess the impact of temperature change on stream flow by simulating the stream flow under different future temperature change scenarios.

1.3 Scope and limitation of the study

Scope of this study can be summarized as follows:

- (1) For runoff estimation from snowmelt to the river during snow melting period, zonal snow cover area, temperature and precipitation data as an input for the model are used to simulate runoff in the SRM model with parameters range derived from specific year by calibration. The simulated runoff are validated accordance with the derived parameter range from the calibration process using Nash Sutcliffe Efficiency (NSE), Percent Bias (PBIAS) and the volume difference (D_v) for accuracy assessment and acceptance of the model. The validated model year is then used to simulate the total contribution to runoff from the snowmelt and rainfall.

- (2) After having accepted the model with its optimum parameters range, the model is further applied for studying the impact of temperature change on the existing SCA and to simulate the snowmelt runoff under different hypothetical scenarios by increasing the average temperature by 1 to 3°C.

1.4 Study area

Punatshang Chu River traverses from North to South, its trajectory passing through five different districts of the country in the descending order: Gasa (North), Punakha, Wangduephodrang, Tsirang and Dagana (south), and the overall basin measuring total area of 9,760.35 sq.km. The basin shares a common boundary with Tibet-China in the North and India in the South. In the northern region, the basin generally covers some of the tallest Himalayan peaks sheltering large glacier lakes and associated glacio-fluvial deposits. It is observed that the fluvial outwash plains containing significant quaternary as the river traverses to the southern foothills (Duran-Ballen, Shrestha, Wang, Yoshimura and Koike, 2012).

The study area is the upper region of Punatshang Chu basin covering three districts: Gasa, Punakha and Wangduephodrang (partially), with a total area of 5664.42 km² encompassing geographical area between 28° 14'N and 27° 27'N and 89° 19'E and 90° 22'E is dissected by discharge gauging station located at latitude and longitude of 27° 27'N and 89° 54'E from the overall basin (Figure 1.1). The topography of the study area varies from altitude of 1,180 to 7,087 m amsl.

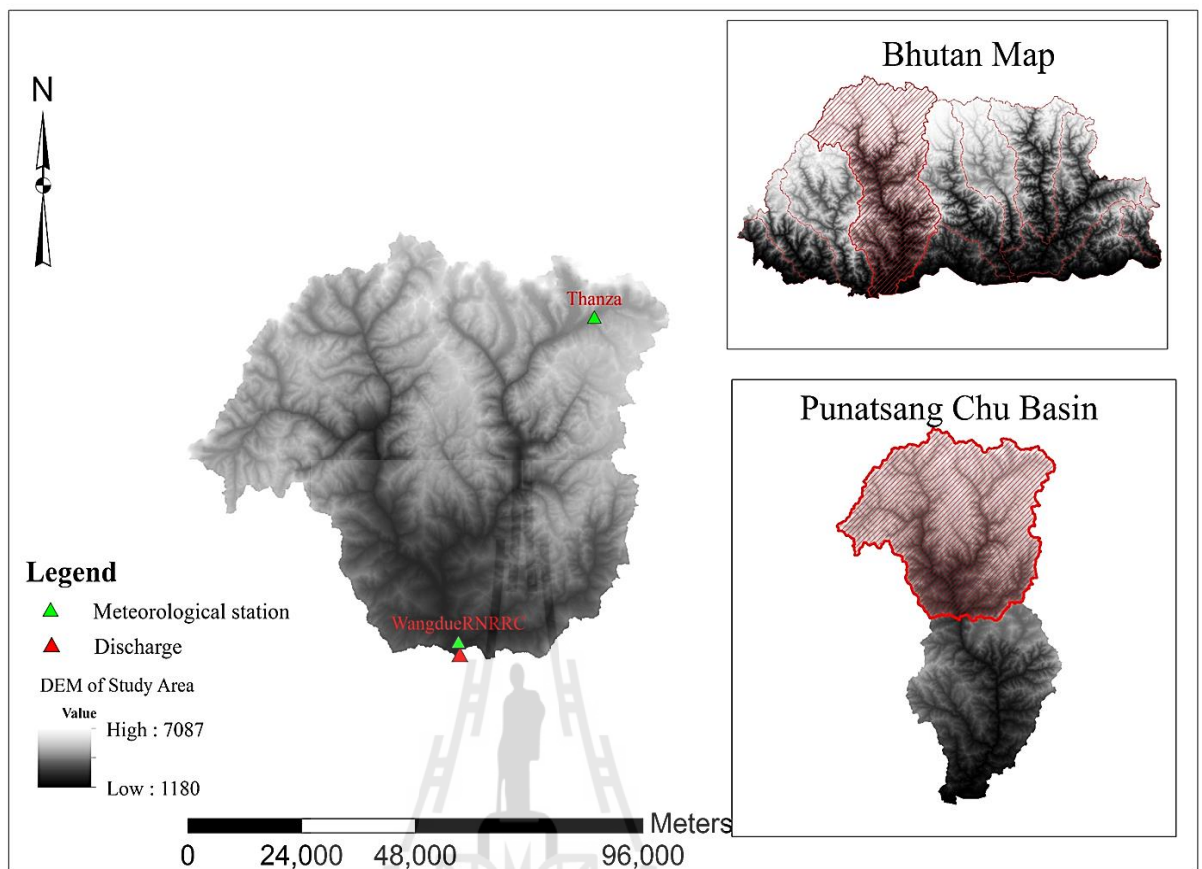


Figure 1.1 Map depicting the study area extent.

1.5 Benefits of the study

(1) Gain information on the total runoff from snow during the melting period and the derived SRM parameters range of different zones which can be used for future research.

(2) Complete understanding of the effect of temperature change on the snow and glacier residing on the Himalayas and understand the future scenario of water level conceived by the impact of climate change.

(3) Accomplish comprehensive trend of the depletion of snow cover over the study period from the MODIS satellite images.

CHAPTER II

BASIC CONCEPTS AND LITERATURE REVIEWS

Basic concepts include (1) snowmelt runoff model, (2) structure of SRM (3) data required for executing the model and (4) accuracy assessment and relevant literatures are reviewed in this chapter.

2.1 Snowmelt runoff model (SRM)

In general, many models have been created around the world over the last four decades to describe snowmelt runoff. These can be divided into two broad categories, (1) statistical and (2) physical. A statistical model utilizes statistical relationships between inputs and outputs. A physically based model describes the physical process that relates inputs to outputs. In turn, these models can be applied in lumped or distributed mode. A lumped model describes catchment processes with single “catchment average” values. A distributed model divides a catchment into sections and carries out model calculation for each section. A lumped model can be considered as a single section distributed model, or equally, a distributed mode can be considered as a series of small lumped models. The two more common ways of subdividing an area of interest for snowmelt modelling is into elevation zones, or into grid squares (Haq, 2008).

The Snowmelt Runoff Model (SRM) is designed to simulate and forecast daily stream flow in mountain basins where snowmelt is a major runoff factor. SRM was initially developed by Martinec in 1975 in small European basins. With its credibility in studying about snow, now recently, it has also been applied to evaluate the effect of a climate change on seasonal snow cover and runoff. Moreover, the SRM employs deterministic approach and it runs without calibrating the model parameters and this model needs only six parameters for accurate simulation (Butt and Bilal, 2011).

Initially, the SRM was applied to small basins, however with the advent of satellite remote sensing technology in the field of snow cover, now this model is being extensively used for larger and larger basins. Recently, the runoff was modelled in the basin of the Ganges River, which has an area of 917,444 km² and an elevation range from 0 to 8,840 meters above mean sea level. Contrary to the original assumptions, there appears to be no limits for application with regard to the basin size and the elevation range (Martinec, Rango, and Roberts, 2007). The SRM, which is termed as Matinec-Rango model, can be defined as a simple conceptual and degree day model which can be applied to mountain basis of various sizes and elevations, and the distinct feature of the SRM from other models is the need of inputting area of an elevation zone covered by snow (Rango and Katwijk, 1990).

Runoff computation by the SRM model appears to be relatively easily understood. As of now, the model has been applied by various agencies, institutes and universities in over 112 basins, situated in 29 different countries. SRM also successfully underwent tests by the World Meteorological Organization with regard to runoff simulations (WMO, 1986) and to partially simulated conditions of real time

runoff forecasts (Matinec et al., 2007; DeWalle and Rango, 2008; Butt and Bilal, 2011).

According to Jain et al. (2012), the snowmelt models have two basic approaches towards calculating the amount of snowmelt occurring from a snowpack: (1) energy budget method and (2) temperature index method.

Mays (2011) expressed the energy budget expression mathematically as follows:

$$Q_m = Q_{sn} + Q_{ln} + Q_h + Q_e + Q_g + Q_p - \Delta Q_i, \quad (2.1)$$

where Q_m is the total energy available for snowmelt, Q_{sn} is shortwave radiation, Q_{ln} is long-wave net radiation, Q_h is convection from the air (sensible energy), Q_e vapor condensation (latent energy), Q_g is conduction from the ground, Q_p is the energy contained in rainfall and ΔQ_i is the rate of change in the internal energy stored in the snow per unit area of snow. During periods of warming, the net flux of heat ΔQ_i is into the snow, and during periods of cooling, the net flux ΔQ_i is out of the snowpack.

The energy budget approach attempts to make the process as physically based as possible. The goal is to simulate all energy fluxes over time and space. This approach is extremely data intensive, requiring vast amounts of input data either to force an initial run of a model, or to calibrate it based on historical data before running a forecast. Too often, this approach suffers from inadequate data supply or simply that the level of data is unwarranted for the purpose at hand.

In light of the intensive data requirements necessary for the energy budget approach, an alternative method known as the temperature index or degree day approach allows for snowmelt calculation with much less data input. The basis of the temperature index approach is that there is a high correlation between snowmelt and air temperature, due to the high correlation of air temperatures with the energy

balance components which make up the energy budget equation. The temperature index model is popularly used for operational purpose due to following reason (He, Parajka, Tian, and Bloschl, 2014):

1. Wide availability of air temperature data
2. Relatively easy interpolation and forecasting possibilities of air temperature.
3. Generally good model performance
4. Computational simplicity.

There are several temperature index based snowmelt models like the SSARR Model, the HEC-1 and HEC-1F Models, the NWSRFS Model, the PRMS Model, the SRM and the GAWSER Model. Amongst these model, the SRM is widely used for modeling in Himalayan basin. The SRM uses snow-covered area as input instead of snowfall data, but it does not simulate the base flow component of runoff. In other words, the SRM model does not consider the contribution to the groundwater reservoir from snowmelt or rainfall, nor its delayed contribution to the stream flow in the form of base flow (Singh and Jain, 2003 and Jain et al., 2012).

According to Martine et al. (2007), the SRM model can be used for the following purposes: (1) simulation of daily flows in a snowmelt season, in a year, or in a sequence of years, (2) short term and seasonal runoff forecasts, and (3) evaluating the potential effect of climate change on the seasonal snow cover and runoff.

2.2 Structure of SRM

Each day, the water produced from snowmelt and from rainfall is computed, superimposed on the calculated recession flow and transformed into daily discharge from the basin according to the following equation:

$$Q_{n+1} = [C_{Sn} \cdot \alpha_n (T_n + \Delta T_n) S_n + C_{Rn} \cdot P_n] \cdot A \frac{10000}{86400} (1 - k_{n+1}) + Q_n \cdot k_{n+1}, \quad (2.2)$$

where Q = average daily discharge [$\text{m}^3 \text{s}^{-1}$],

C = runoff coefficient expressing the losses as a ratio (runoff/precipitation),

with C_S referring to snowmelt and C_R to rain,

α = degree day factor [$\text{cm}^\circ\text{C}^{-1} \text{d}^{-1}$] indication the snowmelt depth resulting from 1 degree-day,

T = number of degree days [$^\circ\text{C}\cdot\text{d}$],

ΔT = the adjustment by temperature lapse rate when extrapolating the temperature from the station of the average hypsometric elevation of the basin or zone [$^\circ\text{C}\cdot\text{d}$],

S = ratio of the snow covered area to the total area,

P = precipitation contributing to runoff [cm]. A preselected threshold temperature called critical temperature, T_{CRIT} , determines whether this contribution is rainfall and immediate. If the precipitation is determined by T_{CRIT} to be new snow, it is kept on storage over the hitherto snow free area until melting condition occur,

A = area of the basin or zone [km^2],

k = recession coefficient indicating the decline of discharge in a period without snowmelt or rainfall: ($k = \frac{Q_{n+1}}{Q_n}$ where $n, n+1$ are the sequence of days during a true recession flow period).

n = sequence of days during the discharge computation period.

Equation 2.2 is written for a time lag, L between the daily temperature cycle and the resulting discharge cycle of 18 hours. In this case, the number of degree days measured on the n day corresponds to the discharge on the $(n+1)$ day. Various lag times can be introduced by a subroutine.

$$\frac{10000}{86400} = \text{conversion from cm.km}^2\text{d}^{-1} \text{ to m}^3 \text{ s}^{-1}$$

T, S and P are available to be measured or determined each day, C_R, C_S , lapse rate to determine $\Delta T, T_{\text{CRIT}}, k$ and the L are parameters which are characteristics for a give basin or, more generally, for a give climate.

If the elevation range of the basin exceeds 500 m, it is recommended that the basin should be subdivided into elevation zones. For an elevation range of 1500 m and three elevation zones A, B and C, the model equation becomes:

$$Q_{n+1} = \left\{ [C_{SA_n} \alpha_{A_n} (T_n + \Delta T_{A_n}) S_{A_n} + C_{RA_n} P_{A_n}] A_A \cdot \frac{1000}{86400} + [C_{SB_n} \alpha_{B_n} (T_n + \Delta T_{B_n}) S_{B_n} + C_{RB_n} P_{B_n}] A_B \cdot \frac{1000}{86400} + [C_{SC_n} \alpha_{C_n} (T_n + \Delta T_{C_n}) S_{C_n} + P_{A_n}] A_C \cdot \frac{1000}{86400} \right\} (1 - k_{n+1}) + Q_n k_{n+1} \quad (2.3)$$

The indices A, B and C refer to the respective elevation zones (Figure 2.1) and a time lag of 18 hours is assumed.

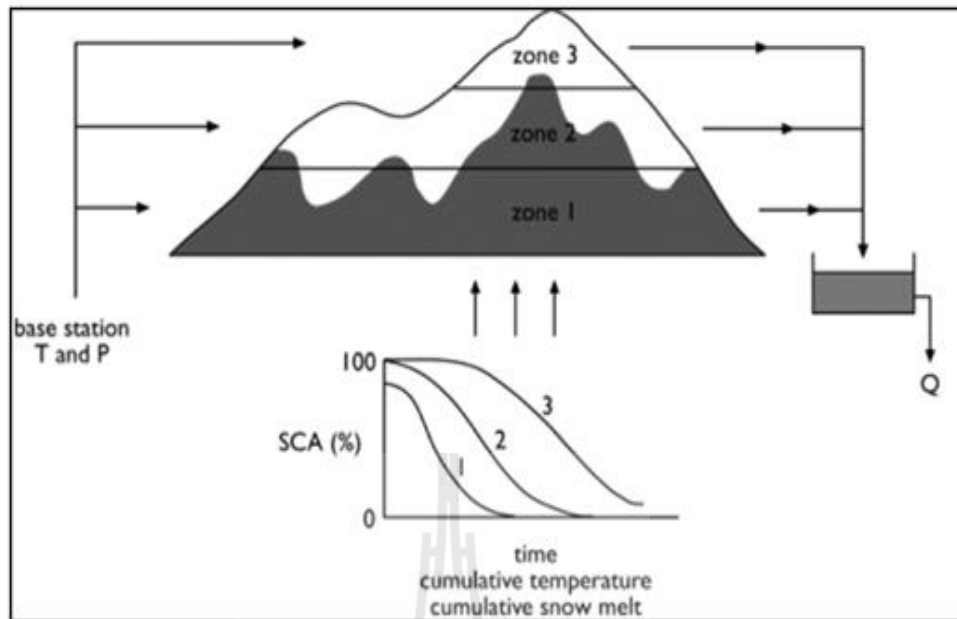


Figure 2.1 The structure of the SRM

Source: Ferguson (1999).

2.3 Data required for executing the model

The necessary input data for running the model can be grouped as follows

2.3.1 Basin characteristics

2.3.1.1 Basin and zone areas

The basin boundary is defined by the location of the stream gauge (or some arbitrary point on the stream course) and the watershed divide is identified on a topographic map. According to user requirement, the basin boundary can be drawn at a different map scale and elevation zones can be delineated in intervals of about 500 m after examining the elevation range between the stream gauge and the highest point in the basin. (Martinec et al., 2007).

Conventionally, for delineating the watershed a topographic map can be used and, further the elevation range of the watershed can be calculated manually taking the height difference of gauge station and the highest point in the basin. After defining the basin boundary, with aid of some intermediate topographic contour lines the area-elevation curve can be constructed (Refer Figure 2.2).

Now with the advent of satellite remote sensing and information technology, many of the above steps deployed for generating area-elevation curve can be expedited through the use of computer analysis and a Digital Elevation Model (DEM) (Martinec et al., 2007 and DeWalle and Rango, 2008).

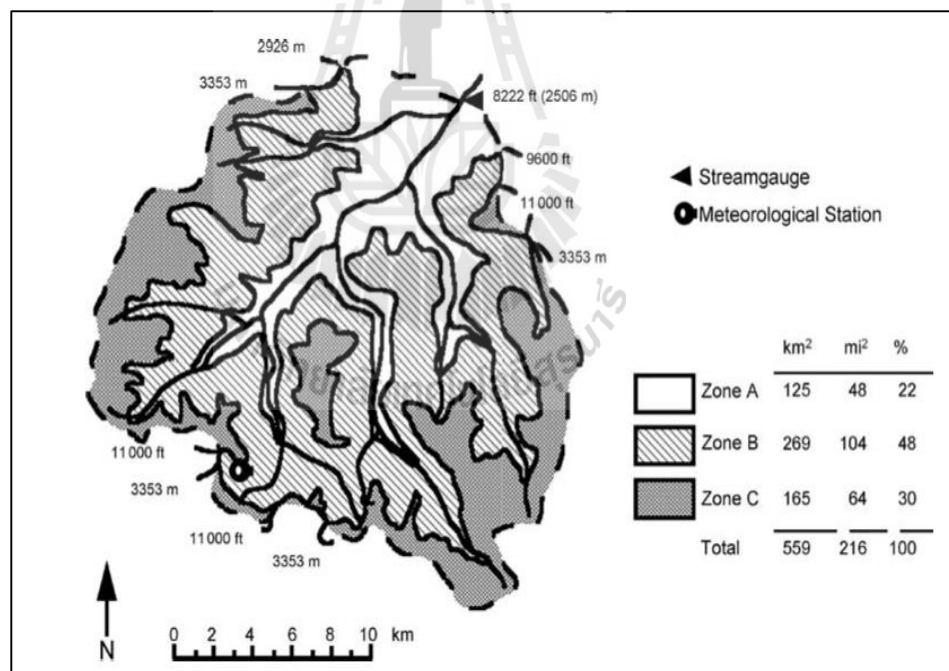


Figure 2.2 Elevation zone and areas of the South Fork of Rio Grande Basin, Colorado, USA.

Source: Martinec et al. (2007) and DeWalle and Rango (2008).

2.3.1.2 Area-elevation curve

By using the zone boundaries and other selected contour lines in the basin, the areas enclosed by various elevation contours can be determined by planimetry (Egdir, 2003). These data can be plotted (area vs. elevation) and area-elevation (hypsothetic) curve derived as shown in the Figure 2.3 for the South Fork basin as an example.

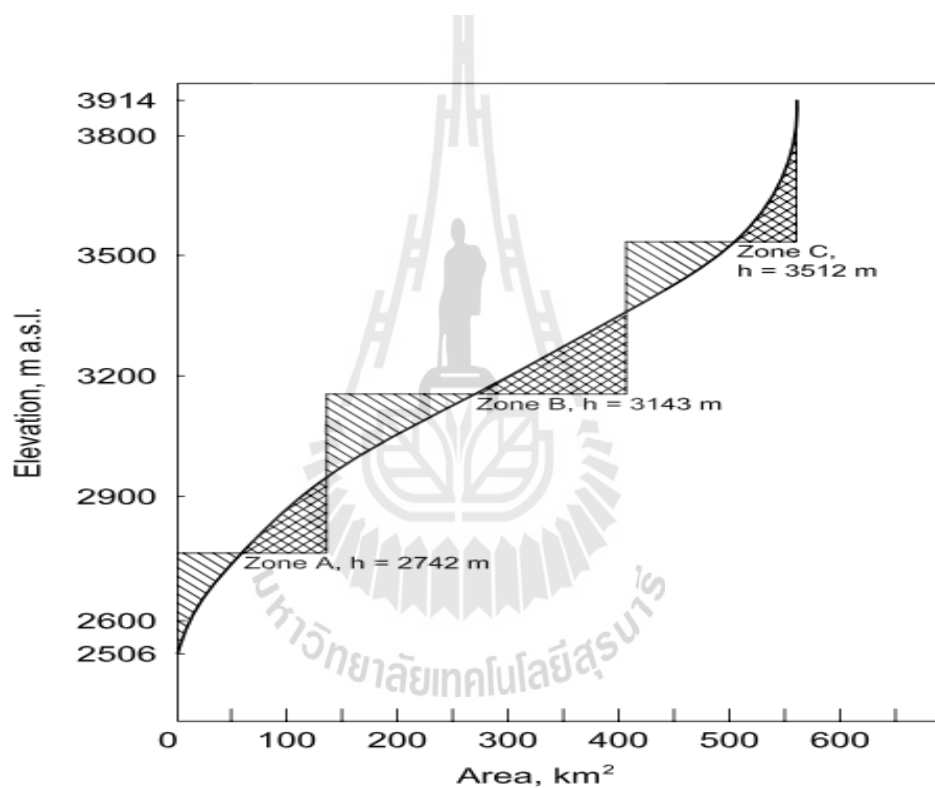


Figure 2.3 Determination of the zonal mean hypsothetic elevation using area-elevation curve for the South Fork of the Rio Grande basin.

Source: Martinec et al. (2007) and DeWalle and Rango (2008).

With help of the DEM, the area-elevation curve can also be derived automatically using computer algorithm in an image processing system. The zonal mean hypsothetic elevation, \bar{h} , can then be determined from this curve by balancing

the areas above and below the mean elevation as shown in Figure 2.3. The \bar{h} value is used as the elevation to which base station temperatures are extrapolated for the calculation of zonal degree days (Martinec et al., 2007).

2.3.2 Variables

For the model, variables basically describe the actual field observed meteorological measurements and its condition for the simulated year. And these set of data are obtained through in-situ measurement, except for snow cover area which can be defined by using satellite remote sensing data.

2.3.2.1 Temperature

Martinec et al. (2007) affirm that in order to compute the daily snowmelt depths, the number of degree days must be determined from temperature measurements or, in a forecasting mode, from temperature forecasts.

In SRM there are two options to input temperature measurement, either as daily mean temperature, T_{avg} or two temperature values on each day, i.e., T_{max} and T_{min} . This input temperature is then extrapolated from the base station elevation to the hypsometric mean elevation of the respective zones and the temperature data can be either from single or multiple stations. As measurement of correct air temperature is difficult, so it would be advisable to adopt one good temperature station (even if located outside the basin) which may be preferable to several less reliable stations, as measurement of correct air temperature is difficult (DeWalle and Rango, 2008).

Further, the average temperatures refer to a 24 hour period starting always at 06.00 hrs, they become degree days T [$^{\circ}\text{C}\cdot\text{d}$]. The altitude adjustment ΔT in Equation 2.2 in Section 2.2 is computed as follows:

$$\Delta T = \gamma (h_{\text{st}} - \bar{h}) \cdot \frac{1}{100} \quad (2.4)$$

where γ = temperature lapse rate [$^{\circ}\text{C}$ per 100 m], h_{st} = altitude of the temperature station [m] and \bar{h} = hypsometric mean elevation of a zone [m].

2.3.2.2 Precipitation

In mountain basins, it is extremely difficult to evaluate the representative areal precipitation. And moreover, quantitative precipitation forecasts are seldom available for the forecast mode. Similarly to temperature input, precipitation input can be assigned either a single, basin-wide precipitation input (from one station or from a “synthetic station” combined from several stations) or different precipitation inputs zone by zone (DeWalle and Rango, 2008).

In case if only low altitude precipitation stations data are used then the precipitation input may be underestimated in basins with a great elevation range. In such scenario, it is highly recommended to extrapolate precipitation data to the mean hypsometric altitudes of the respective zones by an altitude gradient, for instance 3% or 4% per 100 m (Martinec et al., 2007). However, if there are two stations at different altitudes, it is possible to assign the averaged data to the average elevation of both stations and to extrapolate by an altitude gradient from this reference level to the elevation zones. It should be kept in mind that the increase of precipitation amounts with altitude does not continue indefinitely but stops at a certain altitude, especially in very high elevation mountain ranges (Martinec et al., 2007 and DeWalle and Rango, 2008).

According to the suggestion of Martinec et al. (2007) if the precipitation is used by zone-wise and only one weather station is available, then the same precipitation values must be input to each elevation zone.

2.3.2.3 Snow cover area

Fuladipanah and Jorabloo (2012) suggested that snow covered area being a dynamic variable, it can be calculated through three methods: (1) direct measurement (2) using satellite data and (3) snow line calculation. It is a typical feature of mountain basins that the areal extent of the seasonal snow cover gradually decreases during the snowmelt season. Depletion curves of the snow coverage can be interpolated from periodical snow cover mapping so that the daily values can be read off as important input variables to SRM. The snow cover can be mapped using different methods such as terrestrial observation (for very small basins), by aircraft photography (during the flood emergency) and, of recent, the most efficiently method is by remote sensing satellites techniques. Nevertheless, the accuracy of mapped area by satellite undoubtedly depends on the spatial resolution of the remote sensor mounted on the satellite (Martinec et al., 2007 and DeWalle and Rango, 2008). The derivation of SCDCs as shown in Figure 2.4 from SCA classified using Landsat images shown in Figure 2.5 and Table 2.1 refers more about the available remote sensing satellites for mapping snow cover area.

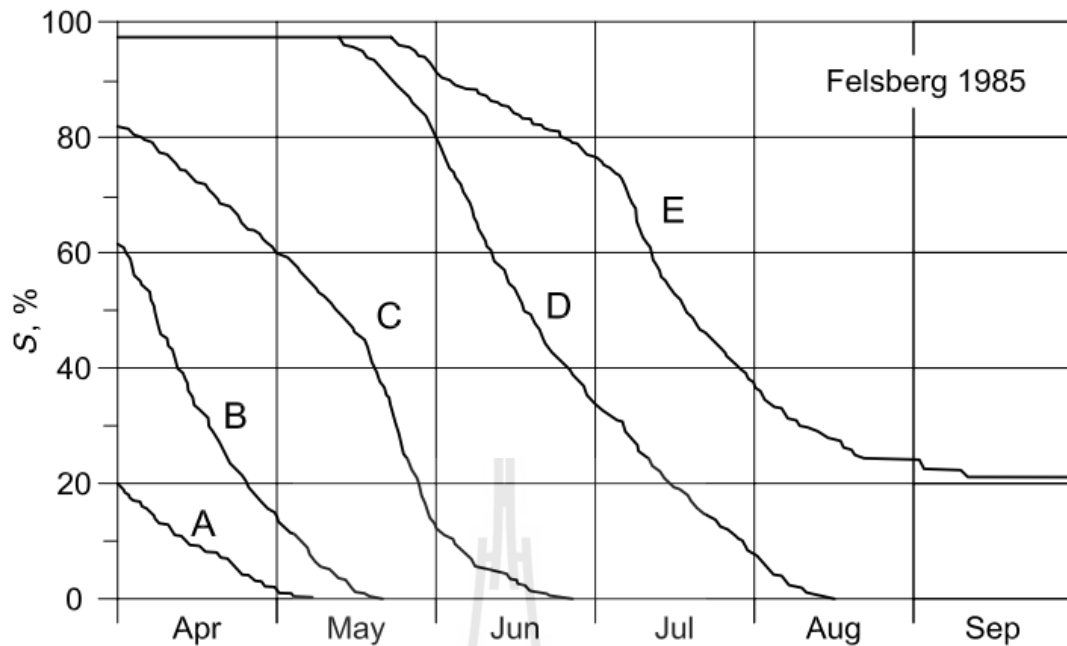


Figure 2.4 Depletion curves of the snow coverage for 5 elevation zones of the basin Felsberg, derived from the Landsat imagery shown in Figure 7. A: 560-1100 m (amsl), B: 1100-1600 m (amsl). C: 1600-2100 m (amsl). D: 2100-2600 m (amsl). E: 2600-3600 m (amsl).

Source: Martinec et al. (2007) and DeWalle and Rango (2008).

Like NDVI (Normalized Difference Vegetation Index), for mapping snow cover areas NDSI (Normalized Difference Snow Index) can be implemented (Butt and Bilal, 2011). NDSI is a band-ratioing algorithm (MODIS Reflective Solar Bands) of band 4 (0.545 – 0.565 μm) and band 6 (1.628-1.652 μm) and is given in equation as:

$$NDSI = \frac{MODIS(B4) - MODIS(B6)}{MODIS(B4) + MODIS(B6)} \quad (2.5)$$

where $MODIS(B4)$ is MODIS band 4 and $MODIS(B6)$ is MODIS band 6.

Table 2.1 List of remote sensing data for mapping snow cover area.

Platform-Sensor	Spectral Bands	Spatial resolution	Minimum area size	Repeat period
Aircraft-Orthophoto	Visible/NIR	2 m	1 km ²	flexible
IRS – Pan	Green to NIR	5.8 m	2 km ²	24 days
IRS -LISS-II	1 – 3 Green to NIR	23 m	2.5 – 5 km ²	24 days
IRS – WiFS	1 Red / 2 NIR	188 m	10 – 20 km ²	5 days
SPOT-HRVIR	1 – 3 Green to NIR	2.5 – 20 m	1 – 3 km ²	26 days
Landsat- MSS	1 – 4 Green to NIR	80 m	10 – 20 km ²	16 – 18 days
Landsat- TM	1 – 4 Green to NIR	30 m	2.5 – 5 km ²	16 – 18 days
Landsat- ETM-Pan*	Visible to NIR	15 m	2 – 3 km ²	16 – 18 days
Terra/Aqua- MODIS	1 Red / 2 NIR	250 m	20 – 50 km ²	1 day
Terra/Aqua- MODIS	3 – 8 Blue to MIR	500 m	50 – 100 km ²	1 day
NOAA-AVHRR	1 Red / 2 NIR	1.1 km	10 – 500 km ²	12 hr
Meteosat-SEVIRI	1 – 3 Red to NIR	3 km	500 – 1000 km ²	30 min
Meteosat-SEVIRI	12 Visible	1 km	10 – 500 km ²	30 min

Source: Matinec et al. (2007).

Acronym: ASTER = Advanced Spaceborne Thermal Emission and Reflection Radiometer, AVHRR = Advanced Very High Resolution Radiometer, HRVIR = High Resolution Visible and Near Infrared, IRS = Indian Remote Sensing, LISS = Linear Imaging Self-scanning Sensor, MIR = Middle Infrared, MODIS = Moderate Resolution Imaging Spectroradiometer, MSS = Multi-Spectral Scanner, NIR = Near Infrared, Pan = Panchromatic, SEVIRI = Spinning Enhanced Visible and Infrared Imager, SPOT = Satellite Pour l'Observation de La Terre, TM = Thematic Mapper, WiFS = Wide Field Sensor, ETM-Pan = Enhanced Thematic Mapper – Panchromatic

(*) Landsat 6 and 7 only (**) Depends on availability

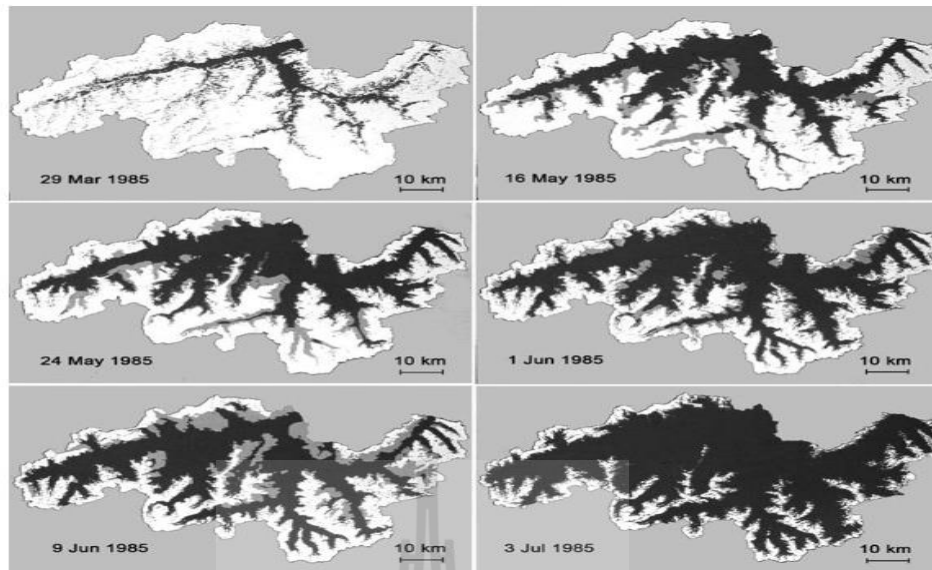


Figure 2.5 Sequence of snow cover maps from Landsat 5- MSS, Upper Rhine River at Felsberg, 3250 km², 560-3614 masl.. Black is snow free, gray is cloud covered and white is snow covered areas.

Source: Martinec et al. (2007) and DeWalle and Rango (2008).

Three threshold values are used before assigning the pixels as snow cover, i.e. NDSI is greater than 0.4 (Hall, Riggs, and Salomonson, 1995), reflectance in band 2 (0.841 – 0.876 μm) is greater than 11% and reflectance in band 4 (0.545 – 0.565 μm) is greater than 10%. The threshold value of bands 2 and 4 are used to eliminate water and dark pixels in an image, respectively. Thus, a pixel is mapped as snow if it has an $\text{NDSI} \geq 0.4$, band 2 reflectance greater than 11% and band 4 reflectance greater than 10%. The runoff volume during the snowmelt season is directly correlated to the SCA. Therefore, in the SRM, SCA estimates on weekly basis are required (Butt and Bilal, 2011). Snow cover depletion curves (SCDCs) can be analyzed from high temporal snow cover mapping to get daily values of percentage of SCAs (see Figure 2.4 and 2.5).

Note that cloud typically has high reflectance in the VNIR and the value decreases slowly in shortwave infrared wavelength (SWIR), while snow has high reflectance in visible and NIR and the value decreases significantly in the SWIR (see Figure 2.6).

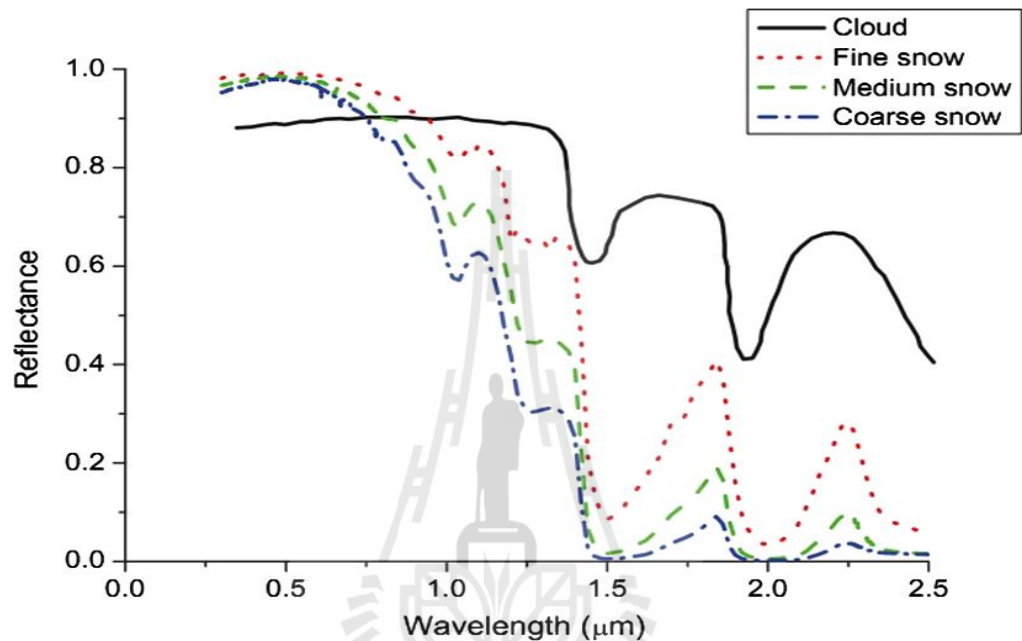


Figure 2.6 Spectral reflectance curves of typical cloud and snow.

Source: Shahabi, Khezri, Ahmed, and Musa (2014).

2.3.3 Parameters

The SRM parameters are not calibrated or optimized by historical data. They can be either derived from measurements or estimated by hydrological judgment taking into account the basin characteristics, physical laws and theoretical relations or empirical regression relations. Occasional subsequent adjustments should never exceed the range of physically and hydrologically acceptable values (Martinec and Rango, 1986; Martinec et al., 2007 and DeWalle and Rango, 2008). Following are the parameters allied with the SRM:

2.3.3.1 Runoff coefficient of snow and rain (C_S and C_R)

The difference between the melt volume and the runoff volume is considered a loss and is assumed to be infiltration into the soil and groundwater storage. These losses are expected to return to the stream during the event, but may contribute to base flow. Infiltration losses under snowpack are difficult to base on the soil and land cover characteristics because of varying frozen ground condition. Instead, the infiltration or loss parameter may be selected based on calibrating the model so that runoff volumes computed from a known volume of snowmelt agree with measured volumes of runoff from a watershed (USDA NRCS, 2004).

In other words, the runoff coefficient in the SRM deals with losses or in other words, it can be explained as the difference between the available water volume (snowmelt + rainfall) and the outflow from the basin. It takes care of all the losses between the snowmelt and the outflow from the watershed (Martinec et al., 2007 and DeWalle and Rango, 2008).

Mathematically, the runoff coefficient (C_R) is the ratio of runoff to snowmelt (M) and the coefficient varies widely from watershed to watershed from as little as 0.1 to more than 0.9. The ratio may be related to soil and cover type and to total precipitation, and it varies seasonally, generally decreasing as evapotranspiration losses increase as the melt progresses (USDA NRCS, 2004). The runoff coefficient can be expressed as:

$$C_R = \frac{\text{Runoff}}{M} \quad (2.6)$$

2.3.3.2 Degree day Factor (α)

According to He et al. (2014), the temperature index model is based on an assumed relationship between ablation and air temperature and calculates the

daily snowmelt, M (mm d^{-1}), by multiplying the difference between the daily temperature and the melt threshold value, $T - T_o$ ($^{\circ}\text{C day}^{-1}$), with the snowmelt degree day factor or α ($\text{mm } ^{\circ}\text{C}^{-1}\text{d}^{-1}$).

In other words, the degree day factor is the ratio of the snowmelt to concurrent degree days or it is the amount of snowmelt that would result due to one degree day. This factor commonly ranges from 0.05 to 0.1 inches per degree Fahrenheit day, but is difficult to obtain since the snowmelt cannot be measured directly, so the rate of runoff must be used in lieu of the rate of snowmelt (Shawcroft, 1985).

A degree day is the departure of one degree Fahrenheit ($32^{\circ}\text{F} = 0^{\circ}\text{C}$) for one day of the mean daily temperature from a specified base temperature. The mean daily temperature is simply an average of the daily maximum and minimum temperatures. In this case, the base temperature was 32°F . For example, if the mean daily temperature for a given day were 37°F , this would represent 5 degree days.

The α [$\text{cm } ^{\circ}\text{C}^{-1}\text{d}^{-1}$] converts the number of degree days T [$^{\circ}\text{C}\cdot\text{d}$] into the daily snowmelt depth M [cm]:

$$M = \alpha \cdot T \quad (2.7)$$

where $T = (T_i - T_b)$, T_i = index air temperature ($^{\circ}\text{C}$) and T_b = base temperature (usually 0°C). Mean daily temperature is the most commonly used index of air temperature for snowmelt (Prasad and Roy, 2005). The value of degree day factor, α according to Martinec and Rango (1986) in SRM computation is determined from the following empirical relation whenever snow density data were available:

$$\alpha = 1.1 \cdot \frac{\rho_s}{\rho_w} \quad (2.8)$$

where α = the degree day factor [$\text{cm } ^\circ\text{C}^{-1}\text{d}^{-1}$], ρ_s = density of snow and ρ_w = density of water.

Additionally, Fuladipanah and Jarabloo (2012) stated that the degree day factor has direct affect in snowmelt runoff, because it converts the snow cover to snowmelt expressed in depth of water. It was concluded by He et al. (2014) that spatial variations of basin topography, such as elevation, terrain slope, aspect and terrain shading change the spatial energy conditions for snowmelt and lead to significant variation in α .

2.3.3.3 Temperature lapse rate (γ)

To distinguish the precipitation falls as rain or snow, it is essential to quantify the distribution of temperature in complex terrain for accurately modeling stream flow and ecosystem distributions, and for understanding decadal trends in snowpack and glacier volume. Due to sparse network of sensors measuring surface temperature in mountains, combined with the influence of local factors like cold air pooling and inversion, such a quantification is challenging. With seldom availability of such measurements, therefore, the empirical relationship between surface temperature and elevation are frequently used for studying temperate lapse rate (Minder, Mote, and Lundquist, 2010).

According to Harlow et al. (2004), the lapse rates can be defined as the rate of change of temperature with height and can be expressed mathematically as follows:

$$T = T_o - \gamma \cdot dz \quad (2.9)$$

where T_o is the temperature at the base location, T is the temperature at a second station, γ is the lapse rate and dz is the difference in elevation between the two

locations. Generally, the common method adopted to determine the temperature lapse rate is by employing the historical data observed at temperature stations located at different altitudes are available.

However, either in the absence of meteorological stations or if the manually recording of air temperature is erroneous, then in such situation the land surface temperature (LST) maps can be generated from satellite images, which are known to be an attractive and logical alternatives. As an output, LST maps prepared from the satellite images will be continuous datasets (Jain et al., 2010).

2.3.3.4 Critical temperature (T_{CRIT})

The critical threshold temperature, T_{CRIT} , determines whether measured daily precipitation is rain or snow. This is of particular importance for models which simulate the build-up of the snow cover from precipitation data. The SRM directly deploys remote sensing of the snow cover, and does not depend on this parameter during the accumulation period. This parameter, T_{CRIT} , is required only during the snowmelt season in order to decide whether a precipitation immediately contributes to runoff, or, if $T < T_{CRIT}$, whether a melt season snowfall took place. In this case, SRM automatically keeps the newly fallen snow in storage until it is melted on subsequent warm days, thus contributing as a “delayed rainfall” to the runoff (Martinec and Rango, 1986; Martinec et al., 2007 and DeWalle and Rango, 2008). Martinec and Rango (1986) confirmed from the direct observation, T_{CRIT} is generally higher than 0 °C or 32 °F (Figure 2.7).

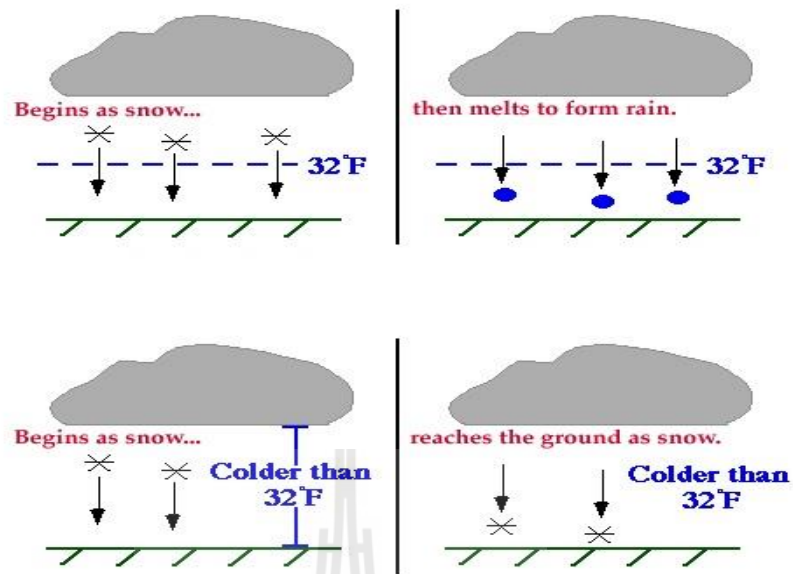


Figure 2.7 The diagram depicts the role of critical temperature to distinguish the precipitation to be rain or snow.

Source: University of Illinois (2014).

2.3.3.5 Rainfall contribution area (RCA)

When precipitation is determined to be rain, it can be treated in two ways. In the initial situation, it is assumed that rain falling on the snowpack early in the snowmelt season is retained by the snow which is usually dry and deep. Rainfall runoff is added to snowmelt runoff only from the snow-free area, that is to say the rainfall depth is reduced by the ratio snow-free area/ zone area. Now, if rain falls on this snow cover, it is assumed that the same amount of water is released from the snowpack so that rain from the entire zone area is added to snowmelt. The melting effect if rain is neglected because the addition heat supplied by the liquid precipitation is considered to be small (Martinec et al., 2007 and DeWalle and Rango, 2008).

2.3.3.6 Recession coefficient (k)

Martinec and Rango (1986) validated that a good way of determining the value, k is by analyzing the historical discharge data. It is evident from the Equation 2.2 that the SRM model is very much sensitive to this value /parameter as (1-k) is the proportion of the daily melt water production which immediately appears in the runoff. Thus, while using SRM model, the value k should be evaluated carefully. In particular, its variability in relation to the current discharge should be taken into account by determining the constants x, y in the following equation:

$$K_{n+1} = xQ_n^{-y} \quad (2.10)$$

Figure 2.8 shows such evaluation for the alpine basin Dischma (43.3 km², 1,668-3,146 m amsl.). Values of Q_n and Q_{n+1} are plotted against each other and the lower envelope line of ballpoints is considered to indicate the k-values. Based on the relation $k = Q_{n+1}/Q_n$, it can be derived that for example k₁ = 0.677 for Q_n = 14 m³s⁻¹ and k₂ = 0.85 for Q_n = 1 m³s⁻¹. This means that k is not constant, rather its value increases with decreasing Q_n value.

The constants x and y must be determined for a given basin by solving the equation:

$$k_1 = xQ_1^{-y} \quad (2.11)$$

$$k_2 = xQ_2^{-y} \quad (2.12)$$

Further, the above equation can be written as

$$\log k_1 = \log x - y \log Q_1$$

$$\log k_2 = \log x - y \log Q_2$$

For the given value of k_1 and k_2 and substituting it, the above equations yield values as follows:

$$\log 0.677 = \log x - y \log 14$$

$$\log 0.85 = \log x - y \log 1$$

$$x = 0.85 \text{ and } y = 0.086$$

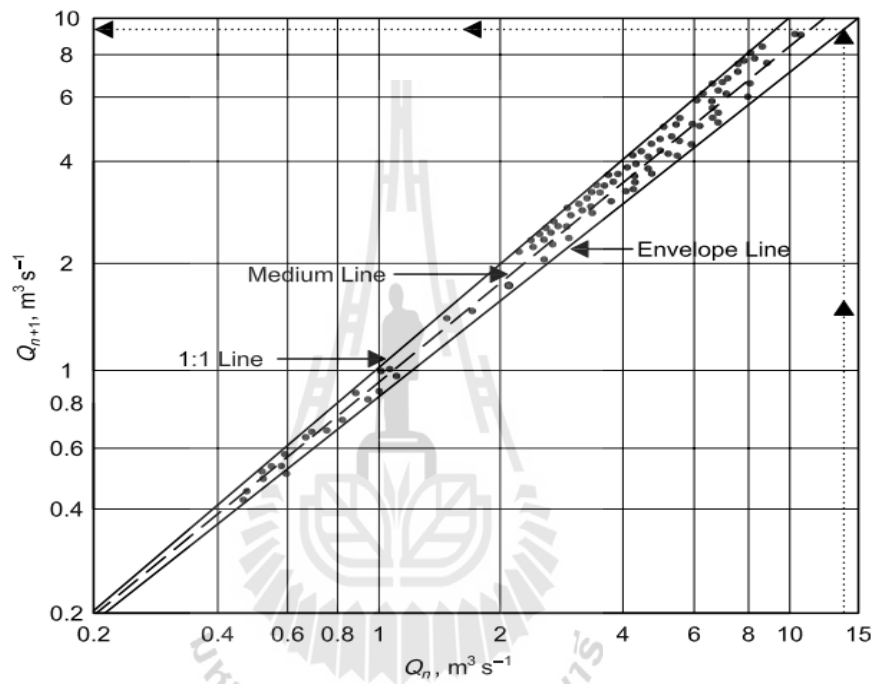


Figure 2.8 Recession flow plot Q_n vs. Q_{n+1} for the Dischma basin in Switzerland.

Either the slope envelope line or the dashed medium line is used to determine k -values for computing the constants x and y in the Equation 2.10.

Source: Martinec and Rango (1986) and Martinec et al. (2007).

In the case of ungauged basins with insufficient historical data, then x and y can be derived indirectly from the size of the basin according to Martinec and Rango (1986) and Matinec et al. (2007) by using the following equation:

$$k_{Nn} = \left[x_M \left(\frac{Q_{avgM}}{Q_{avgN}} \cdot Q_{Nn-1} \right)^{-y_M} \right]^{\frac{4}{\sqrt{A_M/A_N}}} \quad (2.13)$$

where x_M and y_M are the known constants for the basin M , Q_{avg_M} and Q_{avg_N} are average discharge values from the basin M and the new basin N ; and A_M and A_N are the areas of the respective basins. Equation 2.13 indicates that the recession coefficient are generally higher in large basins than in small basins.

2.3.3.7 Time lag (L)

The characteristic daily fluctuation of snowmelt runoff enables the time lag to be determined directly from the hydrographs of the past years. If for example, the discharge starts rising each day around noon, it lags behind the rise of temperature by about 6 h. Consequently, temperature measured on the n th day correspond to discharge between 1200 h on the n^{th} day and 1200h on the $(n+1)^{\text{th}}$ day. Discharge data, however, may only be published for midnight-to-midnight intervals and would need adjustments in order to be compared with stimulated values (Martinec and Rango, 1986; Martinec et al., 2007 and DeWalle and Rango, 2008).

Conversely, the simulated values can be adjusted to refer to the midnight-to-midnight periods. Figure 2.9 below illustrates the procedure for different time lags. For instance, $L= 6$ hours, 50% of input computed for temperature and precipitation of the n^{th} day (I_n) plus 50% of I_{n+1} results in then $n+1$ day's runoff after being processed by the SRM computer program:

$$L = 6\text{h}, 0.5I_n + 0.5 I_{n+1} \rightarrow Q_{n+1} \quad (2.14)$$

Similarly,

$$L = 12\text{h}, 0.75I_n + 0.25 I_{n+1} \rightarrow Q_{n+1} \quad (2.15)$$

$$L = 18\text{h}, I_n \rightarrow Q_{n+1} \quad (2.16)$$

$$L = 6\text{h}, 0.25I_n + 0.75 I_{n+1} \rightarrow Q_{n+1} \quad (2.17)$$

According to Martinec et al. (2007) and DeWalle and Rango (2008) this procedure is preferable for a mountain basin with area not exceeding 5000 km² to evaluate L by calculating the velocity of overland flow and channel flow. It has been shown by environmental isotope tracer studies that overland flow is not a major part of the snowmelt runoff as previously believed (Martinec et al., 2007). There is increasing evidence that a major part of melt water infiltrates and quickly stimulates a corresponding outflow from the groundwater reservoir. With the runoff concept in mind, the seemingly oversimplified treatment of the time lag in the SRM model is better understood.

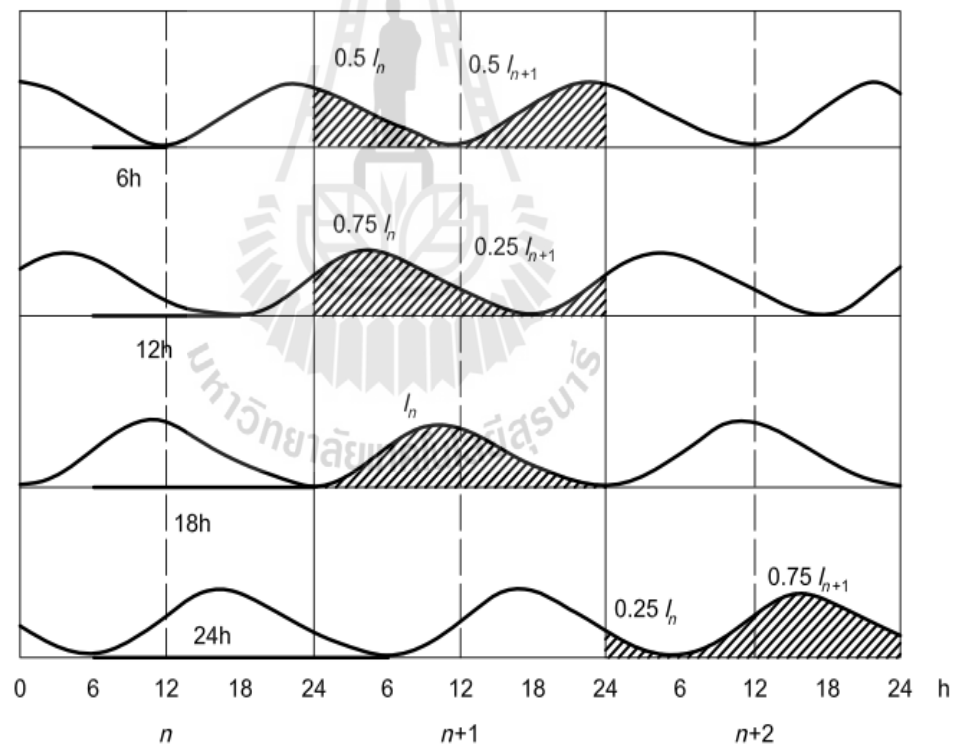


Figure 2.9 Snowmelt hydrographs illustrating the conversion of computed runoff amounts for 24-hours periods to calendar day periods. The various time lags (bold lines) are taken into account by proportions of the daily inputs, I

Source: Martinec and Rango (1986) and DeWalle and Rango (2008).

If the hydrographs are not available or if their shape is distorted by reservoir operations, the time lag can be estimated according to basin size and by analogy with other comparable basins. Generally, the time lag in a basin increases as the snow line retreats.

If there is some uncertainty, L (percentage in Equation 2.14 to 2.17) can be adjusted in order to improve the synchronization of the simulated and measured peaks of average daily flows. It should be noted that similar effect results from an adjustment of the recession coefficient.

Martinec and Rango (1986) concluded that almost all the models, which underwent WMO test are, are calibrated with the time lag. However, these results appear to be of little help to determine the proper values. Contradictory time lags have been calibrated by different models. However, if the time lags for the all models participating in the WMO intercomparison test are averaged for each basin, the resulting values support the expected relation between L and basin size:

Basin W-3 (8.42 km²): 3.0 h

Dischma (43.3 km²): 2.0 h

Dunajec (680 km²): 10.5 h

Durance (2170 km²): 12.4 h

Usually, the parameters of the L , α , and k can be evaluated more accurately by on site measurements, weather records, and hydrological data analysis with certain empirical formulas. The remaining parameters, namely k , T_{CRIT} , RCA , and L , are derived from basin characteristics such as geographical location, vegetation cover, topography, soil condition, evapotranspiration, physical laws, and complex interaction between them (Abudu, Cui, and King, 2012).

2.4 Accuracy assessment

2.4.1 Accuracy criteria

The SRM computer program facilitates with a graphical display of the computed hydrograph and measured runoff. From this graphical display, one can assure qualitatively whether the simulation is successful or not. In addition, the SRM model uses two well established accuracy criteria, namely, the Nash-Sutcliffe Efficiency, NSE and the volume difference, D_V .

1. The Nash-Sutcliffe Efficiency (NSE)

NSE is computed as follows:

$$NSE = 1 - \frac{\sum_{i=1}^n (Q_i - Q'_i)^2}{\sum_{i=1}^n (Q_i - Q')^2} \quad (2.18)$$

where Q_i is the measured daily discharge, Q'_i is the computed daily discharge, Q' is the average measured discharge of the given year or snowmelt season and n is the number of daily discharge values.

NSE ranges between $-\infty$ and 1, with $NSE = 1$ being the optimal value. Values between 0 to 1 are general reviewed as acceptable levels of performance, whereas values ≤ 0 indicates that the mean observed value is a better predictor than the simulated value, which indicates unacceptable performance.

2. The Deviation of the Runoff Volumes, D_V is computed as follows:

$$D_V = \frac{(V_R - V'_R)}{V_R} \times 100 \quad (2.19)$$

where V_R is the measured yearly or seasonal runoff volume and V'_R is the computed yearly or seasonal runoff volume.

3. The "Coefficient of Gain from Daily Means," DG

The coefficient of gain from daily means is shown as follows (WMO, 1986; Martinec and Rango, 1989 and Martinec et al., 2007)

$$DG = 1 - \frac{\sum_{i=1}^n (Q_i - Q'_i)^2}{\sum_{i=1}^n (Q_i - Q')^2} \quad (2.20)$$

where Q_i is the measured daily discharge, Q'_i is the computed daily discharge, Q' is the average measured discharge from the past years for each day of the period and n is the number of days.

Thus, NSE compares the performance of a model with “no model” (average discharge) and DG with a “seasonal model” (long term average runoff pattern). Negative values signal that the model performed worse than “no model” or worse than the “seasonal model”.

4. Percent Bias (PBIAS)

PBIAS measure the average tendency if the simulated data to be larger or smaller than their observed counterparts. The optimal value is 0, with low-magnitude values indicates accurate model simulation. Positive values indicate model underestimation bias, and negative values indicates model overestimation bias (Moriasi, Arnold, Van Liew, Bingner, Harmel, and Veith, 2007).

$$PBIAS = \frac{\sum_{i=1}^n (Q_i - Q'_i)}{\sum_{i=1}^n (Q_i)} \times 100 \quad (2.21)$$

where Q_i is the measured daily discharge, Q'_i is the computed daily discharge

Kult, Choi and Choi (2014) provided performance rating for NSE and PBIAS to justify the accuracy of the model as shown in Table 2.2

Table 2.2 Performance ratings for NSE and PBIAS.

NSE Statistics	PBIAS Statistics	Rating
$0.75 < R^2 \leq 1.00$	$ \text{PBIAS} < 10\%$	Very good
$0.65 < R^2 \leq 0.75$	$10\% \leq \text{PBIAS} < 15\%$	Good
$0.50 < R^2 \leq 0.65$	$15\% \leq \text{PBIAS} < 25\%$	Satisfactory
$R^2 \leq 0.50$	$ \text{PBIAS} \geq 25\%$	Unsatisfactory

Source: Kult et al. (2014).

2.4.2 Accuracy criteria in model tests

The World Meteorological Organization (WMO) organized an international comparison of snowmelt runoff models in which hundreds of model runs were performed in six selected test basins. Table 2.3 shows a summary of all numerical values of NSE, DG and D_v published by WMO (1986).

Table 2.3 Results of model performance in the WMO project (10 years, snowmelt season)

Group	Model	D_v max (%)	D_v(%)	Avg.1-NSE²	Avg.1-DG	1-NSE_{min}²	1-DG_{min}
A	UBC	-23	8.13	0.27	0.37	1.9	1.53
B	CEQ	-25	7.37	0.33	0.56	1.37	2.34
C	ERM	65.7	15.3	0.7	0.91	5.83	3.27
D	NAM	51	10.9	0.31	0.49	1.75	2.8
E	TANK	45.9	7.9	0.24	0.36	1.22	2.29
F	HBV	23.2	6.82	0.29	0.5	0.96	4.49
G	SRM	-28	5.97	0.19	0.29	0.39	0.79
H	SSARR	25.4	7.3	0.29	0.51	0.76	1.45
I	PRMS	24.2	10.6	0.37	0.57	0.9	2.52
J	NWS	28.1	7.43	0.23	0.25	0.68	1.24

Source: Martinec et al. (2007).

UBC = University of British Columbia, CEQ = CEQUEAU, HBV = Hydrological Simulation, SRM= Snowmelt Runoff Model, SSARR = Stream flow Synthesis and Reservoir Regulation; PRMS= Precipitation Runoff System Modelling, NWS = National Weather Service. ERM= Effective Rainfall routed by Muskingum method.

2.5 Literature reviews

Aggarwal, Thakur, Bhaskar and Garg (2014) working under the Water Resources Department, Indian Institute of Remote Sensing , Dehradun, India carried out a research on snowmelt runoff with the title “ Integrated approach for snowmelt runoff estimation using temperature index model, remote sensing and GIS.” For this research, the authors integrated temporal SCA and DEM derived from satellite remote sensing with GIS and then used in temperature index model for estimating the snowmelt runoff in Alakhnanda and Bhagirathi river basins which are part of the head reach Sub-basin of the Ganga River. The authors derived SCA for Bhagirathi and Alakhnanda River for the period years of 2002 - 2007 and 2000 - 2008 respectively, from remote sensing data and DEM was used to derive the elevation zones and aspect maps. The input data such as temperature, precipitation and discharge data were obtained from Indian Meteorological Department and Central Water Commission and after inputting temperature, precipitation and SCA in SRM model, the overall accuracy for estimating snowmelt for Alakhnanda River in terms of NSE is 84% – 90% for years 2000 and 2008, and 74% - 84% in Bhagirathi River for 2002-2007. Further, the authors concluded that SRM needs only basic meteorological and SCA information and has the capability to simulate changed climate scenarios, the effect of climate change on SRM can be simulated in future studies.

Fuladipanah and Jorabloo (2012) conducted a study on estimation of snowmelt and rainfall runoff for water management programs in Gharasoo basin, West-North of Iran during the time period of 20th February, 1998 to 5th June, 1998. In this study, an attempt has been made by the authors to estimate daily discharge using the SRM based on a degree day method. During the research, the data between the time periods of 19th February, 1997 to 21st May, 1997 were used for calibrating the model by dividing the study area into five different elevation zones. For this purpose of calculating percentage of snow covered area, they opted for snow line method and deployed isohyet map to estimate the mean precipitation in each zone. The authors considered 2°C as the critical temperature for the study area and applied exponential regression equation for estimating the value of degree day factor for zone areas. With aid of calibration period data, the snowmelt and rainfall runoff coefficients were calculated. They applied the model accuracy criteria, NSE and D_v , and the output results were 78.11 and -14.24% and 79.56 and -9.21% during the calibration and validation periods respectively, which on the basis of the output the authors concluded that there was a good agreement between measured and calculated daily discharge.

SCA being the fundamental source of water for hydrological cycle for some region and further, accurate measurement of rive discharge from snowmelt can help manage much need water required for hydropower generation and irrigation purpose. Butt and Bilal (2011) applied the SRM for water resource management in the Upper basin of the Astore River in northern Pakistan for the years 2000 to 2006. For this study, the Shuttle Radar Topographic Mission (SRTM) data were used to generate the DEM of the region and various variables, namely SCDCs, temperature and precipitation, and parameters (degree day factor, recession coefficient, runoff

coefficients, time lag, critical temperature and temperature lapse rate) are used as input in the SRM. However, snow cover data is said to be most important input to the SRM. The authors used MODIS data to estimate the SCA using the NDSI algorithm which helps to differentiate between snow cover pixels from other land features pixels. To validate the quality and accuracy of the SRM model, NSE and D_V were used. The output of the research for year 2000 to 2006 resulted an average value 87% for NSE, 1.18% for D_V and the correlation coefficient between the measured and computed runoff is 0.95. Further, the authors concluded that a high level accuracy is possible to achieve during the snowmelt season. Nonetheless, the authors endorsed that the SRM in conjunction with MODIS snow cover product is very useful for water resource management in the Astore River and can also be used for runoff forecasts in the Indus River basin in northern Pakistan.

Alam, Shakil, Romshoo, and Bhat (2011) conducted a study on estimating snowmelt runoff using SRM in the Kolahoi watershed western Himalayas for the year 2001. In this research it broadly sensitizes about the use of SRM (degree day drive model) aided with remote sensing satellite data for calculating the snow covered area. The study area was divided in 10 different elevation zones each with elevation difference of 10 meters. Daily temperature (min and max) has been extrapolated to each zone using temperature lapse rate derived using observed data of meteorological station located outside the watershed. And depletion curves of the snow cover have been interpolated from periodical snow cover mapping using monthly Landsat-TM data and the daily values were derived which are needed as an important input variables to the SRM. Individual runoff from snow covered area and snow free area for every elevation zone are calculated separately. However, the measured runoff data

is not required as input for running the simulation but it has been used for validating the model results. For this research, the simulation revealed the volume difference of only 7.8% between the measured runoff (79.1 m³/sec) and computed runoff (72.9 m³/sec). With such good agreement between the measured runoff and computed runoff, the authors concluded that the SRM proved to be a reliable tool for estimating the snowmelt runoff especially in the ungauged mountainous snow covered catchments.

Nabi, Latif, Rehman, and Azhar (2011) applied SRM in the upper Indus basin which has high mountains covered with snow and glaciers. The core reason behind the application of SRM in the basin is due mainly to difficulty in measuring the hydrological and hydraulics data in the rugged and inhospitable terrain of the basin. The authors used SRM to estimate the snow melt runoff in Astor basin during the year 2000 with input data consisting of daily temperature, precipitation and division of catchment in to different zone on the basis of elevation difference. As usual, the elevation zones were extracted from the DEM of the area and the snow depletion curves were generated using Landsat TM satellite data on a monthly basis. The output of their research work was a discharge hydrograph. The model performance were validated using the statistical parameters such as NSE and D_v in percentage. The values yielded by the SRM were 91 and 9.01% for NSE and D_v respectively for simulation mode and on the basis of the statistical results, the authors concluded that model performance was good. Hence, it encourages to use the temperature index approach for snowmelt runoff estimation in the Indus basin.

Zhang et al. (2007) applied the SRM model to Kaidu River basin to study the influence of the characteristics such as large basin area, sparse gauge stations, mixed

runoff supplied by snowmelt and rainfall with area receiving spatially heterogeneous precipitation, on the variables and parameters of the SRM and to discuss the corresponding determination strategy to improve the accuracy of snowmelt simulation and forecast. The results obtained from this study revealed that (1) the temperature controls the overall tendency of simulated runoff and is dominant to simulation accuracy, as the measured daily mean temperature cannot represent the average level of the same elevation in the basin and that directly inputting it to the model leads to inaccurate simulations. (2) For the conflict between the limited gauge station and remarkably spatial heterogeneity of rainfall, it is not realistic to compute rainfall for each elevation zone. After the measured rainfall is multiplied by a proper coefficient and adjusted with runoff coefficient for rainfall, the measured rainfall data can satisfy the model demands. (3) Adjusting time lag according to the variation of snowmelt and rainfall position can improve the simulation precision of the flood peak process. (4) Along with temperature, the rainfall increases but cannot be completely monitored by limited gauge stations, which results in precision deterioration.

Prasad and Roy (2005) carried out a study on the Beas basin, Western Himalayan, India to estimate snowmelt runoff for hydropower generation plans and the water management during the non-monsoon season. In this research, an attempt has been made to estimate snowmelt runoff on a 10 days average basis in Beas basin up to Pandoh dam during May, 1998 and November, 1999 using SRM, which is a degree day method. The required inputs for the SRM were derived from existing maps, satellite data, meteorological and hydrological data. The relief of the basin was divided into 12 elevation zones of 500 meter each and the temperature was extrapolated to these elevation zones using temperature lapse rate calculated using the

observed temperature at seven stations within the basin. The authors deployed Indian Remote Sensing Satellite (IRS-1C/1D Wide Field Sensor (WiFS) for generating the snow covered area of the study area which was further used for differentiating the snow covered area from snow free area for each elevation zones. They, however, derived the degree day factor from literature and runoff coefficients for snow and rain were derived using the observed data. The total discharge data at the dam site was computed by a weighted sum of runoff components from all the elevation zones and came up with an output results of 85.4% for NSE and D_v of +4.6%, so the authors concluded that is a good agreement between the observed and computed runoff.

Gómez-Landesa and Rango (2002) jointly conducted a study on “Operational snowmelt runoff forecasting in Spanish Pyrenees using the snowmelt runoff model”. Having used SRM for simulating and forecasting the daily discharge of several basin of the Spanish Pyrenees, the authors focus on using NOAA-AVHRR data for mapping the snow cover area and to develop a procedure to estimate retrospectively the accumulated snow water equivalent volume with the SRM. The snow cover in each pixel is obtained as product of a linear combination of NOAA channels 1 and 2. Real-time snowmelt forecasts are generated with the SRM using area snow cover as input variable. The authors reassure that for a basin without a historical discharge and meteorological data, the SRM provides an estimation of the daily snowmelt discharge. Here in this research, the forecasted stream flow was integrated with recession stream flow generating the total snowmelt volume which is obtained as a function of time. This function converges asymptotically to the net stored volume of water equivalent of the snowpack. Plotting this integral as a function of time, it was possible to estimate for each basin both the melted snow water equivalent (SWE) and the SWE

remaining in storage at any point in the snowmelt season. The authors state that Spanish hydropower companies use results from the SRM to improve water resource management.



CHAPTER III

DATA, TOOLS AND RESEARCH METHODOLOGY

This chapter is subdivided into following subtopics (1) Data, (2) Tools and (3) Research methodology.

3.1 Data

3.1.1 Temperature and precipitation

The meteorological data (daily temperature and precipitation) of weather stations within Upper Punatshang Chu basin are operated by Department of Hydro-met Services under the Ministry of Economic Affairs (MoEA). Meteorological data of the identified 8 weather stations (3 Class A and 5 Class C) of 22 stations in the basin, which fall within the study area, are firstly collected and examined for data preparation. Some details related to weather stations in the study site are shown in the Table 3.1

The meteorological data of 8 available weather stations were collected for year 2005-2009 and after verification of data contents of the weather stations, the meteorological data (i.e., precipitation and temperature) of Wangdue RNRRC (13640046) station situated at elevation 1,180 meters (amsl) was used as input data. Wangdue RNRRC and Thanza stations were used for calculating temperature lapse rate of the study area.

Table 3.1 List of weather stations within the study.

No	Station			Latitude	Longitude	Elevation	Observation
	Id	Station Name	Station Type				Year (Starting)
1	13670046	Punakha	A	27.5817	89.8664	1236	1990
2	13640046	Wangdue RNRRC	A	27.4867	89.9008	1180	1990
3	13760046	Gasakhatey	A	27.9000	89.7164	2760	2003
4	13550046	Nobding	C	27.5478	90.1528	2600	1996
5	13530046	Samtengang	C	27.5243	90.0000	1960	1990
6	12200046	Lingshi	C	27.8479	89.4347	4136	2004
7	12760045	Thinleygang	C	27.5058	89.8062	2210	2012
8	13700046	Yebesa	C	27.6301	89.7636	2062	2007
9	N/A	Thanza	AWS	28.0800	90.20800	4159	2002

3.1.2 Discharge

The hydrological data (daily discharge) of gauging station, Wangdue (13490045) are operated since 1991 by Department of Hydro-met Services under the Ministry of Economic Affairs (MoEA) was collected for year 2005-2009 and used for assessing the SRM model accuracy.

3.1.3 Digital elevation model (DEM)

Considering the fact that Advanced Spaceborne Thermal Emission and Reflection Radiometer (ASTER) and Shuttle Radar Topographic Mission (SRTM) provide with a global Digital Elevation Model (DEM) at different resolution are found to be useful particularly in the field of study of geomorphology, archaeology, forestry and environment, and hydrology. With this, the research work carried out by Forkuor

and Matthuis (2012) revealed that when ASTER and SRTM DEM compared with reference DEM, SRTM DEM was found to be “closer” to the reference DEM. Thus, the research concluded the SRTM DEM is more accurate than ASTER DEM. Based on the above result, the SRTM DEM for the study was downloaded from the CGIAR Consortium for Spatial Information (CGIAR-CSI) website (<http://www.cgiar-csi.org>) for this study. The collected STRM DEM is further used to generate basin characteristics.

3.1.4 MODIS snow product

The Moderate Resolution Imaging Spectrometer (MODIS) on the Terra and Aqua platforms has 36 selected, narrow spectral bands ranging in ground resolution from 250 to 1000 m. With reference to Riggs, Hall, and Salomonson (2006), MODIS Snow Products User’s guide subdivides snow product of the sensor in seven different categories in terms of spatial and temporal resolution, nominal data array dimensions and map projection (Refer Table 3.2). When compared to other satellite platforms, MODIS-derived SCA is most suitable for use in snowmelt model because of a higher spatial resolution (500 m) and location accuracy (Tekeli, Akyurek, Sorman, Sensoy, and Sorman, 2005). Although MODIS provides both daily and 8-day snow cover products, the 8-day maximum snow cover extent (MOD10A2) product was used to minimize cloud cover. Zhang, Xie, Yao, Li, and Duan (2014) and Li and Williams (2008) concluded that composite MOD10A2 and MYD10A2 products present lower cloud coverage and higher snow percentage compared to the daily products of MOD10A1 and MYD10A1.

An algorithm, NDSI has been developed to map SCA by Hall, Riggs and Salomonson (2001), and Hall, Riggs, Salomonson, DiGirolamo, and Bayr (2002) using these particular products and moreover, the products demonstrated the capability to detect and discriminate snow from clouds (Tekeli et al., 2005).

Results of the snow algorithm, NDSI, are stored as coded integers in the snow cover scientific data sets (data arrays) of the Hierarchical Data Format- Earth Observation System (HDF-EOS) product file. The snow algorithm identifies pixel as being snow, snow-covered lake ice, cloud, land, water, or other condition. The condition identified by the algorithm is listed in Table 3.3.

From the listed snow products, MODIS Terra, MOD10A2 and Aqua, MYD10A2 with spatial and temporal resolution of 500 m and 8-day respectively which can be freely downloaded from National Aeronautics and Space Administration (NASA) website (<http://reverb.echo.nasa.gov/reverb>) is deployed for calculating zonal SCA. In this study, 225 scenes of MOD10A2 and 225 scenes of MYD10A2 were downloaded. Figure 3.1 displayed an example of MOD10A2 and MYD10A2 snow products.

Table 3.2 Summary of the MODIS snow products.

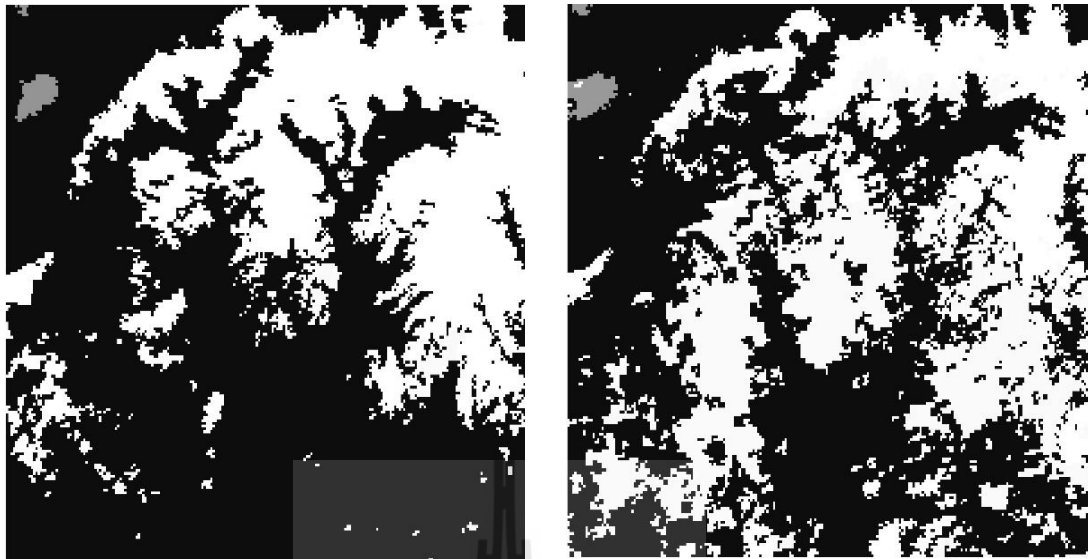
Earth Science Data	Product Level	Nominal Data Array Dimensions	Spatial Resolution	Temporal Resolution	Map Projection
MOD10_L2	L2	1354 km by 2000 km	500m	swath (scene)	None.
MOD10L2G	L2G	1200km by 1200km	500m	day of multiple coincident swaths	Sinusoidal
MOD10A1	L3	1200km by 1200km	500m	day	Sinusoidal
MYD10A1	L3	1200km by 1200km	500m	day	Sinusoidal
MOD10A2	L3	1200km by 1200km	500m	eight days	Sinusoidal
MYD10A2	L3	1200km by 1200km	500m	eight days	Sinusoidal
MOD10C1	L3	360° by 180° (global)	0.05° by 0.05°	day	Geographic
MOD10C2	L3	360° by 180° (global)	0.05° by 0.05°	eight days	Geographic
MOD10CM	L3	360° by 180° (global)	0.05° by 0.05°	month	Geographic

Source: Riggs et al. (2006).

Table 3.3 Interpretation key for MODIS Snow Product.

Integer/ Pixel Value	Meaning
0	Missing data
1	No decision
11	Night / Darkness
25	Land -- no snow detected
37	Lake/ Inland Water
39	Ocean
50	Cloud Obscured
100	Lake Ice
200	Snow
254	Detector Saturated
255	Fill Data -- No data expected for pixel

Source: Riggs et al. (2006).



(a) MOD10A2

(b) MYD10A2

Figure 3.1 Example of MOD10A2 and MYD10A2 snow products.

3.2 Tools

3.2.1 WinSRM model

The WinSRM model is a conceptual, degree day, hydrologic model that can be used to simulate daily runoff, and to forecast snowmelt and rainfall in mountainous region. This model has proved to be valuable for use in Himalayan regions where meteorological and gauging field networks are sparse (Immerzeel, Droogers, de Jong and Bierkens, 2010). So, this model is used for studying the snowmelt runoff and impact of changing temperature on the snow cover area.

3.2.2 ERDAS imagine

ESRI ArcMap is the main component ArcGIS geospatial processing programs of Environmental Systems Research Institute (ESRI) and is used primarily to view, edit, create, and analyze geospatial data. ArcMap allows the user to explore

data within a data set, symbolize features accordingly, and create maps. For the study, hydrology toolbox and model builder module was used.

3.2.3 MODIS Reprojection Tools (MRT)

MRT enables users to read data files in HDF-EOS format (MODIS Level-2G, Level-3, and Level-4 land data products), specify a geographic subset or specific science data sets as input to processing, perform geographic transformation to a different coordinate system/cartographic projection, and write the output to file formats other than HDF-EOS. See more at: https://lpdaac.usgs.gov/tools/modis_reprojection_tool#sthash.4u7e42hg.dpuf.

3.2.4 MODIS Snow tools

MODIS Snow Tool has been developed in MENRIS, ICIMOD in order to facilitate processing and analysis of daily and 8-day standard MODIS snow products (MOD10A1, MOD10A2, MYD10A1 and MYD10A2). It is designed to be able to handle a large amount files. The core program is written in C language and the Graphic User Interface (GUI) is written in Visual C#. The core program is developed as an individual standalone executable program and it supports the batch processing. The programs uses the GDAL (Geospatial Data Abstraction Library), JPEG library, GeoTiff library and Dr. Honda image processing library which are distributed as General Public License version > 2.0. The current version of MODIS Snow Tool includes only image processing module, no visualization module is integrated at the moment. The release version is 1.0 Beta version. MODIS Reprojection Tool can be used to mosaic and reproject standard MODIS level 3 products.

3.2.5 MATLAB

MATLAB is a high-level language and interactive environment for numerical computation, visualization, and programming. MATLAB can be used to analyze data, develop algorithms, and create models and applications. The language, tools, and built-in math functions enable to explore multiple approaches and reach a solution faster than with spreadsheets or traditional programming languages, such as C/C++ or Java. This software was used to interpolate the snow cover area of missing day between two consecutive 8-day snow products. For this purpose, the Piecewise Cubic Hermite Interpolation technique (Li and Williams, 2008) was used.

3.3 Research methodology

The chronological flow of research methodology is schematically displayed in Figure 3.2 representing three main components: (1) input data preparation, (2) Runoff simulation during snowmelt period by SRM model, and (3) Impact of temperature change on streamflow. Detail of each component is separately described in the following section.

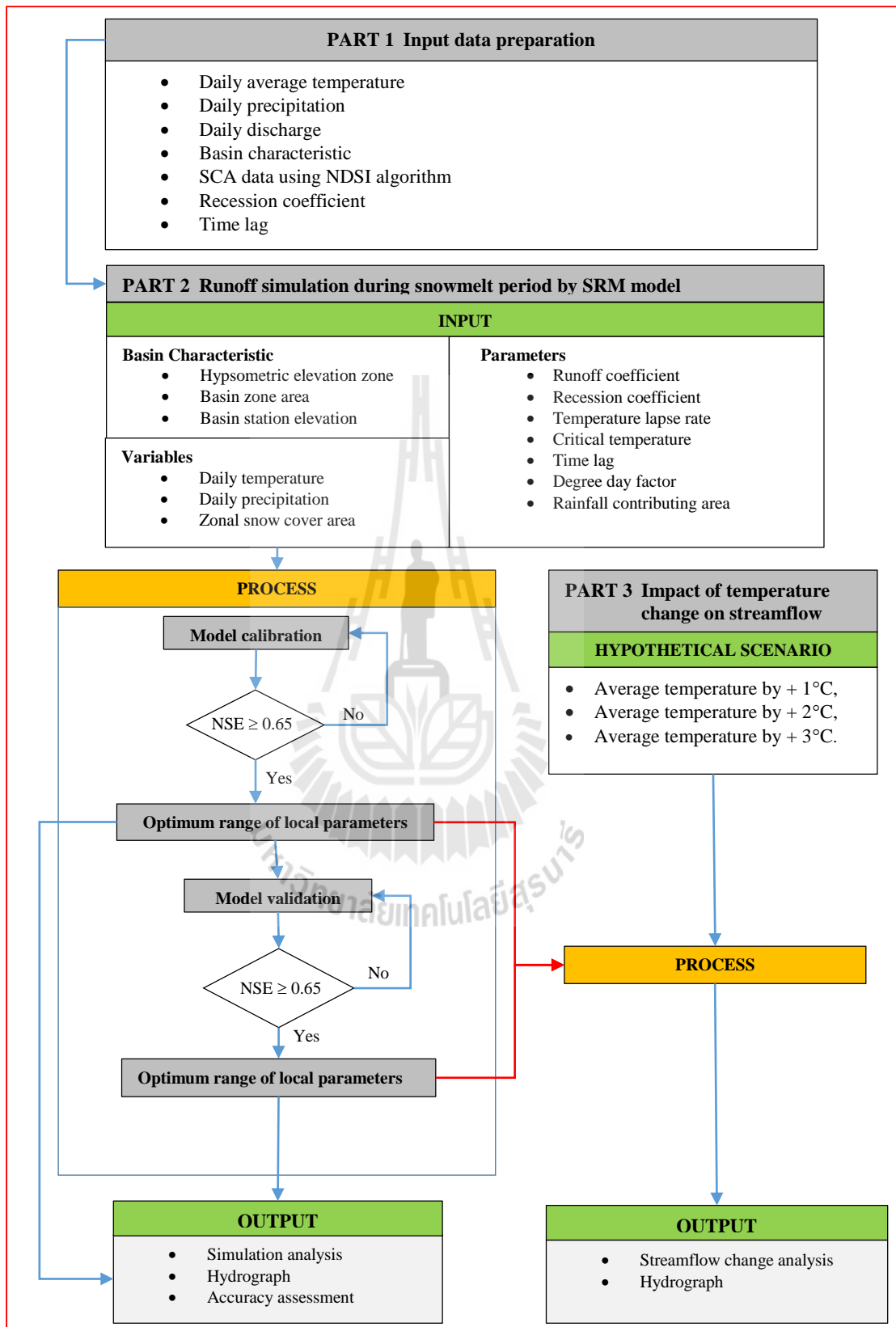


Figure 3.2 Workflow diagram of research methodology.

3.3.1 Input data preparation

3.3.1.1 Hydro-meteorological data

The hydro-meteorological data (daily temperature, precipitation and discharge) which are recorded manually and supplied in raw format were converted to time series format using MS Excel for executing the model. Daily average temperature is derived using observed maximum and minimum temperature reading.

3.3.1.2 Basin characteristics

With help of Hydrology Tools in the ESRI ArcMap software, the downloaded DEM is processed by applying certain tools such as fill to correct some errors of DEM and flow direction, flow accumulation, and snap pour point to extract watershed boundary. Following paragraph briefly explain working principal of above stated tools:

a. Fill tool

Due to the resolution of data or rounding of elevation to the nearest integer value often cause errors such as sinks and peaks in the data. All these errors (sinks and peaks) should be corrected to ensure proper delineation of basins and streams. In case if these errors are left uncorrected, then a derived drainage network may be discontinuous. The tool corrects these errors by iterating until sinks within the specified z limit are filled. In similar fashion, the tool can be used to eliminate the peak error caused by spurious cells with elevation greater than would be expected given the trend of the surrounding surface (ESRI, 2015) (Figure 3.3 and 3.4).

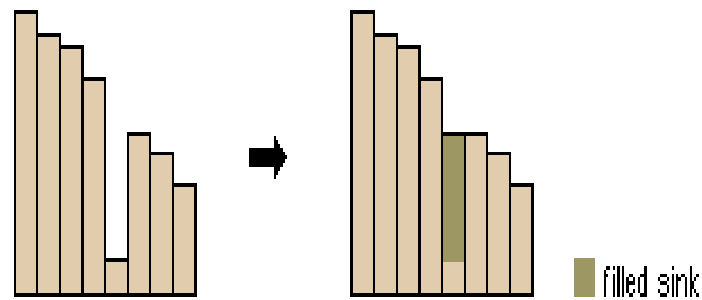


Figure 3.3 Profile view of a sink before and after running fill.

Source: ESRI (2015).

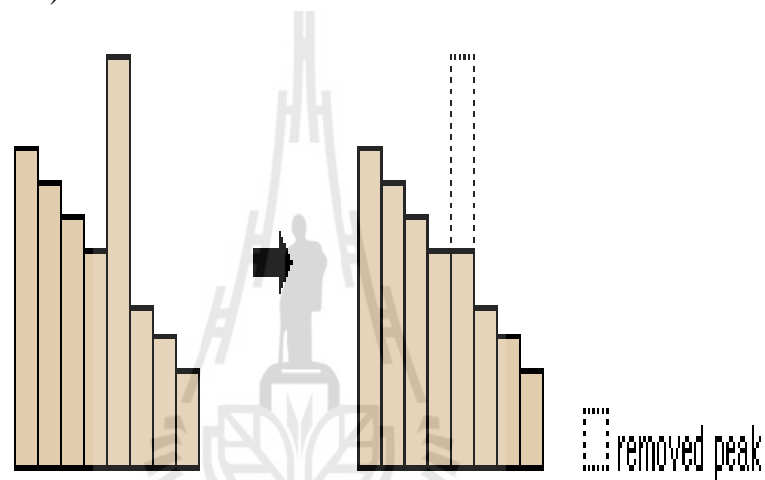


Figure 3.4 Profile view of a peak before and after running fill.

Source: ESRI (2015).

b. Flow Direction

Flow Direction is one of the tools of hydrology in ArcGIS software with ability determine the direction of the flow from every cell in the raster. This tool takes input a surface and outputs a raster showing the direction of flow out of each cell. For determining the direction of the flow, the tool takes up eight valid output directions relating to the eight adjacent cells into which flow could travel (Figure 3.5). This approach is commonly referred to as an eight-direction (D8) flow model (ESRI, 2015).

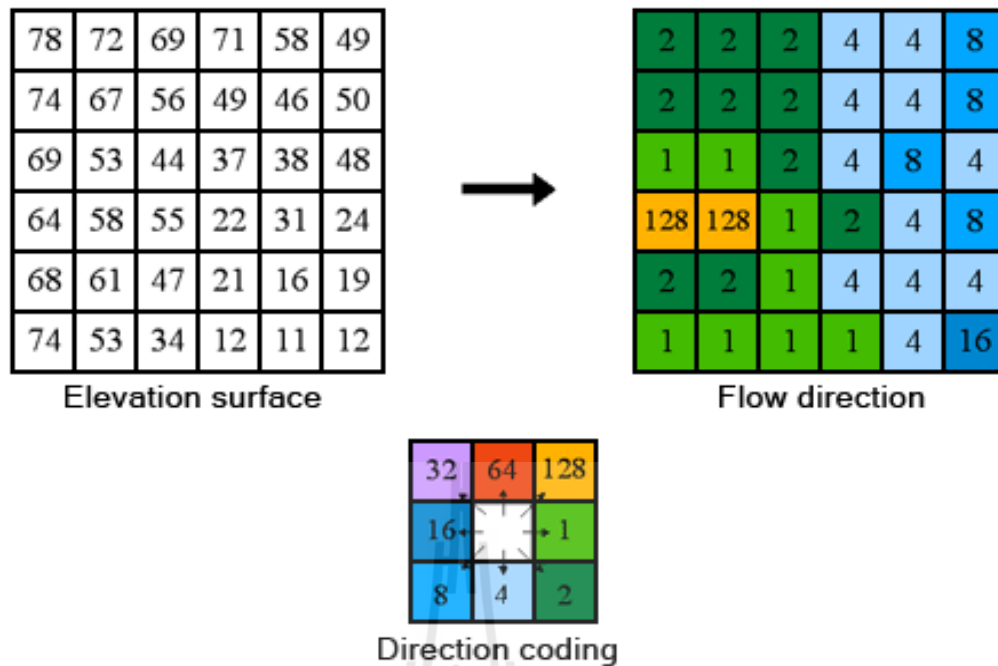


Figure 3.5 The coding of the direction of flow.

Source: ESRI (2015).

c. Flow Accumulation

This tool calculates accumulated weight of all cells flowing into each downslope cell in the output raster. If no weight is provided, a weight of 1 is applied to each cell, and the value of cells in the output raster is the number of cells that flow into each cell. Here, this tool uses the input as the output map of the flow direction operation. The output map of this operation contains cumulative hydrologic flow values that represent the number of input pixels which contribute any water to any outlets; the outlets of the largest streams, rivers etc. will have the largest values (ESRI, 2015). (See Figure 3.6).

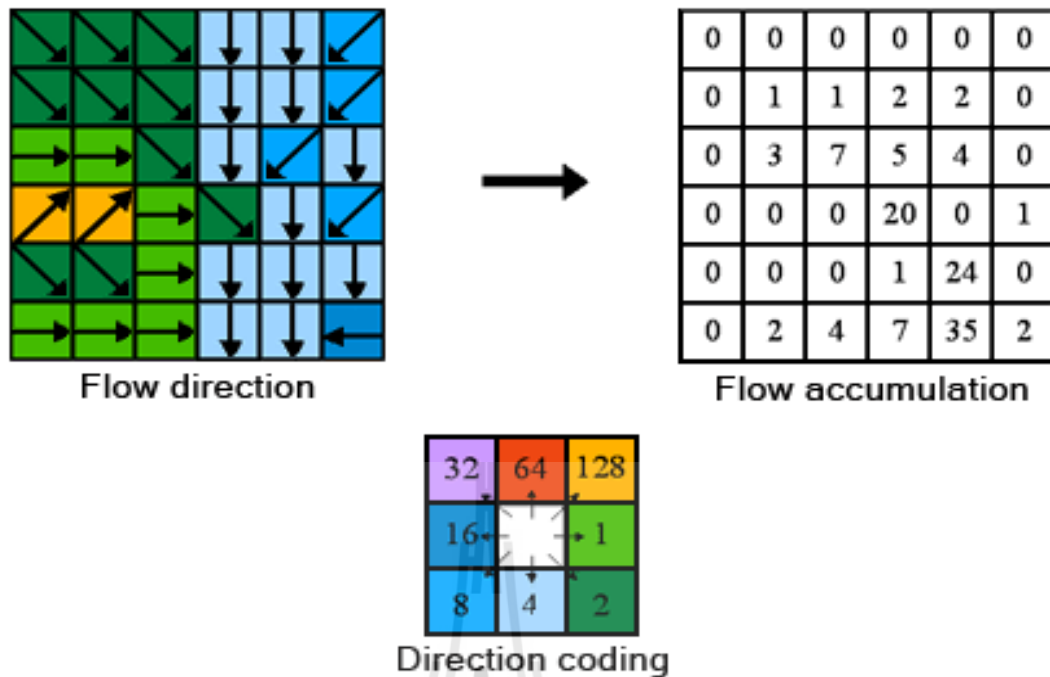


Figure 3.6 Determining the accumulation flow.

Source: ESRI (2015).

d. Snap pour point

The proposed watershed boundary should be delineated from the point where the discharge gauging station is located, the snap pour point tool can be used for this purpose. Usually, snap pour point tool snaps the discharge points to the cell of the highest flow accumulation within a specified distance.

After extracting basin boundary by applying the DEM-processing hydrologic tools, the basin boundary is subdivided into different elevation zones using Reclassify tool in ESRI ArcMap and the area of each zone is calculated based on the resolution of DEM and pixel counts. Herein, a curve is plotted between the cumulative zone area and elevation range, and the zonal mean hypsometric

elevation, \bar{h} , is calculated from the curve by balancing the areas above and below the mean elevation.

3.3.1.3 Snow cover area (SCA) extraction

The MODIS products obtained for the study area in a HDF format are re-projected to UTM, Zone 45 N projection with reference datum WGS1984 and converted from HDF to *.tiff format using MRT tool software.

According to Gurung, Giriraj, Aung and Shretha, (2011) cloud cover is a major issue in summer to map snow cover due to continuous overcast conditions. To overcome cloud cover to certain degree of extent, cloud filtering approach proposed by Gafurove and Bardossy (2009) is applied in MODIS snow tool. In accordance to the proposed approach, the time lag in the overpass timing of Terra and Aqua allows to reclassify cloud pixel in one of the products with information from the corresponding pixel from the other product. This is done by combining Terra and Aqua snow products as explained in Equation 3.1 below:

$$S(x, y, t) = \max(SA(x, y, t), ST(x, y, t)) \quad (3.1)$$

where y is the index for row (vertical), x the index for column (horizontal), t the index for day (temporal) of pixel S , and SA and ST are the Aqua and Terra pixels respectively.

Gurung et al. (2011) confirmed that the algorithm had removed approximately 40% of the cloud in case of the Hindu Kush Himalaya (HKH) region which comprises mainly of mountain areas (from the Hindu Kush range in the west through Karakoram to the Eastern Himalayan range in the east) from eight countries (Afghanistan, Bangladesh, Bhutan, China, India, Myanmar, Nepal, and Pakistan). After combining Terra and Aqua data of 8 days, if any pixel is identified as a cloud,

then the temporal filter is applied to identify the land feature below the cloud. Initially the same class as give in backward 8-day product is used and subsequently, if the pixel is still identified as cloud, then forward 8-day product is used. The pixels identified as cloud in all three sets of 8-day products are retained as cloud. The relationship is explained in Equation 3.2:

$$S(x, y, t) = 1 \text{ if } S(s, y, t - 8) = 1 \text{ or } S(x, y, t + 8) = 1 \quad (3.2)$$

where $t - 8$, t and $t + 8$ are three consecutive sets of 8-day products; 1 corresponds to snow cover, and 0 land cover.

The spatial filtering is applied selectively only to the cloud pixel and missing data, whereas the other original data are maintained. After applying temporal filters, a large area is found under cloud cover and majority of these cloud pixels are observed during the monsoon season. To remove cloud spatial filter is used with 7 x 7 filter window, which has proved optimal in removing clouds pixels. In the spatial filter, majority of a valid class (but not the cloud class) within 7 x 7 window is used to replace the cloud or missing data pixel, but not the snow/land pixel.

The spatial filtering mostly removes some cloud pixels surrounded by land/snow and some cloud pixels at the edge of the big cloud area. Spatial filter removed additional 5% of the cloud pixels (Gurung et al., 2011). (Refer Figure 3.7)

The output obtained after applying cloud removal algorithm is further used as input to Model Builder module to extract snow cover pixel by creating semi-automate model.

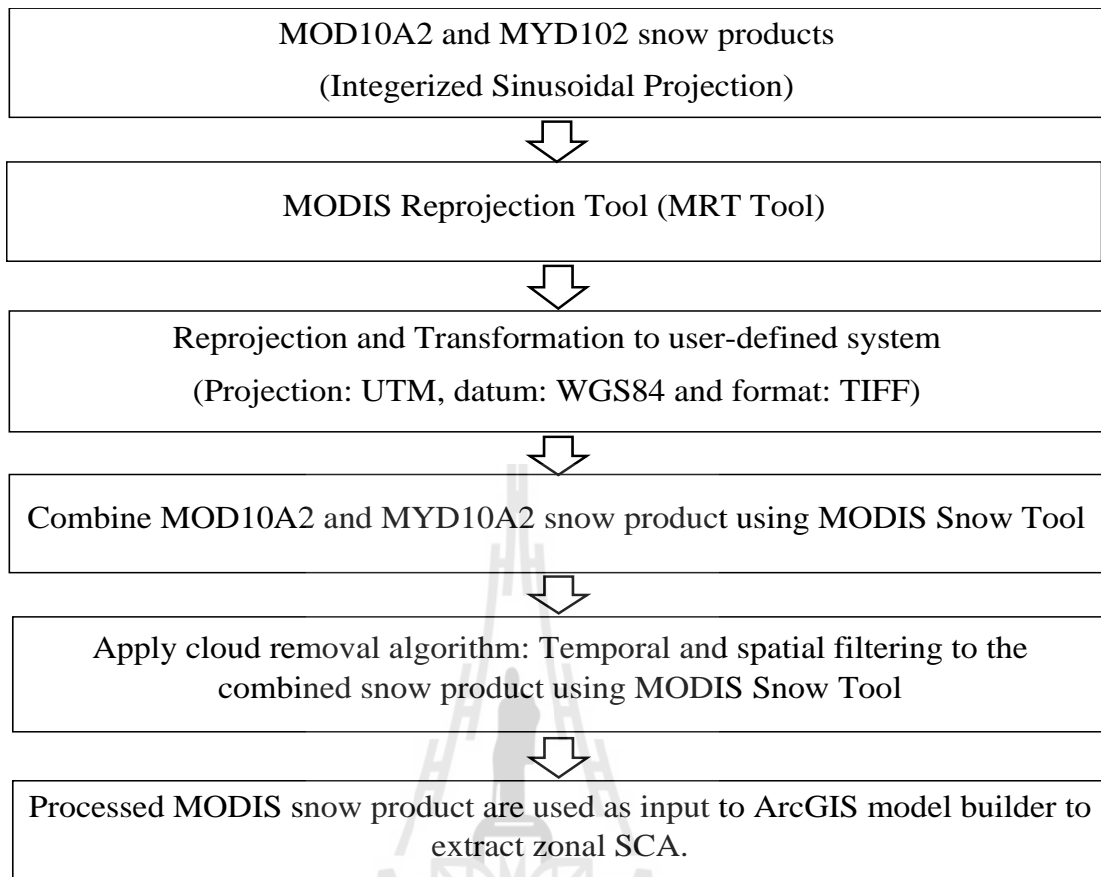


Figure 3.7 Steps involved in combining the MODIS snow product and applying cloud removal algorithm.

3.3.1.4 Initial input parameters

To execute the SRM model, daily temperature, precipitation and SCA are required. Beside these inputs, SRM requires parameters that must be estimated from the meteorological and stream flow records. The model is initialized using the parameters that are reviewed from the literature reviews. Snow cover modeling at Punatshang Chu basin in Bhutan with corrected JRA-25 temperature by Duran Ballen et al. (2012) confirmed the γ of $0.65^{\circ}\text{C}/100\text{ m}$. However, a lapse rate of $0.57^{\circ}\text{C}/100\text{ m}$, calculated using the temperature of Wangdue RNRRC and Thanza

weather stations, was used for extrapolating temperature to each mean hypsometric elevation of zones.

According to literature reviews, the T_{CRIT} of precipitation, the temperature of the surrounding environment is crucial to differentiate whether the precipitation is snow or rain. The T_{CRIT} value varies from basin to basin and the value is slightly above the freezing point (Ma and Cheng, 2003). USACE (1956) reported that the T_{CRIT} ranges between $+1.5^{\circ}\text{C}$ to 0°C . A recent study by Dai (2008) concluded that global synoptic observations estimated that the half point of snow versus rain over the global land surface is 1.2°C . Further, the RCA (rainfall contributing area) for the melt period is set to 1 as rainfall directly contributes to runoff.

Runoff coefficient for rain (C_R) and snow (C_S) is an important parameter in SRM which takes consideration of water losses caused by natural phenomenon such as evapotranspiration and infiltration. The coefficient value varies between 0.1 to more than 0.9 depending upon the size and shape of the watershed (USDA NRCS, 2004).

From the reviewed literature on the degree day factor by Tahir, Chevallier, Arnaud, Neppel, and Ahmand (2011), Hock (2003) and Zhang, Liu and Ding (2006), they clearly mentioned about the degree day factor value calculated in their research ranges from $0.4\text{-}0.5 \text{ cm }^{\circ}\text{C}^{-1}\text{d}^{-1}$ and $0.57\text{-}0.74 \text{ cm }^{\circ}\text{C}^{-1}\text{d}^{-1}$ for snow and ice, respectively, and they concluded that most region above 5,000 m (amsl) are glacier covered. Pandey, Williams, Frey, and Brown (2013) have used $0.3\text{-}0.6 \text{ cm }^{\circ}\text{C}^{-1}\text{d}^{-1}$ for the elevation zone 533 to 4,000 m and $0.5\text{-}0.9 \text{ cm }^{\circ}\text{C}^{-1}\text{d}^{-1}$ for 4,000-5,000 m altitude zone of Tamor river basin, Nepal. Butt and Bilal (2011) used a α as low as $0.2 \text{ cm }^{\circ}\text{C}^{-1}\text{d}^{-1}$ in Upper Indus Basin, Pakistan and Zhang et al. (2014) applied a α

0.3 cm °C⁻¹d⁻¹ in Lake Qinghai, China. And the recent research of Tiwari, Kar and Bhatla (2015) on α value for Himalayan region computed α value range from 0.4-2.4 cm °C⁻¹d⁻¹. Based on the above range, in this study a α factor applied for the simulation range can be varied from 0.2-2.4 cm °C⁻¹d⁻¹.

According to Martinec and Rango (1986), during the WMO intercomparison test of different snowmelt runoff models concluded that there is relation between time lag and basin size. Following are the few observed relation of time lag and basin size:

Basin W-3 (8.42 km²): 3.0 h

Dischma (43.3 km²): 2.0 h

Dunajec (680 km²): 10.5 h

Durance (2,170 km²): 12.4 h

Based on the observed data of WMO test, the following graph was plotted: time lag vs. basin size. Solving the trend equation using the area of Upper Punatshang Chu basin, the L of the study area are 11 h, 12 h and 13 h for zone A, B and C respectively as a result in Figure 3.8.

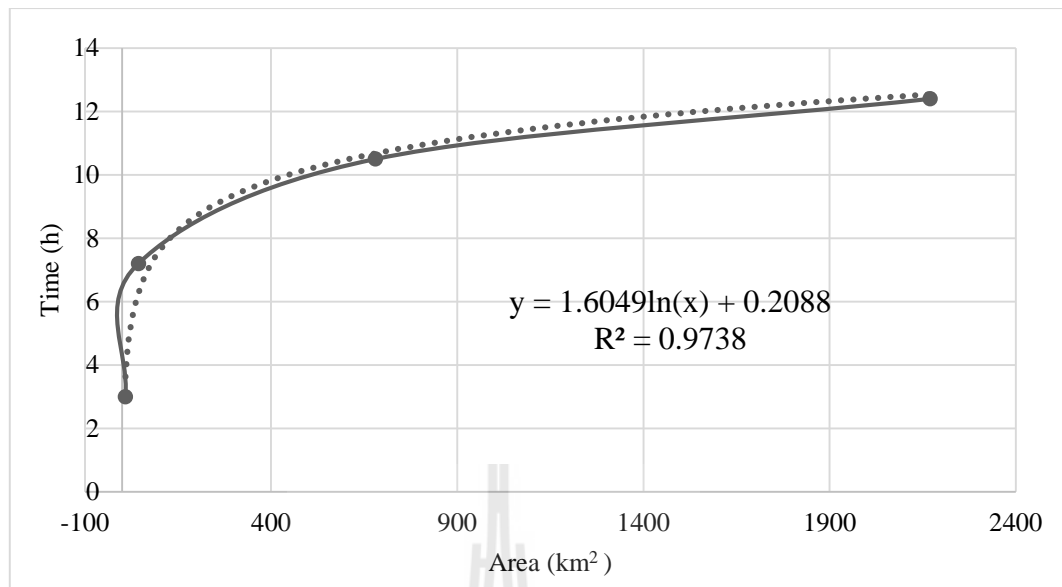


Figure 3.8 Time lag graph of Upper Punatshang Chu Basin.

Recession coefficient (k) is determined by analyzing the historical discharge data and calculated using Equation 2.10 for individual year. In accordance to Martinec, Rango and Major (1983), for k value determination, daily discharge value for the snowmelt season or the whole year are used. The discharge on a given day, Q_n , is always plotted against the value on the following day, Q_{n+1} , as illustrated in earlier Figure 2.8. In this figure, any points above the 1:1 line refer to the rise of the hydrograph and the points below the line to the fall of the hydrograph.

For purpose of SRM model and derivation of the recession equation, only points (excluding $Q_{n+1} > Q_n$) below the 1: 1 line need to be plotted. After having plotted all those points, an envelope line is drawn to enclose most of the points. The lower envelope line represents the extreme discharge decline, i.e., the recession without any partial delay by possible precipitation or snowmelt. This lower envelope line has been found to be valid on small size basins. When the model is applied to large basins, however, it is recommended that the lower envelope line be replaced

with an average line halfway between the lower envelope line and the 1:1 line. The average line should probably be used on basins greater than about 50 sq.km.

3.3.2 Runoff simulation during snowmelt period by SRM model

The working principle of the SRM model is that the model sums up all the discharge from different zones contributed by runoff from the snowmelt and rain, and then superimposed it to calculate recession flow to get the overall flow from the whole basin (Refer Equation 2.2). To elaborate more, during the SRM simulation, degree day factor and zonal degree days are used to determine the snowmelt from the prior day (day n). This results is multiplied with the area of the zone and C_s to determine the percentage of snowmelt that contributes to the river discharge. Likewise, to determine the percent of precipitation to runoff, the results was multiplied with C_R and zonal area.

3.3.2.1 Model Calibration

Ferguson (1999) clearly stated that the SRM model is not regarded as calibration model according to the developers, rather users are urged to use physically based default values for its relatively small number of parameters, apart from the recession constants x and y which must be estimated from discharge data when applying the model to a new basin.

For model calibration, initial parameters sets available in the SRM literature are tested with multiple variables and parameters configuration by trial and error to understand the relationship between inputs and their simulated hydrographs. Basically, the initial parameters can be applied either by zone or basin wide and can be adjusted at a daily or period time step.

The C_S , C_R and α are adjusted during the model calibration and varied seasonally. As stated in an earlier section, the permissible range of value for parameters adjustment during the calibration mode should be strictly monitored. Taking those values obtained from literature and some derived from the historical data into account, the model is iteratively calibrated by accessing NSE value with the range defined by Kult et al. (2014), for the calibration year (2005 and 2006) to obtain the optimum range of local parameters.

When running the model in simulation mode, if a good agreement is not initially achieved, the recommended checklist to solve the problem according to the Martinec et al., 1983 are as follows:

1. Re-evaluate the snow cover depletion curves to check the errors were not made in the drawing the curves. However, this problem is tackled after the launch of Terra and Aqua satellites.
2. Reconsider the lapse rate used in the basin. Often times an average lapse rate may be too high or too low for a particular month resulting in the number of degree days too high or too low. For this study simulation, the locally calculated lapse rate, i.e., $0.57\text{ }^\circ\text{C}/100\text{ m}$ is used.
3. The runoff coefficient may require adjustment if the computed discharge is too high or too low. Typically, the runoff coefficient is the most difficult of the basin parameters to estimate accurately and should be examined closely after any gross errors due to discrepancies in snow cover and lapse rate have been ruled out.
4. The degree day factor should be investigated after the runoff coefficient. Since the degree day factor can be estimated initially from snow density

measurements, less probability of error may be expected. If, however, good snow density values are not available, adjustment of the degree day factor may be necessary to have some effect on the runoff volume. Usually high wind conditions may also result in the end to temporarily increase the degree day factor, where new snow falling on the season snowpack may cause a temporary in the degree day factor.

5. The recession coefficient should be revised if the model reacts too quickly or too slowly in comparison with the actual hydrograph.

3.3.2.2 Model validation

The derived optimum range of parameters value of calibration year is further used to validate model by estimating runoff during snowmelt period for year 2007, 2008 and 2009 by accessing the accuracy using NSE. During the validation process, there is a constant need of changing the parameters value due to change in the average temperature and snow covered areas of validation years.

3.3.2.3 Data output

Main derived output products from data processing under SRM model using the range of optimum parameters are estimated runoff from snowmelt during snow melting period from calibration and validate periods with accuracy assessment statistics.

3.3.3 Impact of temperature change on stream flow

Other than simulating the snowmelt contribution to river discharge from all hydrological years, the impact of temperature change on the streamflow are investigated using three different hypothetical scenarios: (1) average temperature +1°C (2) average temperature +2°C and (3) average temperature +3°C for calibration

and validation periods. This impact was investigated by maintaining all derived parameters and variables constants, except the average temperature.

The output achieved from the investigation are effect of hypothetical scenarios on the average streamflow.



CHAPTER IV

RESULTS AND DISCUSSIONS

Two main results according to specific objectives include (1) snowmelt runoff simulation and (2) assessment of impact of temperature change on stream flow are here presented and discussed in following sections.

4.1 Snowmelt runoff simulation

The key results and findings of snowmelt runoff simulation that is to estimate runoff from the snow during snowmelt period are separately described as following.

4.1.1 Basin characteristics, variables and parameters for SRM model

Prior to the execution of the model, the required data for generating basin characteristics are collected and processed. Similarly the variables data are collected from the concerned agency and organized in a prescribed format of SRM model. Parameter values are based on the literature reviews and some are derived from historical data with generic equations. The following sub sections address briefly on these matters.

4.1.1.1 Basin characteristics.

Basin boundary was extracted using DEM and hydrology tools in ESRI ArcMap, and it was subdivided into three different hypsometric elevation zones:

A: 1,180 -2,500 m, B: 2,501-4,000 m and C: 4,001-7,087 m using reclassify tool (Figure 4.1). The detail of hypsometric elevation zone of Upper Punatshang Chu Basin is summarized in Table 4.1 and the hypsometric curve which was plotted based on the facts as shown in Table 4.1 is presented in Figure 4.2. The individual zone area and its mean hypsometric elevation are the basic basin characteristics used for setting up the model with zone wise approach.

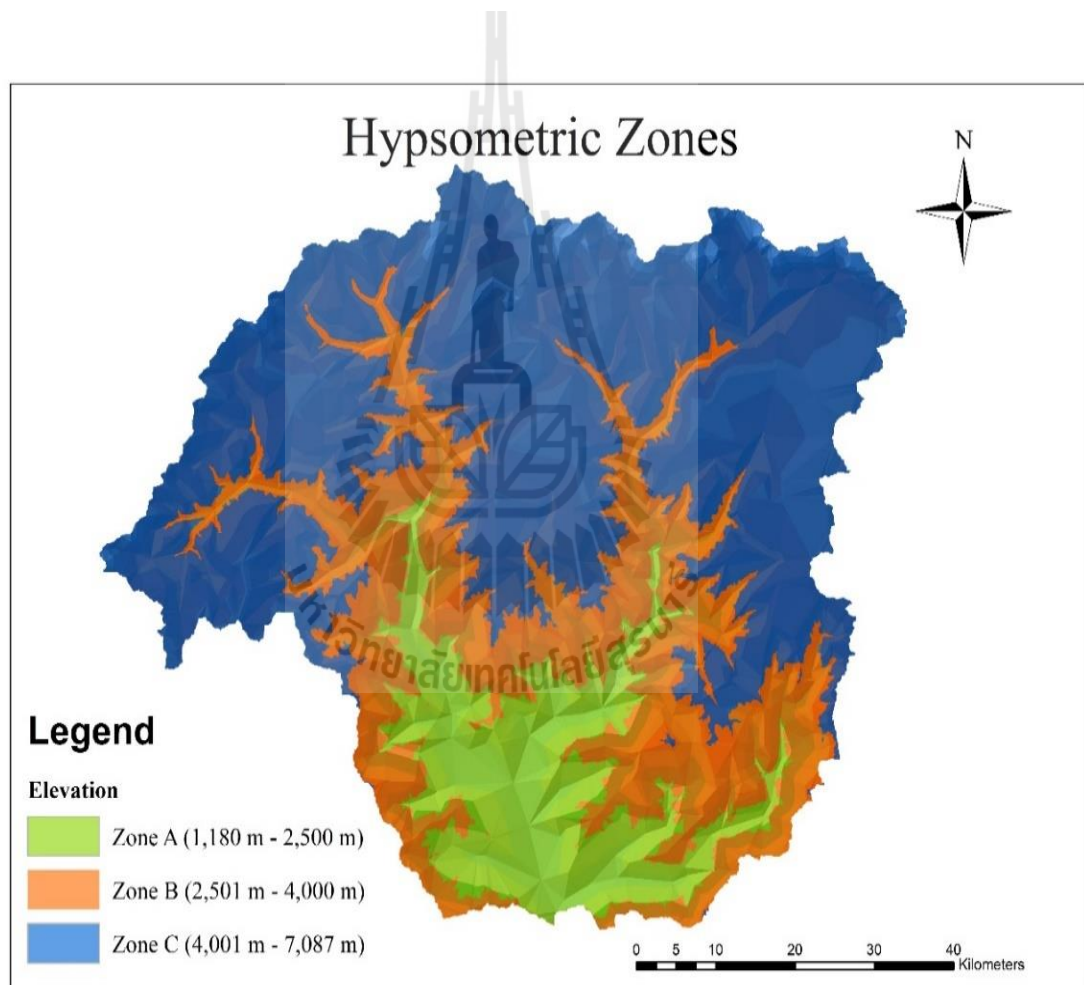


Figure 4.1 Hypsometric elevation zones of Upper Punatshang Chu Basin, Bhutan.

Table 4.1 Summary of the hypsometric elevation zones of Upper Punatshang Chu basin.

Zone	Elevation	Area	Mean Hypsometric	
	interval (m)	(km ²)	%	Elevation (m)
A	1,180-2,500	839.96	14.92	2,019
B	2,501-4,000	1,624.54	28.58	3,278
C	4,001-7,087	3,199.92	56.50	4,678
Total		5,664.42	100.00	

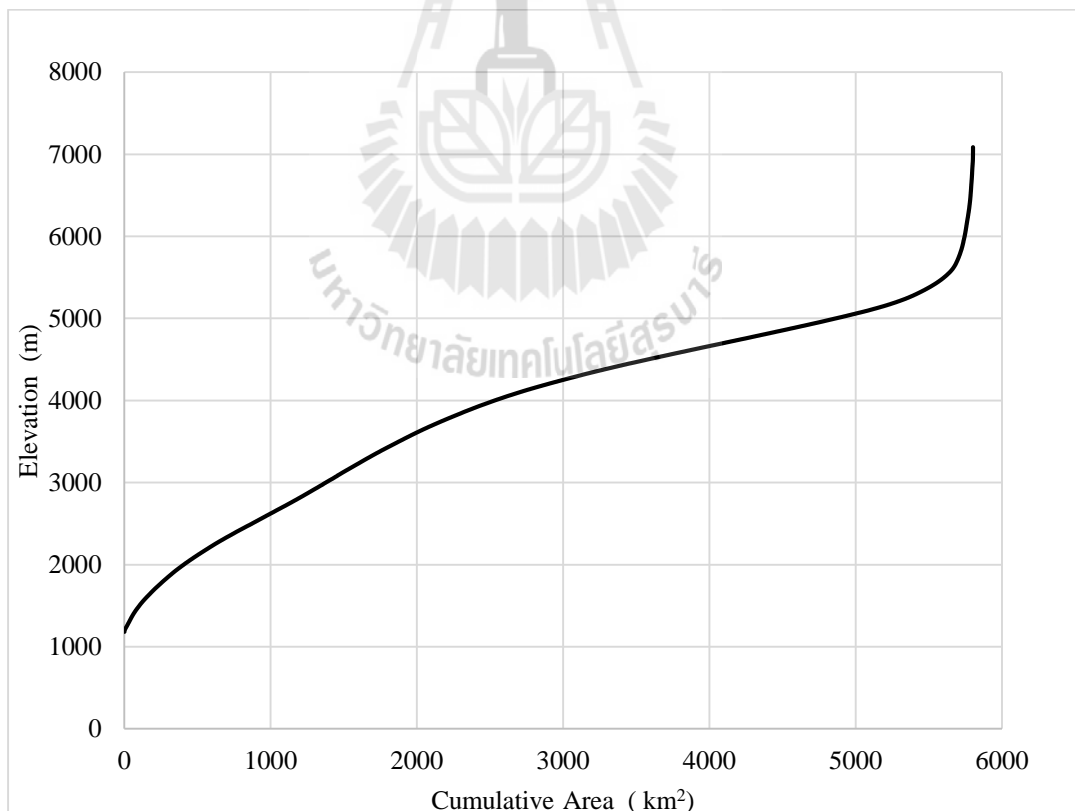


Figure 4.2 Hypsometric curve of Upper Punatshang Chu basin.

4.1.1.2 Temperature and precipitation

Historical data of daily temperature and precipitation observed at Wangdue RNRRC station during snowmelt period (April-August) between 2005 and 2009 were collected and analyzed by averaging daily temperature based on its minimum and maximum values under MS Excel as shown in Figure 4.3 to Figure 4.7.

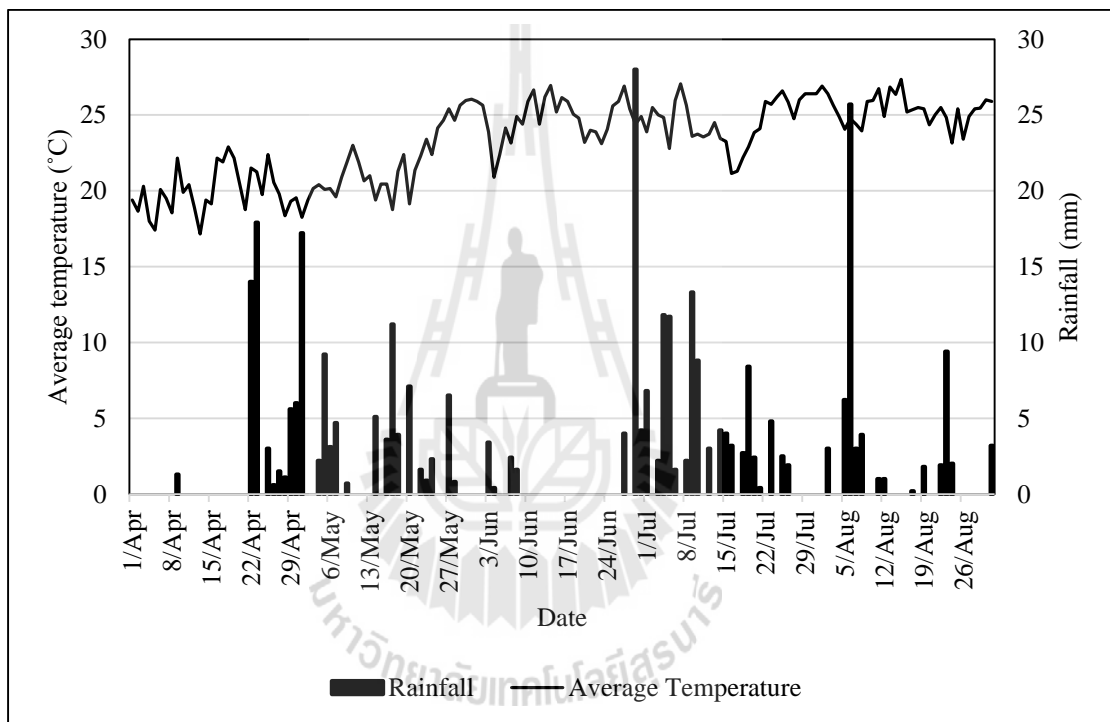


Figure 4.3 Average temperature and rainfall data at Wangdue RNRRC, 2005.

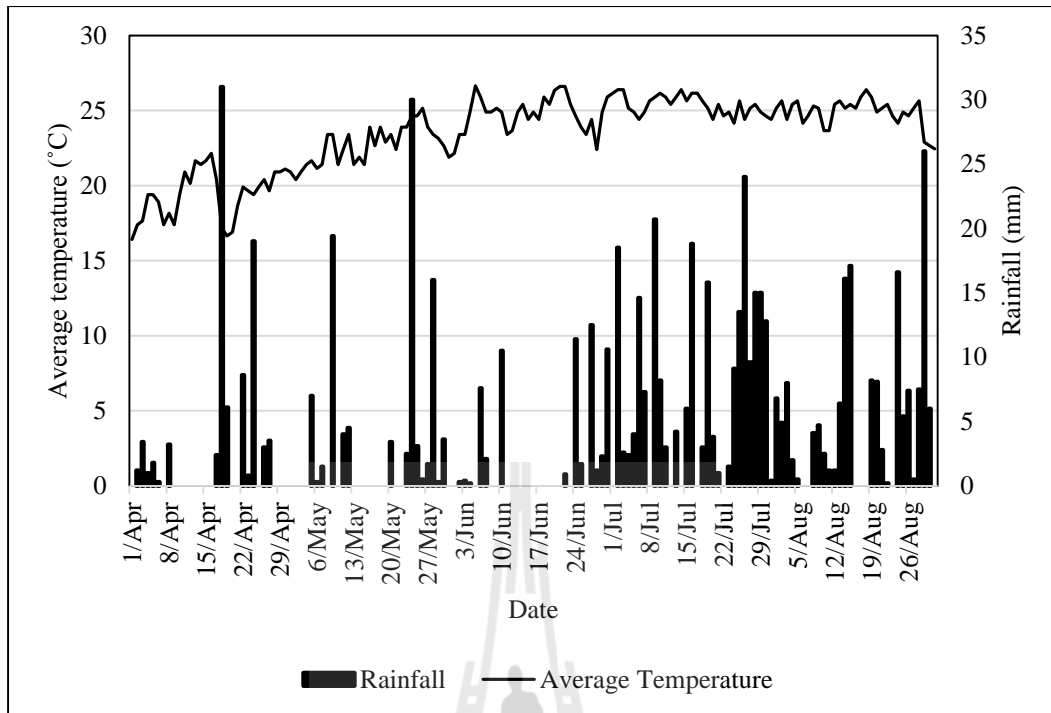


Figure 4.4 Average temperature and rainfall data at Wangdue RNRRC, 2006.

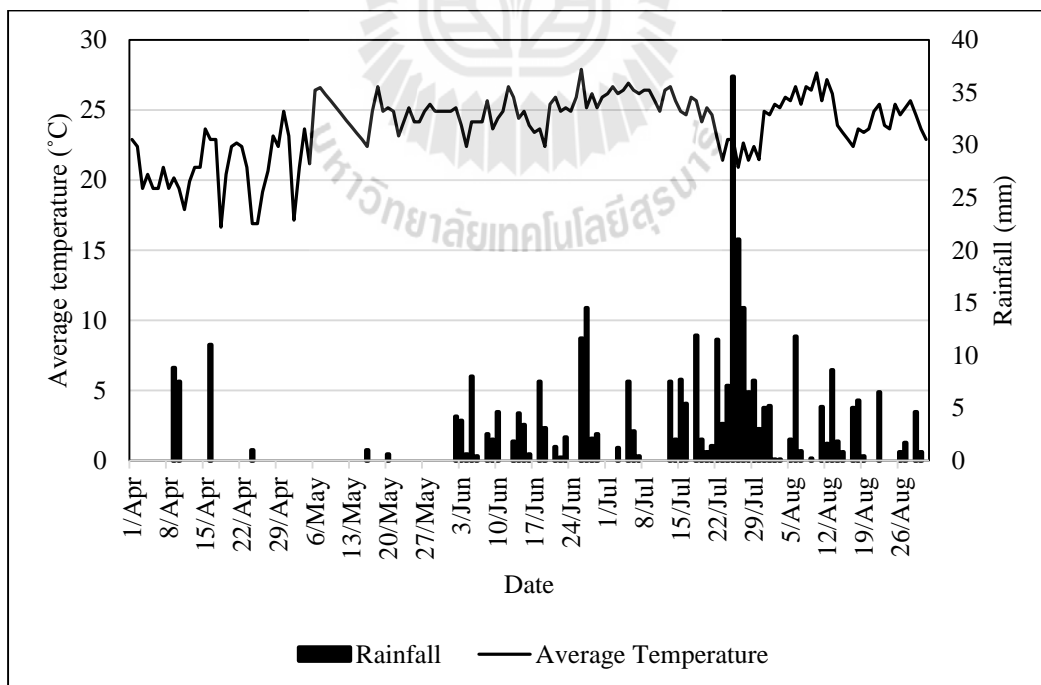


Figure 4.5 Average temperature and rainfall data at Wangdue RNRRC, 2007.

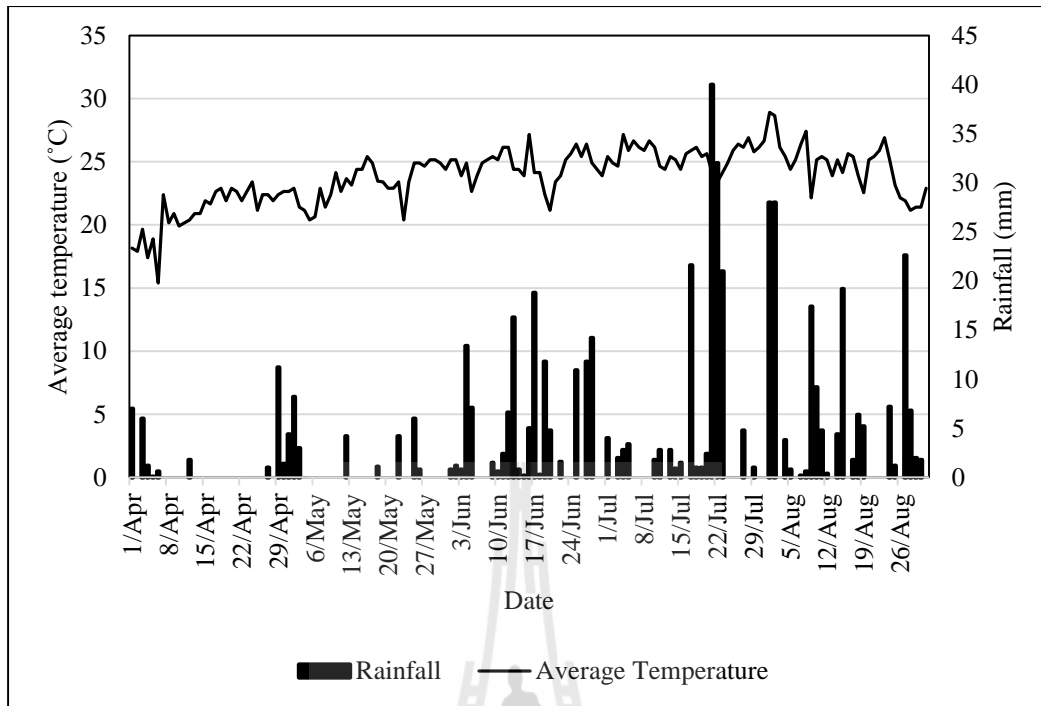


Figure 4.6 Average temperature and rainfall data at Wangdue RNRRC, 2008.

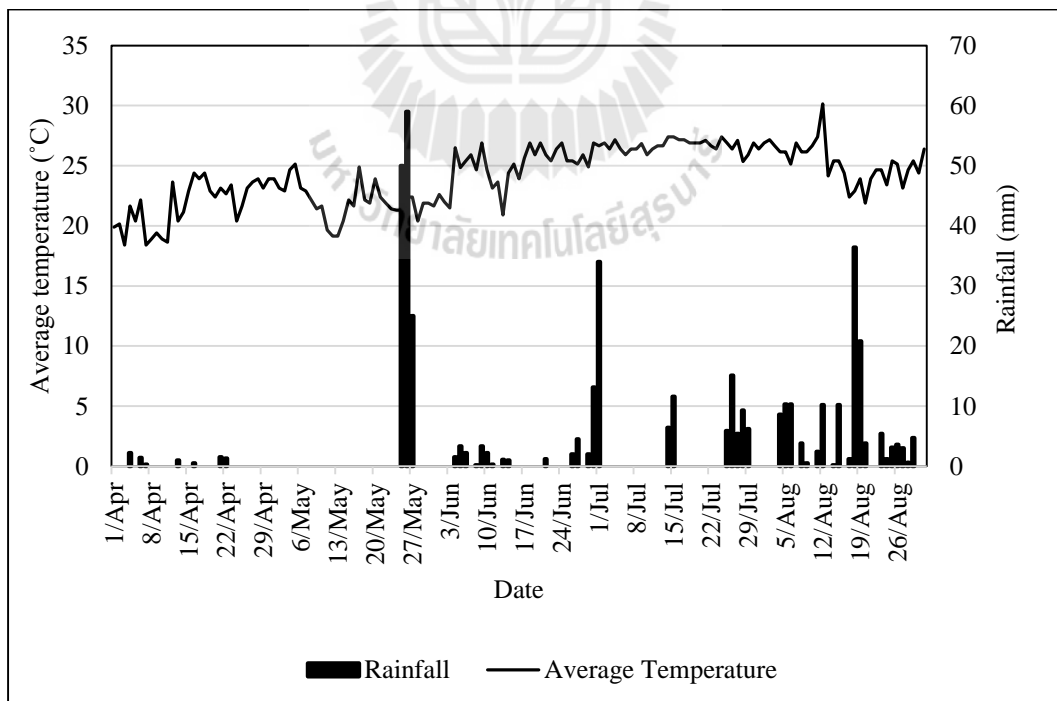


Figure 4.7 Average temperature and rainfall data at Wangdue RNRRC, 2009.

Average rainfall measurements for the snowmelt season recorded at Wangdue RNRRC station are 0.22, 0.42, 0.23, 0.33 and 0.27 cm for hydrological year 2005, 2006, 2007, 2008 and 2009, respectively. Herewith, hydrological year 2005 is relatively dry year with average rainfall of 0.22 cm and hydrological year 2006 is relatively wet year with average rainfall of 0.42 cm. In addition, the highest recorded average monthly rainfall is 0.76 cm in July, 2006 and the lowest recorded average monthly rainfall is 0.05 cm in May, 2007. Furthermore, the highest daily rainfall is recorded on 26 May 2009 with 0.59 cm due to the occurrence of Cyclone Aila in Bay of Bengal on 25-26 May 2009 (Tenzing, 2009).

At Wangdue RNRRC station, the highest daily average temperature recorded on 12 August, 2009 is 30.15°C and lowest recorded daily average temperature is 15.40°C on 6 April 2008. The mean of daily average temperature during snowmelt period of hydrological years 2005, 2006, 2007, 2008 and 2009 are 23.30, 23.41, 23.87, 23.84 and 24.15°C respectively. The highest mean of monthly average temperature of 26.68°C is recorded in July, 2009 and the lowest temperature of 19.37°C is recorded in April, 2006.

4.1.1.3 Snow cover area (SCA)

In this study, the Model Builder module in ERSI ArcMap was used to create semi-automate model incorporating tools like Iterate Raster, Extract by Mask and Extract by Attributes to extract to zonal snow covered area from multiple MODIS snow products (MOD10A2 and MYD10A2) as shown in Figure 4.8.

The snow covered area extracted for every zone after applying the model is used to calculate ratio of SCA which is expressed by dividing SCA by zonal area. This ratio of SCA is then plotted against the time to generate snow covered

depletion curve. The snow cover depletion curves is displayed for 2005-2009 is shown in Figures 4.9 to 4.13.

As a results, it can be observed that the pattern of snow cover area from three zones between 2005 and 2009 is similar with highest snow coverage is Zone C and the lowest snow coverage is Zone A. In comparison, ratio of SCA for Zone A and B of year 2006 are relatively low from other remaining years.

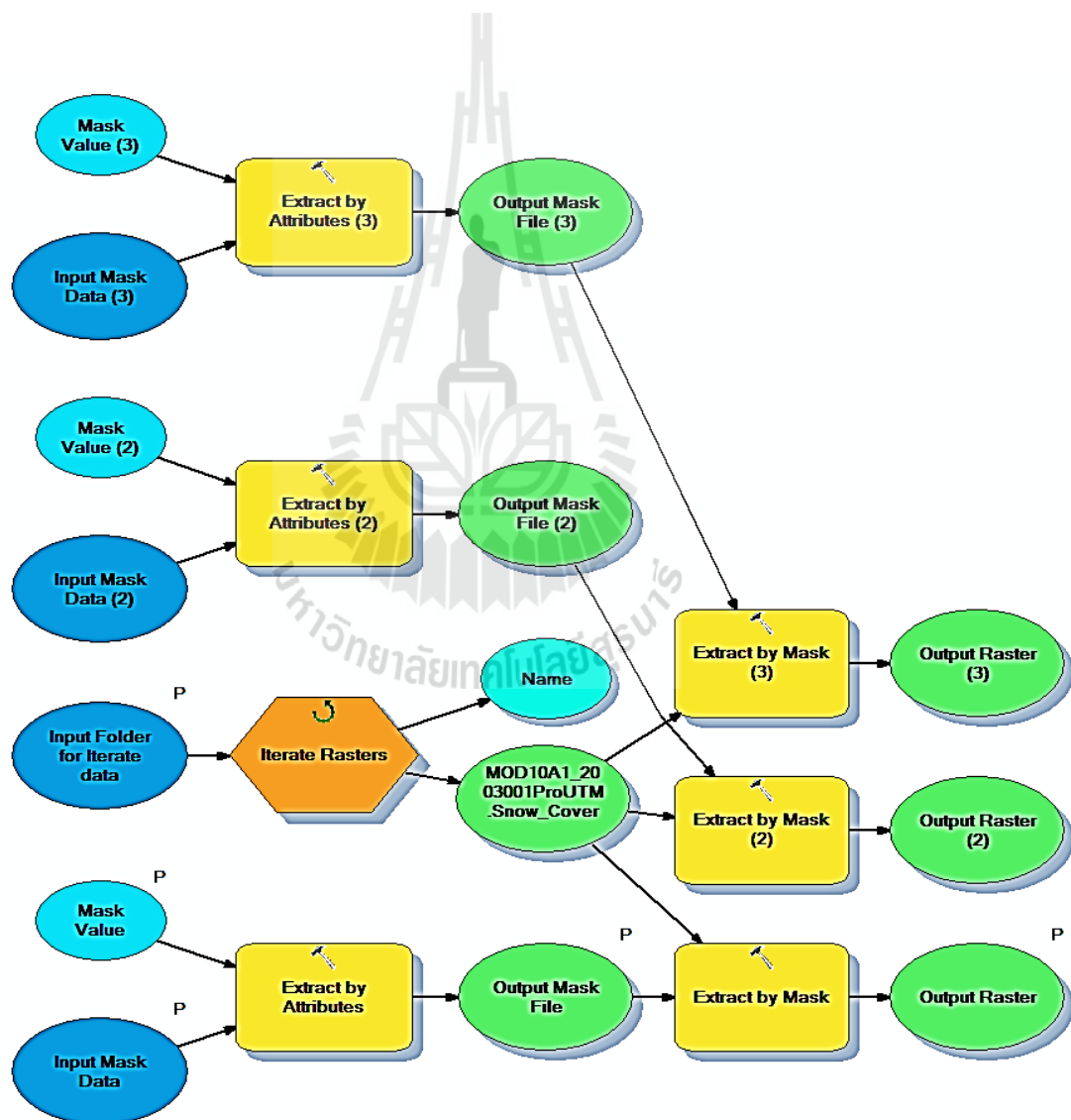


Figure 4.8 Schematic diagram of Model builder for zonal SCA extraction.

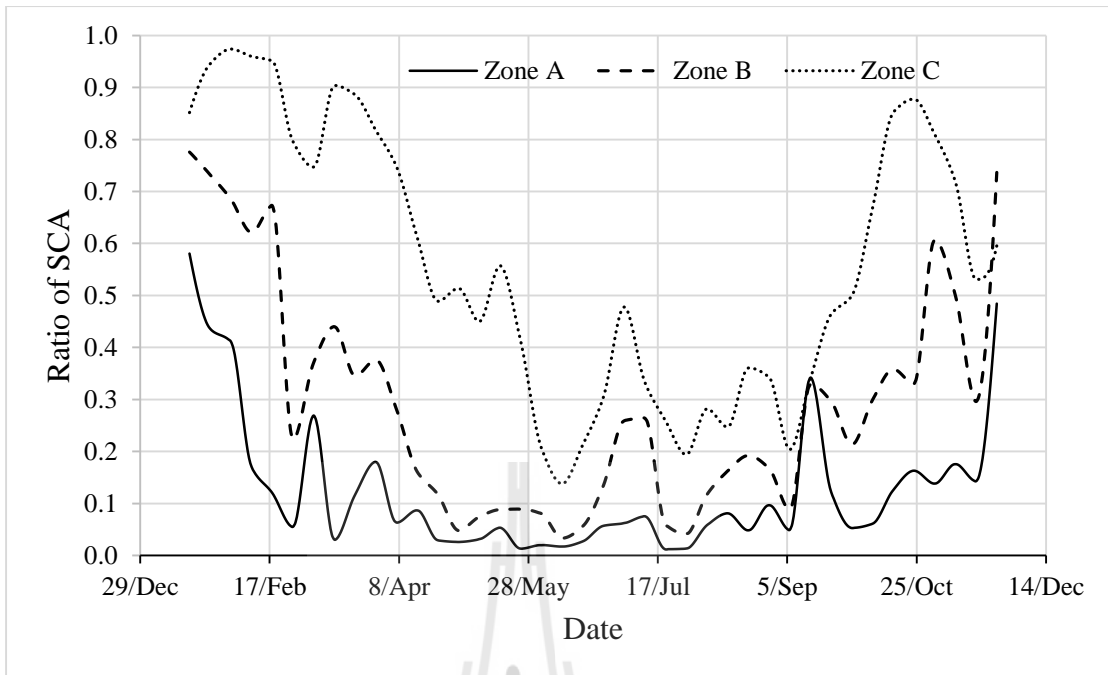


Figure 4.9 Zonal snow cover depletion curve for year 2005.

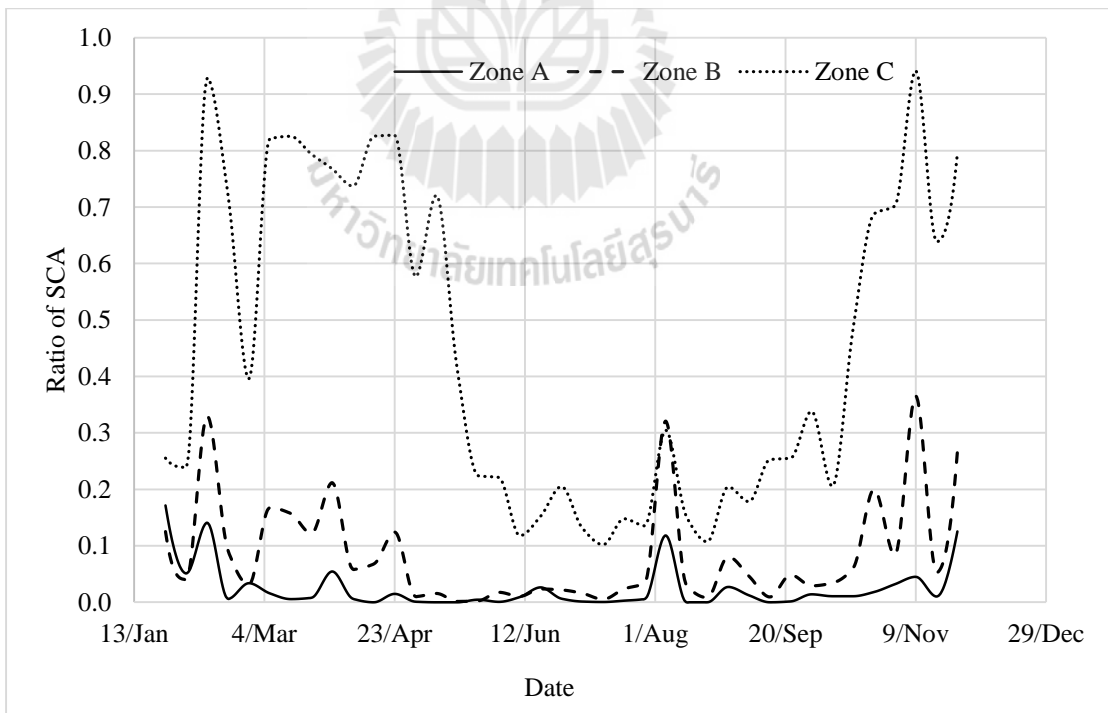


Figure 4.10 Zonal snow cover depletion curve for year 2006.

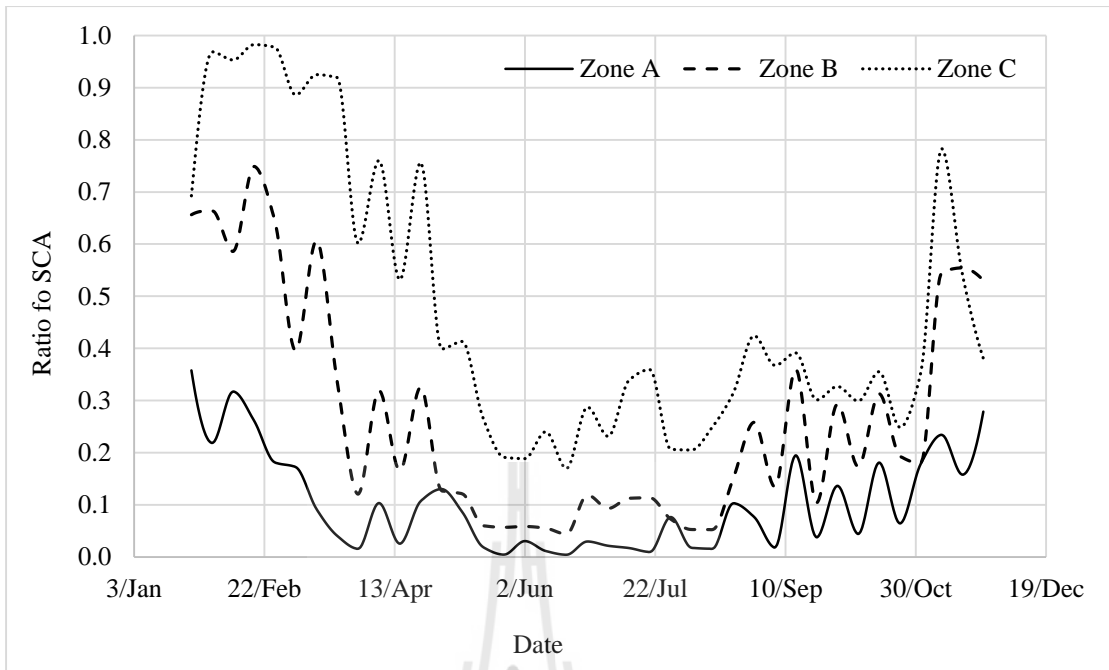


Figure 4.11 Zonal snow cover depletion curve for year 2007.

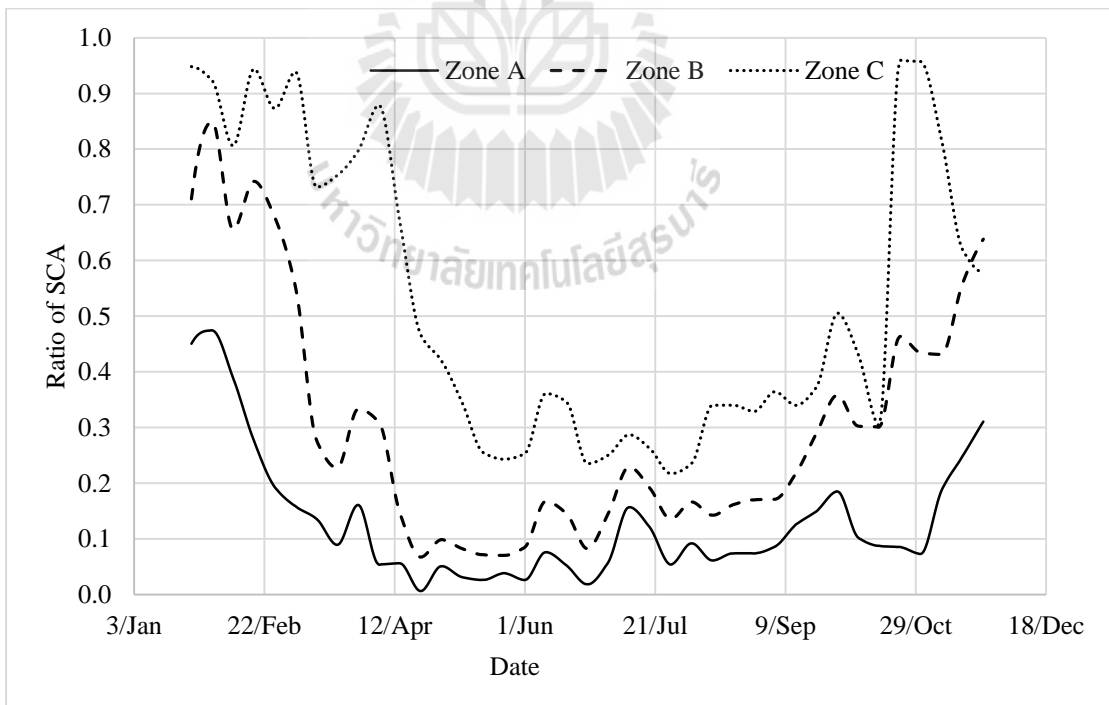


Figure 4.12 Zonal snow cover depletion curve for year 2008.

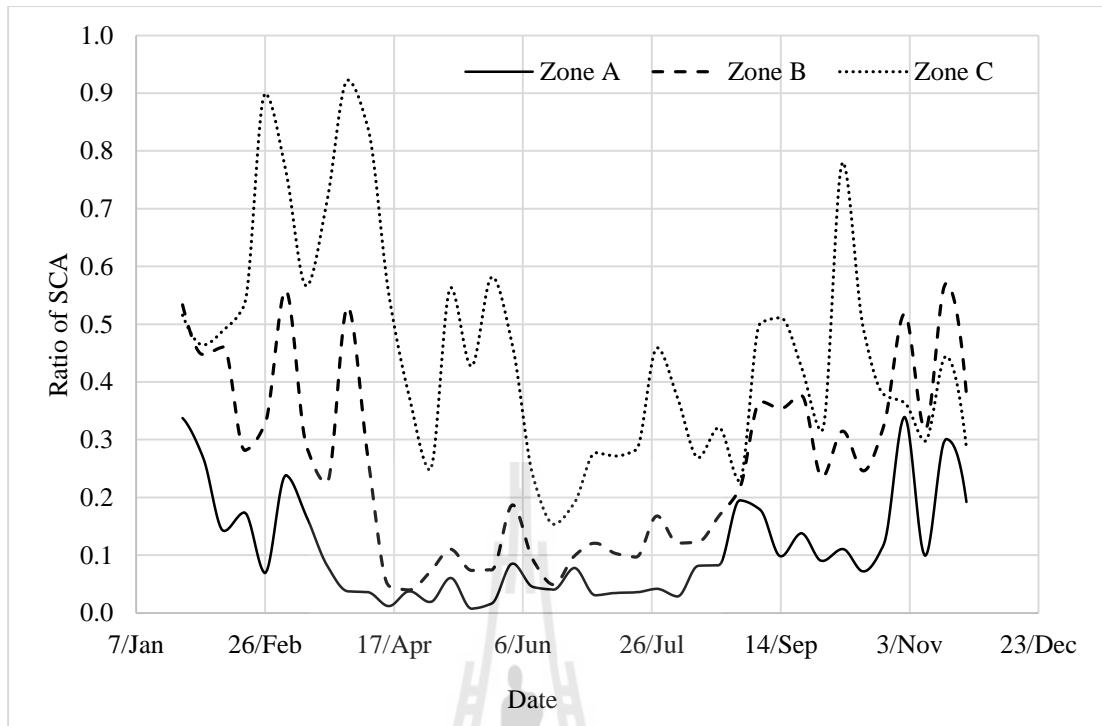


Figure 4.13 Zonal snow cover depletion curve for year 2009.

In addition, percentage of accumulated SCA of individual zone is summarized in Table 4.2 for the melting season between 2005 and 2009. It is observed that the percent of accumulated SCA of Zone A and B for year 2006 are 1.95 and 7.61, respectively, which are different from remaining year whose values varies between 7.09-9.44% for Zone A and 18.88-22.21% for Zone B. Furthermore, the average accumulated SCA in snowmelt season of the hydrological year 2005, 2006, 2007, 2008 and 2009 are 1,480.44, 1,183.19, 1,352.49, 1,434.60 and 1482.79 km², respectively and it is observed that the average accumulated SCA of year 2006 was quite unusual than remaining four hydrological years. This phenomena might be caused by rainfall in the lower zones (A and B) as it was observed at Wangdue RNRRC station of average rainfall during snowmelt period with value of 0.42 cm.

Table 4.2 Accumulated percent of SCA of melt season (April- August) for different hydrological year.

Zone	Percent of SCA of year				
	2005	2006	2007	2008	2009
A	7.43	1.95	7.09	9.44	7.63
B	20.45	7.61	18.88	22.21	19.32
C	59.43	52.81	53.70	56.21	59.79

4.1.1.4 Local recession coefficient extraction

The historical discharge data are used for calculating the recession constants x and y . Here, the discharge data was used to plot a scatterplot with Q_n as abscissa axis and Q_{n+1} as ordinate axis by excluding those discharge $Q_{n+1} > Q_n$. The medium line running in between 1:1 and lower envelop line is used for extracting points to calculate the value of x and y between 2005 and 2009 (see Figures 4.14 to 4.18) and their values are identified as summary in Table 4.3. These values (x , y) are further used to calculate recession coefficient (k) by SRM for indicating the decline of discharge between the sequence of days during a true recession flow period without snowmelt or rainfall during.

Table 4.3 Recession constant value (x and y) for calculating recession coefficient (k) of year 2005-2009.

Recession constant	Year				
	2005	2006	2007	2008	2009
x	0.899	1.051	1.002	0.884	1.007
y	0.010	0.033	0.035	0.008	0.047

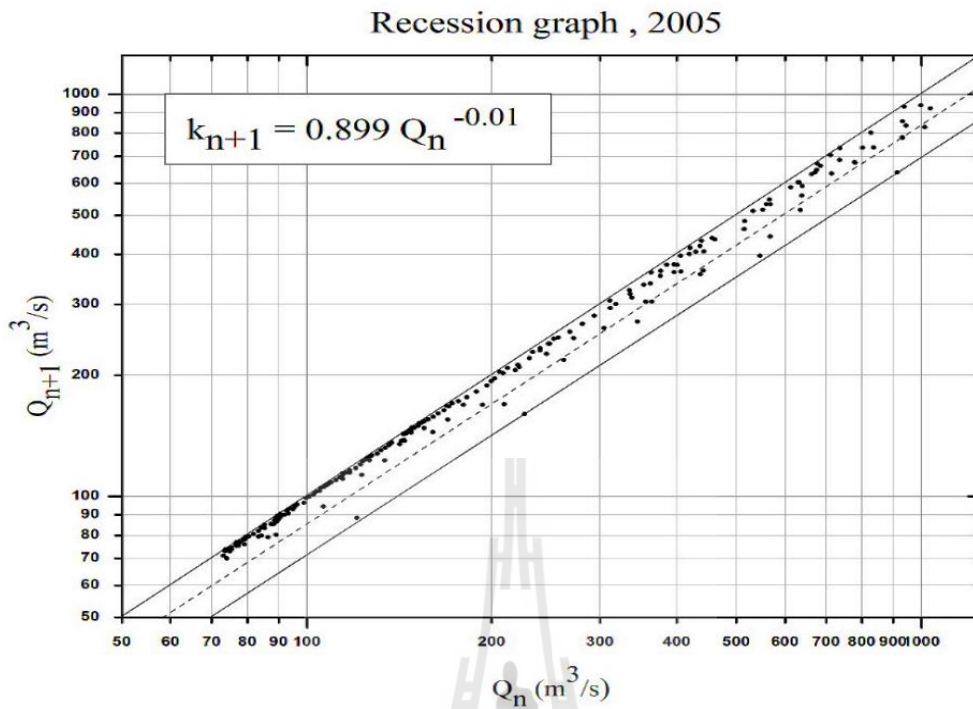


Figure 4.14 Recession graph of 2005.

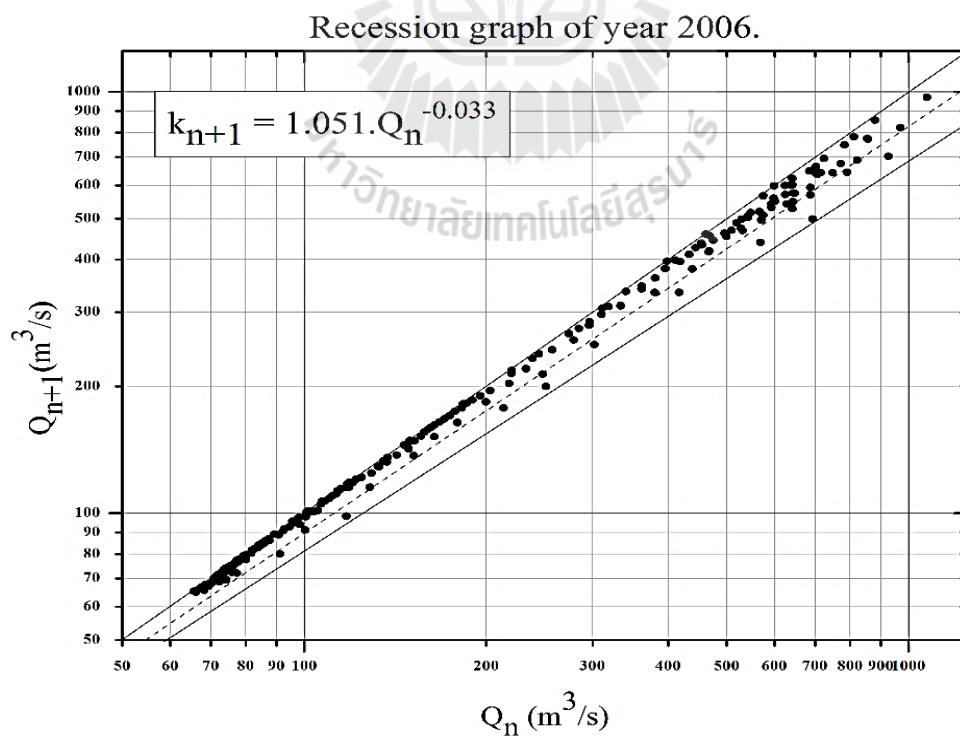


Figure 4.15 Recession graph of 2006.

Recession graph of year 2007.

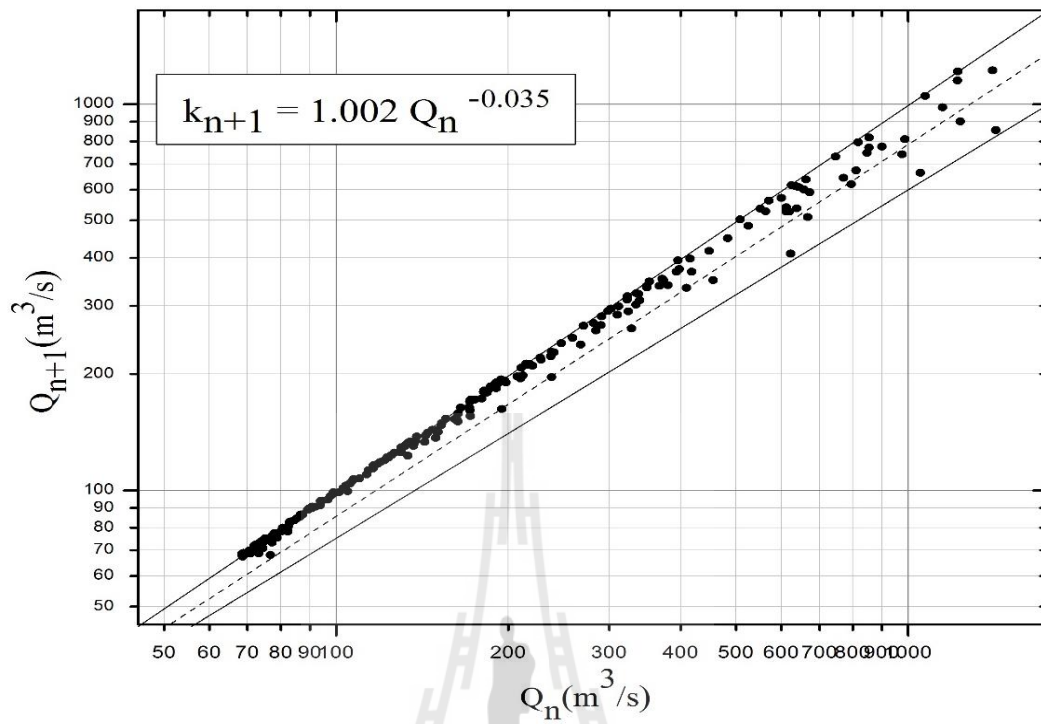


Figure 4.16 Recession graph of 2007.

Recession graph of year 2008.

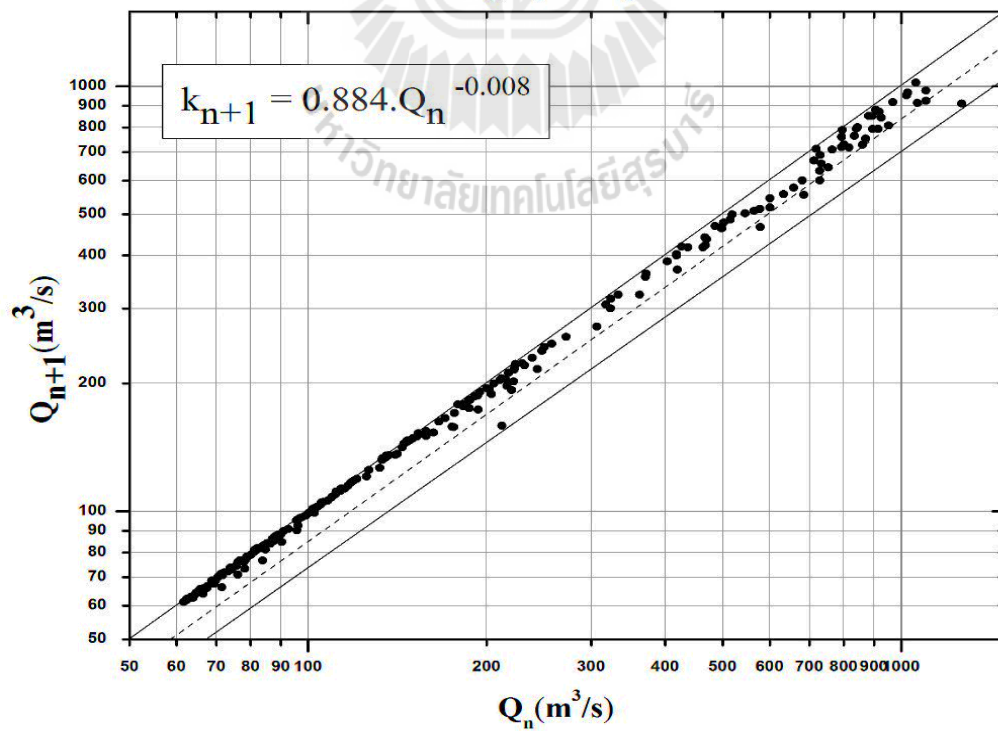


Figure 4.17 Recession graph of 2008.

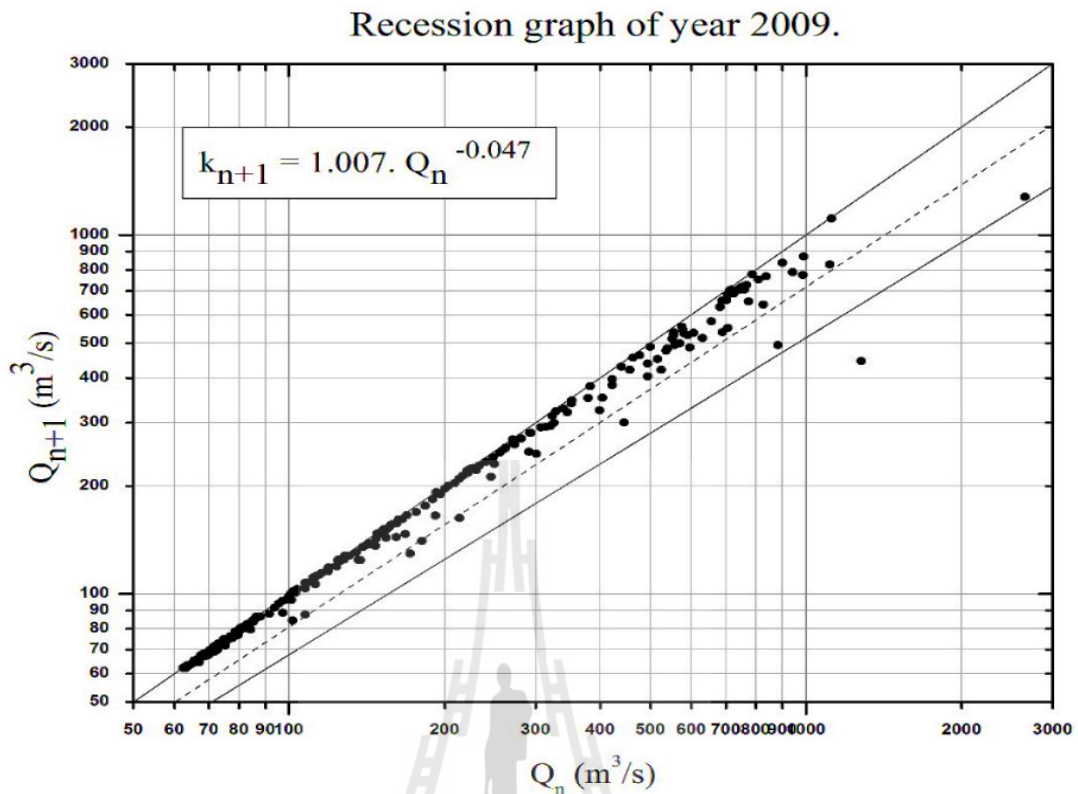


Figure 4.18 Recession graph of 2009.

4.1.2 SRM runoff simulation under calibration process and its optimum range of local parameter

Refer to calibration model under Section 3.3.2.1, selected parameters based on literature reviews including α , C_s , C_r , T_{CRIT} and RCA . These parameters were calibrated for year 2005 and 2006 by varying their value within range limit and iteratively accessing accuracy using NSE within the performance rating range as suggested by Kult et al. (2014).

The SRM model with all its required input data is calibrated iteratively varying the value of parameters on trial and error method and the NSE value obtained were 85.34 and 79.53%, and PBIAS value were 0.63 and 0.36% for the hydrological

year 2005 and 2006, respectively. The optimum range of parameter value derived from calibration periods is summarized in Table 4.4.

The results of calibration year (2005 and 2006) include the simulation hydrograph and statistics data of runoff with accuracy assessment are displayed and summarized in Figures 4.19 and 4.20 and Tables 4.5 to 4.6, respectively.

Table 4.4 Range of optimum local parameters of calibration period.

Year	Calibrated parameters						
	α (cm °C ⁻¹ d ⁻¹)	C _s	C _R	L	RCA	T _{CRIT}	γ (°C/100m)
2005	0.4-1.20	0.20-0.90	0.15-0.85	11 hrs. (Zone A) 12 hrs. (Zone B)	1	1.2	0.57
2006	0.40-2.40	0.20-0.90	0.20-0.90	13 hrs. (Zone C)			

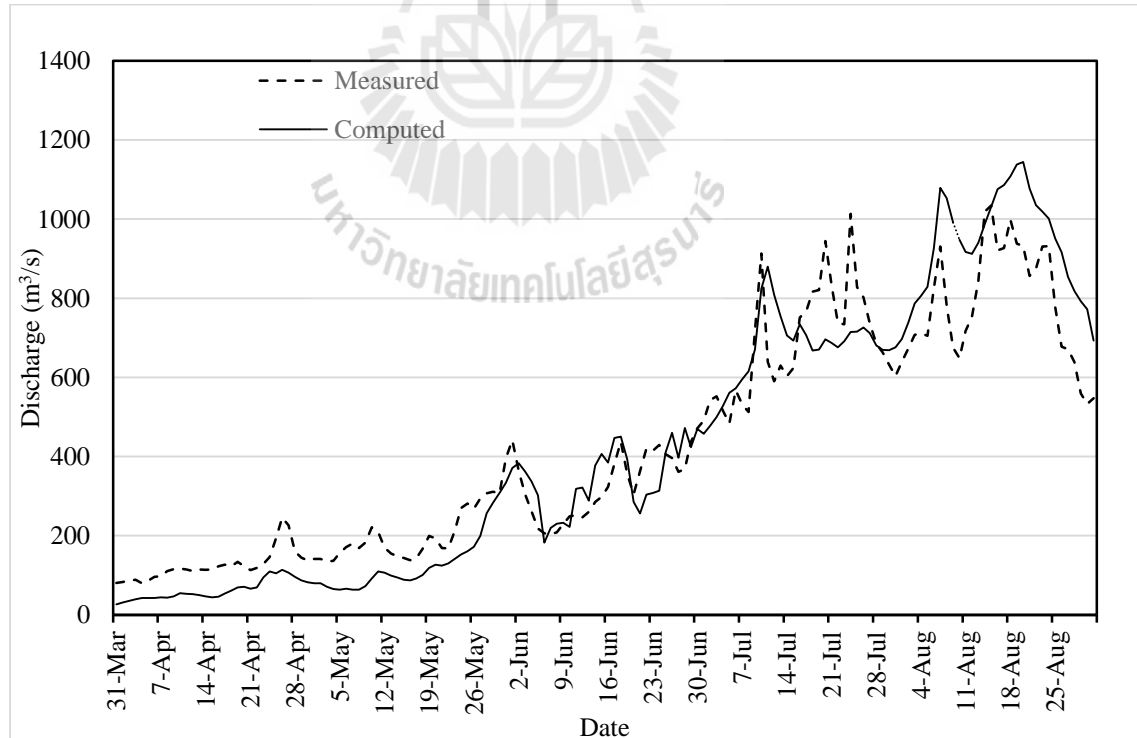


Figure 4.19 Comparison of measured and computed hydrograph of year 2005.

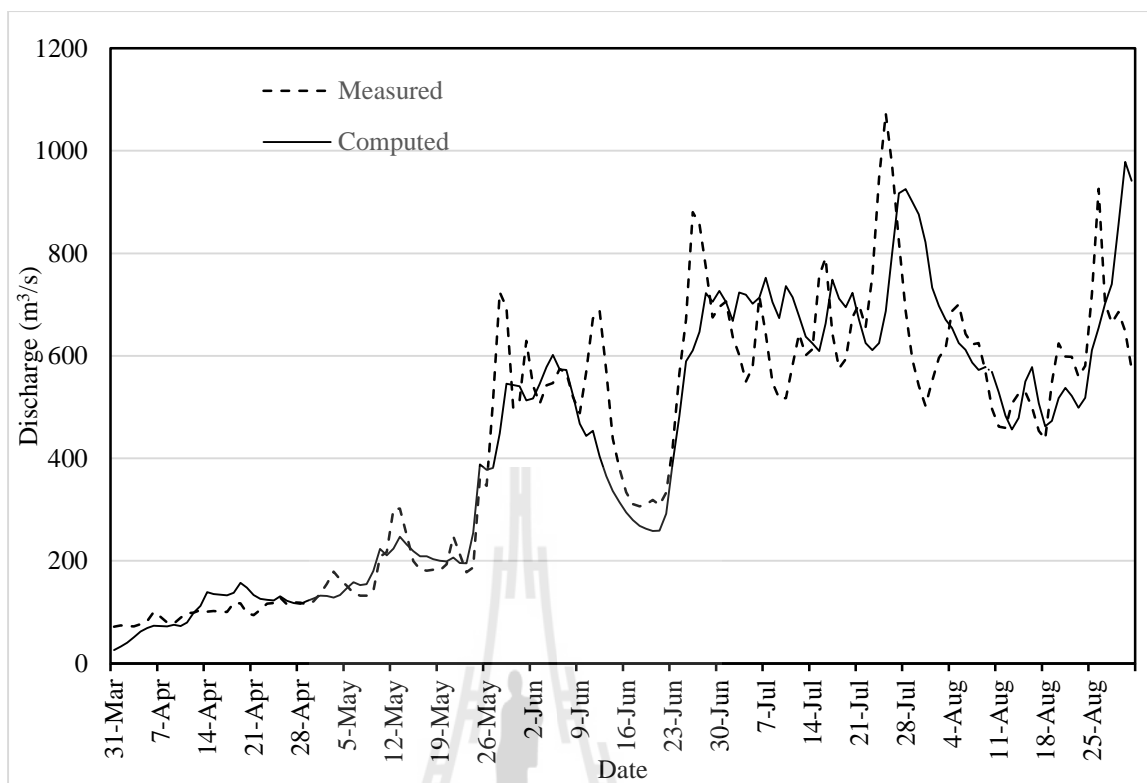


Figure 4.20 Comparison of measured and computed hydrograph of year 2006.

Table 4.5 Statistics data of SRM simulated runoff and its accuracy for year 2005.

Statistics	Quantity
Measured Runoff Volume (10^6 m^3)	5,677.29
Average Measured Runoff (m^3/s)	426.68
Computed Runoff Volume (10^6 m^3)	5,713.29
Average Computed Runoff (m^3/s)	429.39
NSE (%)	85.34
PBIAS (%)	0.63
Volume Difference (%)	-0.63

Table 4.6 Statistics data of SRM simulated runoff and its accuracy for year 2006.

Statistics	Quantity
Measured Runoff Volume (10^6 m^3)	5,739.73
Average Measured Runoff (m^3/s)	431.38
Computed Runoff Volume (10^6 m^3)	5,719.19
Average Computed Runoff (m^3/s)	429.83
NSE (%)	79.53
PBIAS (%)	0.36
Volume Difference (%)	0.36

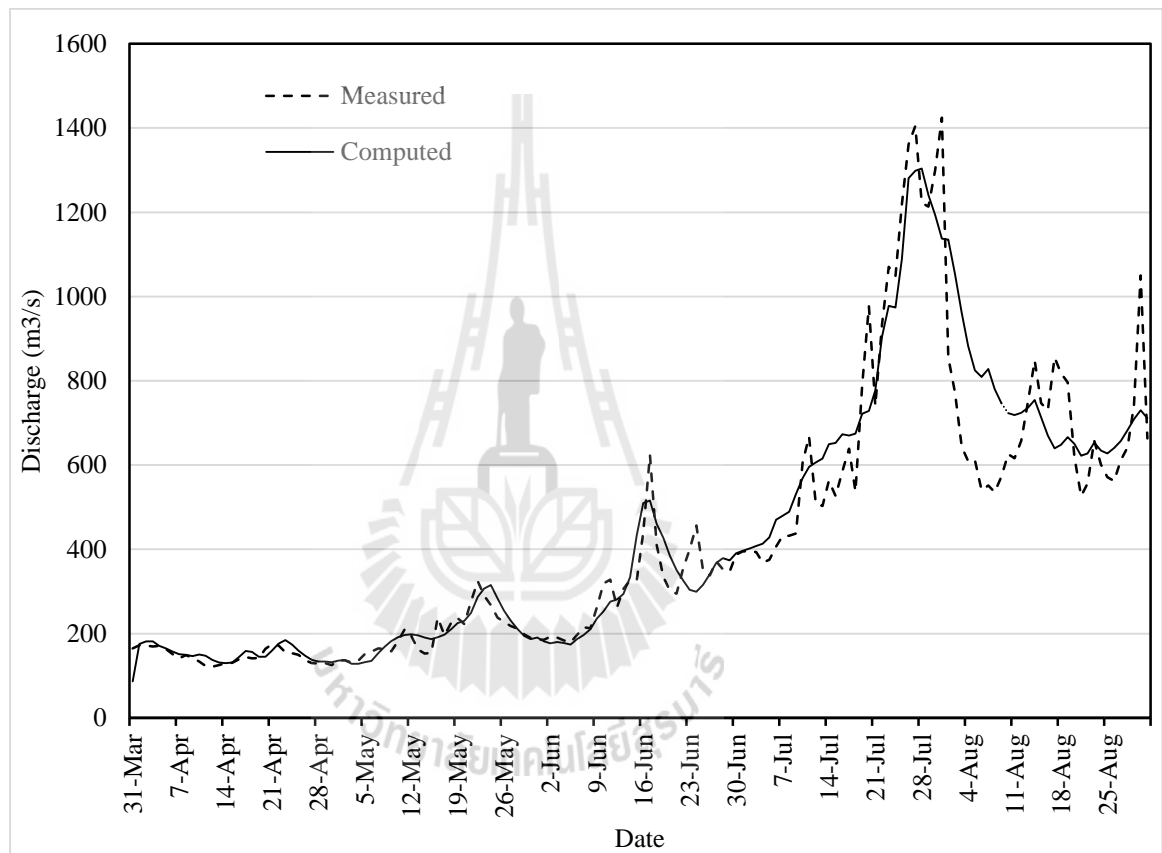
As results, it revealed that the simulated runoff for year 2005 and 2006 from SRM model shows very good performance rating of NSE. The simulated average runoff volume for year 2005 slightly overestimated with D_V of -0.63% but the simulated runoff volume for year 2006 slightly overestimated with D_V of 0.36%.

4.1.3 SRM runoff simulation under validation process and its optimum range of local parameters

Using the derived basin characteristics, local recession coefficient value and initial parameter range from calibration process, the model was set up for validation period (2007, 2008 and 2009) and their NSE values vary between 70.56 and 90.82%. The optimum range of local parameters during validation period is presented in Table 4.7. The validation hydrograph are shown in Figures 4.21 to 4.23 along with statistical results in Tables 4.8 to 4.10.

Table 4.7 Range of optimum local parameters for validation period.

Year	Validated parameters						
	α (cm °C ⁻¹ d ⁻¹)	C _s	C _R	L	RCA	T _{CRIT}	γ (°C/100m)
2007	0.40 - 2.40	0.20 - 0.90	0.20 - 0.85	11 hrs. (Zone A)			
2008	0.40 - 1.20	0.17 - 0.85	0.20 - 0.85	12 hrs. (Zone B)	1	1.2	0.57
2009	0.40 - 1.08	0.20 - 0.85	0.20 - 0.85	13 hrs. (Zone C)			

**Figure 4.21** Comparison of measured and computed hydrograph of year 2007.

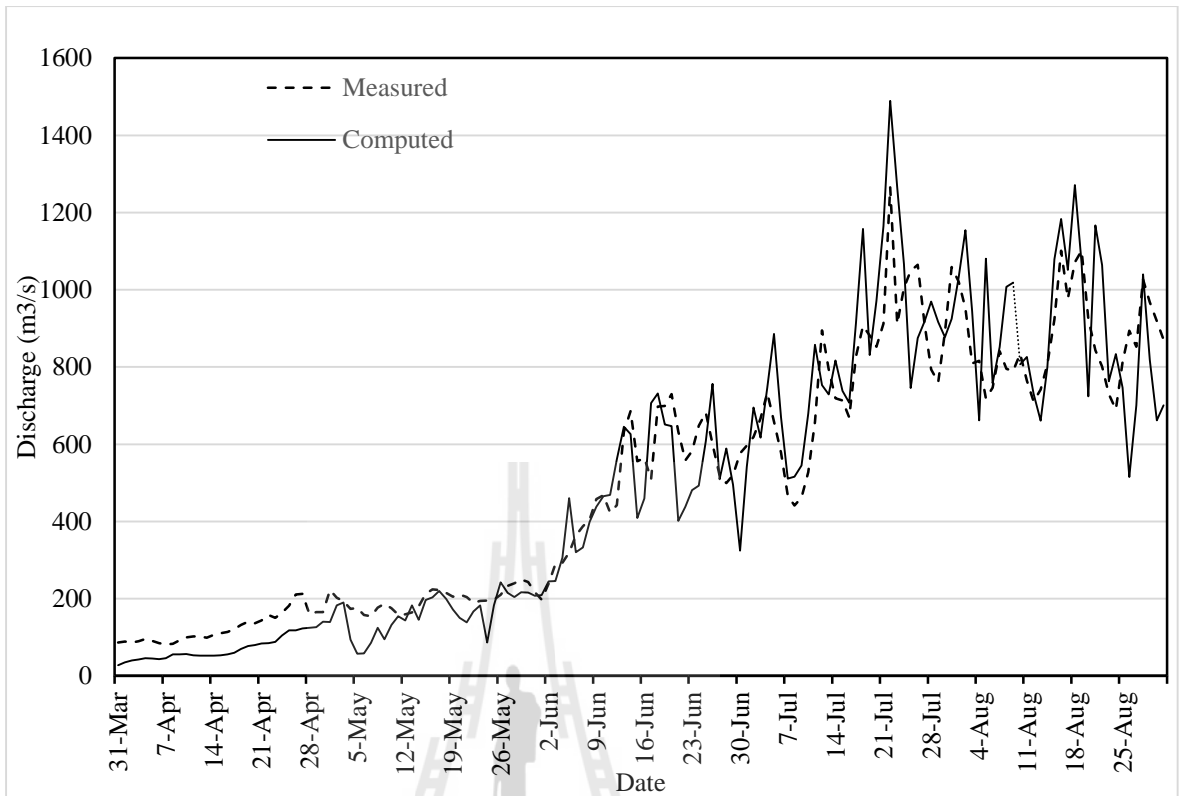


Figure 4.22 Comparison of measured and computed hydrograph of year 2008.

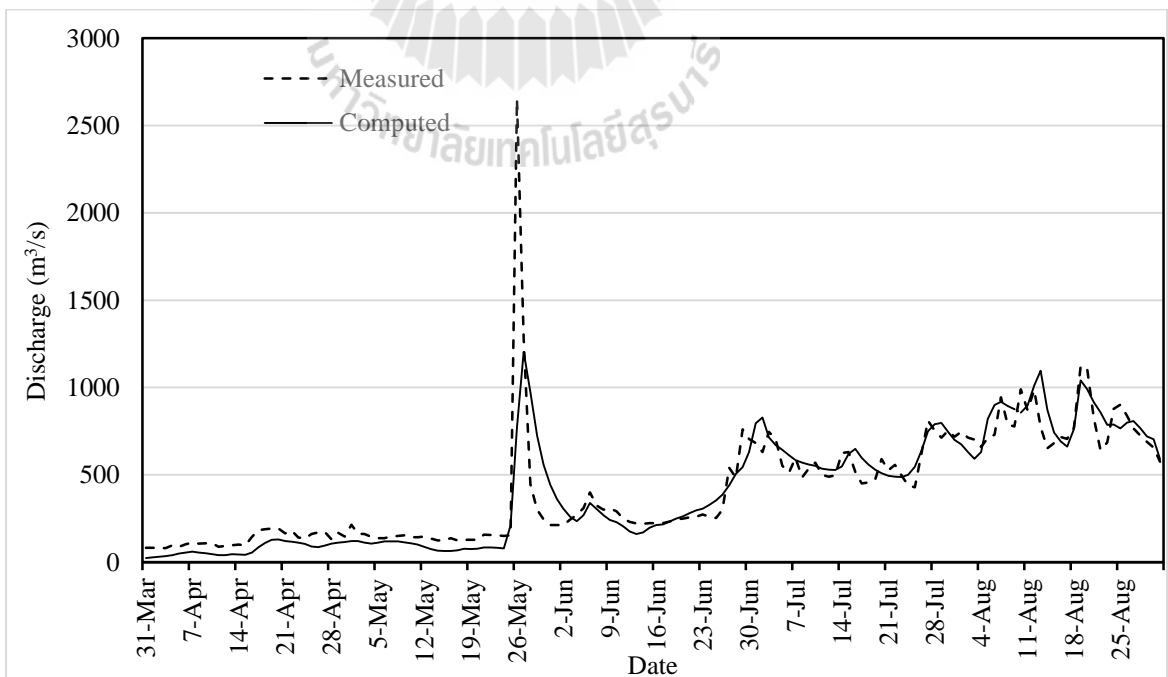


Figure 4.23 Comparison of measured and computed hydrograph of year 2009.

Table 4.8 Statistics data of SRM simulated runoff and its accuracy for year 2007.

Statistics	Quantity
Measured Runoff Volume (10^6 m^3)	5,578.34
Average Measured Runoff (m^3/s)	419.25
Computed Runoff Volume (10^6 m^3)	5,750.92
Average Computed Runoff (m^3/s)	432.22
NSE (%)	90.82
PBIAS (%)	3.09
Volume Difference (%)	-3.09

Table 4.9 Statistics data of SRM simulated runoff and its accuracy for year 2008.

Statistics	Quantity
Measured Runoff Volume (10^6 m^3)	6,593.33
Average Measured Runoff (m^3/s)	495.53
Computed Runoff Volume (10^6 m^3)	6,516.85
Average Computed Runoff (m^3/s)	489.78
NSE (%)	86.65
PBIAS (%)	1.16
Volume Difference (%)	1.16

Table 4.10 Statistics data of SRM simulated runoff and its accuracy for year 2009.

	Statistics	Quantity
Measured Runoff Volume (10^6 m^3)		5,569.92
Average Measured Runoff (m^3/s)		418.61
Computed Runoff Volume (10^6 m^3)		5,400.42
Average Computed Runoff (m^3/s)		405.88
NSE (%)		70.56
PBIAS (%)		3.04
Volume Difference (%)		3.04

The results revealed that the validated runoff for year 2007, 2008 and 2009 show NSE higher than the defined range of performance rating (≥ 0.65). However, the validated runoff for year 2009 comparatively show less NSE value of 70.56% than other hydrological years. The low NSE value for hydrological year 2009 was mainly triggered by Cyclone Aila which hit the Bay of Bengal on 25-26 May, 2009, had a disastrous effect causing flash floods and river flooding events over Bhutan (Figure 4.24). Thus, the river water levels in Wangdue and Punakha districts exceeded the water level recorded in 1994 Glacier Lake Outburst Flood (GLOF) (Tenzing, 2009). Tahir et al. (2011) stated that it is difficult to model the period where there is occurrence of extreme weather condition like cyclone, heavy rainfall and storm. Herewith the simulated average runoff volume for year 2009 is slightly overestimate with D_v of -3.04%.

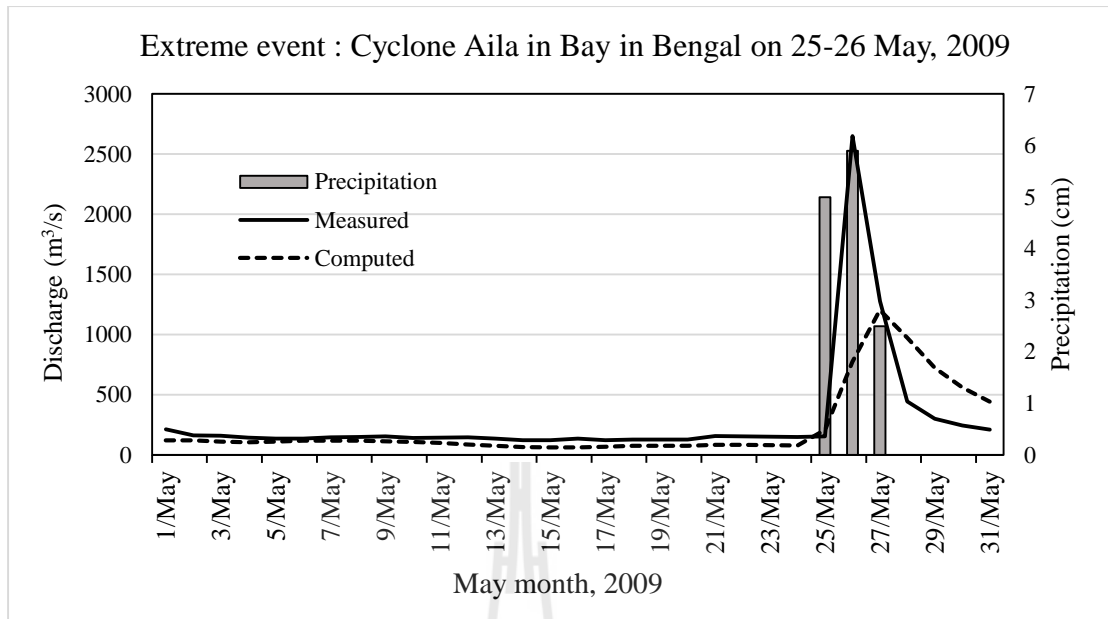


Figure 4.24 Superimposed data of measured and calculated runoff and rainfall of May 2009.

4.1.4 Efficiency of SRM for runoff simulation and their optimum range of local parameter

The SRM model has been applied for simulating the daily flows for the snow melting season of Upper Punatshang Chu Basin for five years. The flow data for the year 2005 and 2006 have been considered for calibrating the model whereas the year 2007, 2008 and 2009 have been considered for validating the model.

The efficiency of the model has been computed based on the daily simulated and observed flow values for five years. The values of the model efficiency, NSE are 85.34, 79.53, 90.82, 86.65 and 70.56% and |PBIAS| are 0.63, 0.36, 3.09, 1.16 and 3.04%, respectively for years 2005, 2006, 2007, 2008 and 2009. The performance of the model in preserving the runoff volume of the entire melting season had been tested based on the criteria computed as percentage difference in observed and

simulated runoff, D_v during the melting period. Their values computed for the year 2005, 2006, 2007, 2008 and 2009 are -0.63, 0.36, -3.09, 1.16 and 3.04%. It is observed that hydrologic year 2007 with maximum NSE value of 90.82% and minimum value of 70.56% for the hydrologic year 2009 caused mainly due to extreme event 'Cyclone Aila' which hit the entire country on 25-26 May, 2009. The overall average NSE value is 82.58% for the whole study period. It is also observed maximum D_v value of 3.04% was computed for hydrologic year 2009 underestimating the average runoff compared to average measured runoff and on the contrary, the hydrologic year 2007 with minimum D_v value of -3.09% overestimating the average computed runoff compared to average measured runoff. The overall average difference in observed and simulated runoff, D_v is 0.17% for the entire study period. The daily simulated and observed flow hydrograph comparison for the study period as shown in Figures 4.18 to 4.23 show that the model has simulated the daily flow reasonably well showing a good agreement with the daily observed flow except few peaks.

At the global level it was found that the least NSE of 70.56% for year 2009 obtained in this study proved to be more accurate than 42 SRM case studies of 112 that have been applied over 112 river basins, located in 29 different countries (See Table 4.11).

At the regional level, many researchers have applied SRM in Himalayan region, namely Kulang, Beas-Manali, Saing, Toutunhe, Gongnisi, Urumqi, Parbati, Buntar, Beas-Thalot, Kabul, Yellow, Brahmaputra basins, the efficiency rating of year 2009 proved to be more accurate than 7 out of 13 SRM applications. Moreover,

average NSE value of 82.58% for years 2005-2009 is higher than 12 out of 13 applications in Himalaya region

Since there is no hydrological study carried out using the SRM model in Bhutan, therefore, the study is compared with three test sites nearby Bhutan. Firstly, the results comparison was made against the research work of Gunjal Silwal (2014) carried out in Dudhkoshi River, Nepal, whose average NSE and D_v are 84 and 4.5727 % respectively, with difference observed in value of NSE is 1.42% and D_v is 4.4063%

The results of the simulation with average NSE of 82.58% proved better than following SRM research carried out by (1) Aggarwal et al. (2014) applied SRM model in Bhagirathi river basin in upper Ganga catchment and the average NSE achieved is 80%, (2) Arya, Gautam, and Murukar (2014) in Dhualigang River, India whose average NSE value for calibration and validation periods resulted 75 and 73% respectively and (3) Zhang et al. (2014) applied SRM model in Qinghai Lake basin and its average NSE value of 73%

Thus, the simulation results achieved for this research work is reasonably good when compared to the above stated results. Herewith, the recommended range of optimum local parameter of SRM for the study area are as follows:

- degree day factor varies between 0.40 and 2.4 $\text{cm}^\circ\text{C}^{-1}\text{d}^{-1}$,
- runoff coefficient value for snow varies from 0.17 to 0.90,
- runoff coefficient value for rain varies from 0.15 to 0.85.

Table 4.11 Details of SRM applications and their results applied by researchers during 1962-1999.

Sl.No	Country	Basin	Size (km ²)	Elev. Range (m amsl)	NSE (%)	Dv [%]	Year
1	USA	EGL (Rocky Mountains)	0.29	3,300-3,450	--	--	1989
2	USA	WGL (Rocky Mountains)	0.6	3,300-3,450	--	--	1989
3	Germany	Lange Bramke (Harz)	0.76	540-700	--	--	1981
4	Germany	Wintertal (Harz)	0.76	560-754	--	--	1981
5	Czech R.	Modry Dul (Krkonose)	2.65	1,000-1,554	96	1.7	1962, 1966
6	USA	GLEES (Rocky M.)	2.87	3,300-3,450	--	--	1989
7	Ecuador	Antisana (Andes)	3.72	4,500-5,760	--	--	1996
8	Argentina	Echaurren	4.5	3,000-4,200	84	7.5	1985
9	Spain	Lago Mar (Pyrenees)	4.5	2,234-3,004	--	--	1965
10	Spain	Llauset dam (Pyrenees)	7.8	2,100-3,000	69	5.5	1999
11	USA	W-3 (Appalachians)	8.42	346-695	81	8.8	1969-1978
12	Germany	Lainbachtal (Allgauer Alps)	18.7	670-1,800	--	--	1978, 1979
13	Spain	Salenca en Baserca (Pyrenees)	22.2	1,460-3,200	72	4.3	1999
14	Spain	Noguera Ribagorzana en Baserca (Pyrenees)	36.8	1,480-3,000	71	3.7	1995
15	Switzerland	Rhone-Gletsch (Alps)	38.9	1,755-3,630	--	--	1979
16	Switzerland	Dischma (Alps)	43.3	1,668-3,146	86	2.5	1973, 1970-79
17	Japan	Sai (Japan Alps)	57	300-1,600	86	--	1979-1981
18	Spain	Tor en Alins (Pyrenees)	60	1,880-3,040	71	7.3	1999
19	Spain	Flamisell en Capdella (Pyrenees)	84	1,440-2,940	68	8.1	1999
20	Spain	Vellós en Añisclo (Pyrenees)	85	1,140-3,360	83	1.5	1999
21	Austria	Rofenache (Alps)	98	1,890-3,771	88	2.4	1992-1993
22	United Kingdom	Feshie (Cairngorms)	106	350-1,265	88	--	1979, 1980
23	Switzerland	Sedrun (Alps)	108	1,840-3,210	79	1.9	1985, 1993

Table 4.11 (Continued).

Sl.No	Country	Basin	Size (km ²)	Elev. Range (m amsl)	NSE (%)	Dv [%]	Year
24	Austria	Tuxbach	116	879-3,062	44	12.7	1996-1998
25	Austria	Schlegeis	121	1,790-3,510	86	8.7	1996-1998
26	Australia	Geehi River (Snowy Mtns.)	125	1,032-2,062	70	6.6	1989-1994
27	USA	American Fork (Utah)	130	1,820-3,580	90	1.7	1983
28	Austria	Venter Ache	165	1,850-3,771	82	5.4	1992
29	Switzerland	Landwasser - Frauenkirch (Alps)	183	1,500-3,146	--	--	1979
30	Switzerland	Massa-Blatten (Alps)	196	1,447-4,191	91	-5.3	1985
31	India	Kulang (Himalayas)	205	2,350-5,000	--	--	---
32	Switzerland	Tavanasa (Alps)	215	1,277-3,210	82	3.1	1985, 1993
33	USA	Dinwoody (Wind River)	228	1,981-4,202	85	2.8	1974, 1976
34	Italy	Cordevole (Alps)	248	980-3,250	89	4.6	1984
35	USA	Salt Creek (Utah)	248	1,564-3,620	--	2.6	---
36	India	Beas-Manali (Himalayas)	345	1,900-6,000	68	12	---
37	Argentina	El Yeso	350	2,475-6,550	91	2.6	1991, 1993
38	Norway	Laerdalselven (Lo Bru)	375	530-1,720	86	5.2	1991
39	Norway	Viveli (Hardangervidda)	386	880-1,613	73	11.3	1991
40	USA	Scofield Dam, Price River (Utah)	401	2,323-3,109	80	5	1996, 1998
41	Spain	Cardós en Tirvia (Pyrenees)	417	1,720-3,240	80	2.6	1999
42	Japan	Okutadami (Mikuni)	422	782-2,346	83	5.4	1984
43	USA	Joes Valley Dam, Cottonwood Creek (Utah)	435	2,131-3,353	83	18.5	1985
44	Spain	Garona en Bossost (Pyrenees)	449	1,620-3,080	75	3	1999
45	Spain	Noguera Pallaresa	450	1,860-2,960	87	3.3	1999
46	USA	en Escaló (Pyrenees) Bull Lake Creek (Rocky Mts.)	484	1,790-4,185	82	4.8	1976
47	Switzerland	Tiefencastel (Alps)	529	837-3,418	55	11.3	1982, 1985

Table 4.11 (Continued).

Sl.No	Country	Basin	Size (km ²)	Elev. Range (m amsl)	NSE (%)	Dv [%]	Year
48	Spain	Valira en Seo d'Urgel (Pyrenees)	545	1,740-3,080	92	0.9	1999
49	USA	Towanda Creek (Appalachians)	550	240-733	78	8.3	1990, 1993, 94
50	Spain	Garona en Pont de Rei (Pyrenees)	558	1,420-3,080	72	2.7	1999
51	USA	South Fork (Colorado)	559	2,506-3,914	89	1.8	1973-79
52	Spain	Noguera Ribagorzana en Pont de Suert (Pyrenees)	573	920-3380	91	-0.6	1999
53	Argentina	Las Cuevas en Los Almendros (Andes)	600	2,500-7,000	--	--	1981
54	USA	Independence R. (Adirondacks)	618	261-702	81	5	1987
55	Chile	Mapocho (Andes)	630	1,024-4,450	42	29.9	1987
56	Poland	Dunajec (High Tatra)	700	577-2,301	73	3.8	1975
57	India	Saing (Himalayas)	705	1,400-5,500	--	--	--- 1973
58	USA	Conejos (Rocky Mts)	730	2,521-4,017	87	1.1	1979
59	Switzerland	Ilanz (Alps)	776	693-3,614	53	8.6	1982, 1985
60	Spain	Cinca en Laspuña (Pyrenees)	798	1,120-3,380	78	5.6	1999 1984
61	China	Toutunhe	840	1,430-4,450	81	2	1986 <199
62	Austria	Ötztaler Ache (Alps)	893	670-3,774	84	9.18	8
63	Argentina	Lago Alumin (Andes)	911	1,145-2,496	--	--	1985 <199
64	China	Gongnisi (Tien Shan)	939	1,776-4,200	80	0.97	9 <199
65	China	Urumqi (Tien Shan)	950	1,880-4,200	62	2.78	9
66	Uzbekistan	Angren	1082	1,200-3,800	63	2.3	--- 1986
67	India	Parbati (Himalayas)	1154	1,500-6,400	73	7.5	~ 1991
68	Canada	Illecillewae (Rocky Mts)	1155	509-3,150	86	7	1976, 1981, 83,84
69	Spain	Segre en Seo d'Urgel (Pyrenees)	1217	360-2,900	--	--	1996 1985
70	India	Buntar (Himalayas)	1370	1,200-5,000	--	--	~ 1991

Table 4.11 (Continued).

Sl.No	Country	Basin	Size (km ²)	Elev. Range (m amsl)	NSE (%)	Dv [%]	Year
71	Chile	Tinguiririca Bajo Briones (Andes)	1460	520-4,500	88	-0.3	1987
72	New Zealand	Hawea (S. Alps)	1500	300-2,500	--	--	1989
73	Switzerland	Ticino-Bellinzona (Alps)	1515	220-3,402	86	-0.6	1994
74	USA	Spanish Fork (Utah)	1665	1,484-3,277	85	1	1983
75	Switzerland	Inn at Tarasp (Alps)	1700	1,235-4,005	77	8	1996
76	Argentina	Tupungato (Andes)	1800	2,500-6,000	63	6.4	1981
77	Switzerland	Inn-Martina (Alps)	1943	1,030-4,049	82	4.3	1990
78	Argentina	Chico (Tierra del Fuego)	2000	N/A	--	--	N/A 1976
79	USA	Boise (Rocky Mts.)	2150	983-3,124	84	3.3	1978 1975
80	France	Durance (Alps)	2170	786-4,105	85	2.6	1979 1976
81	USA	Madison (Montana)	2344	1,965-3,234	89	1.5	1978 <200
82	Uzbekistan	Pskem	2448	1,000-4,200	97	-1	2
83	Morocco	Tillouguit (Atlas)	2544	1,050-3,411	84	0.5	1979
84	Austria	Salzach-St.Johann (Alps)	2600	570-3,666	--	--	>199 1 1976
85	USA	Henry's Fork (Idaho)	2694	1,553-3,125	91	1.5	1979
86	USA	Cache la Poudre (Colorado)	2732	1,596-4,133	--	--	1983
86	USA	Cache la Poudre (Colorado)	2732	1,596-4,133	--	--	1983
87	Chile	Aconcagua en	2900	900-6,100	91	0.9	1987
88	USA	Chababuquito (Andes) Sevier River (Utah)	2929	1,923-3,260	75	5.1	1983 1982 ,85,8 8,89, 92,9
89	Switzerland	Rhine-Felsberg (Alps)	3249	562-3,425	70	7.2	4,96
90	Switzerland	Rhône-Sion (Alps)	3371	491-4,634	97	-2.1	1985 1976 -77,
91	USA	Rio Grande (Colorado)	3414	2,432-4,215	84	3.8	1979

Table 4.11 (Continued).

Sl.No	Country	Basin	Size (km ²)	Elev. Range (m amsl)	NSE (%)	Dv [%]	Year
92	USA	Kings River (California)	4000	171-4,341	82	3.2	1973 -75, 82,88
93	Chile	Maipo en el Manzano (Andes)	4960	850-5,600	77	0.9	1982, 1988
94	India	Beas-Thalot (Himalayas)	5144	1,100-6,400	80	1.5	1986 -87
95	USA	Upper Yakima (Cascades)	5517	366-2,121	92	2.8	1989
96	Uzbekistan	Chatkal	6591	1,000-4,000	81	1.6	---
97	Canada	Sturgeon (Ontario)	7000	N/A	--	--	1967
98	Argentina	Grande (Tierra del Fuego)	9050	N/A	--	--	N/A
99	Canada	Iskut (Coast)	9350	200-2,556	--	--	N/A 1997 -
100	Turkey	Karasu (Upper Euphrates)	10216	1,125-3,487	95	0.25	1999
101	Uzbekistan, Kyrgystan	Karadarya	12056	1,100-4,568	87	4	1996, 98, 1999
102	Tadjikistan	Zerafshan	12214	410-5,500	--	--	---
103	Uzbekistan, Kazakhstan	Kafinirgan *	12369	505-3,005	57	8.6	- 1991
104	USA	Sevier River (Utah)	13380	1,506-3,719	93	4	1983 1972 -
105	USA	Snake River (Idaho)	14897	1,524-4,196	90	0.4	1982 1988 -
106	Tadjikistan	Vakhsh *	37759	1,791-5,291	63	2.8	1990
107	Kyrgystan	Naryn	53237	800-5,000	96	1	---
108	Pakistan	Kabul River (Himalayas)	63657	305-7,690	66	6	1975 1988 -
109	Tadjikistan, Afghanistan	Pyandzh (Pamirs and Hindu Kush)	120534	2,141-5,564	65	5.6	- 1991
110	China	Yellow (Anyemogen Shan)	121972	2,500-5,224	--	--	1993
111	India, Bangladesh	Brahmaputra (Himalayas)	547346	0-8,848	75	-7.5	1995
112	India, Bangladesh	Ganges (Himalayas)	917444	0-8,848	94	8.3	1995

Source: Martince et al. (2007).

4.1.5 Snowmelt simulation and its contribution to river discharge

Based on the above simulation with the defined range of parameters, the amount of contribution of snowmelt depth (in cm) to river discharge is summarized in Table 4.12. Herein, amount of snowmelt depth are reported by elevation zone. It is observed that the total snowmelt depth of year 2006 is relatively low when compared with remaining four hydrological years. This phenomena agree with SCA depletion curve as mentioned in Section 4.1.1.3. This agreement can be confirmed by the relationship between snowmelt depth and average snow covered area between 2005 and 2009 as simple linear regression equation as shown in Figure 4.25.

In addition, it is observed that T_{CRIT} plays important role to categorize precipitation to new snow in Zone C when temperature less than T_{CRIT} (1.2°C).

Table 4.12 Contribution of snowmelt to river discharge.

Snowmelt depth by elevation zone (cm)								
Year	Zone A		Zone B		Zone C		Total	Snowmelt Contribution (%)
	Snow	New snow	Snow	New snow	Snow	New snow		
2005	102	0	193.81	0	165.25	7.86	468.87	3.08
2006	24.07	0	59.61	0	119.46	8.53	211.67	1.38
2007	67.99	0	120.86	0	125	3.83	317.68	2.13
2008	145.30	0	220.06	0	171.32	1.67	538.39	3.05
2009	110.80	0	168.24	0	173.90	0.24	453.20	3.04
Average snowmelt contribution								2.53

By converting total snowmelt depth (cm) in Table 4.12 to total discharge (m^3/s) using conversion factor in Eq. 2.2, snowmelt runoff contribution for Upper Punatshang Chu basin ranges from 1.38 to 3.08% with average contribution of 2.53% during the melt season.

Zhang et al. (2014) confirmed about 3-6% of snowmelt runoff contribution during the melt period. Siderius et al. (2013) observed that in Ganges River basin, the snowmelt contribution represents 1-5% of the total runoff.

Ramamoorthi (1987) and Prasad and Roy (2005) also concluded in their research that the effect of temperature on the variation of seasonal snowmelt runoff from year to year will not be significant since the changes in the temperature during the different years in the snowmelt runoff period is not significant. Hence, snow cover area is the main factor in seasonal snowmelt runoff from major mountainous basin. This concept lead to development of regression relationship between the SCA and runoff, which are extensively applied to places where detail snow studies are not carried out.

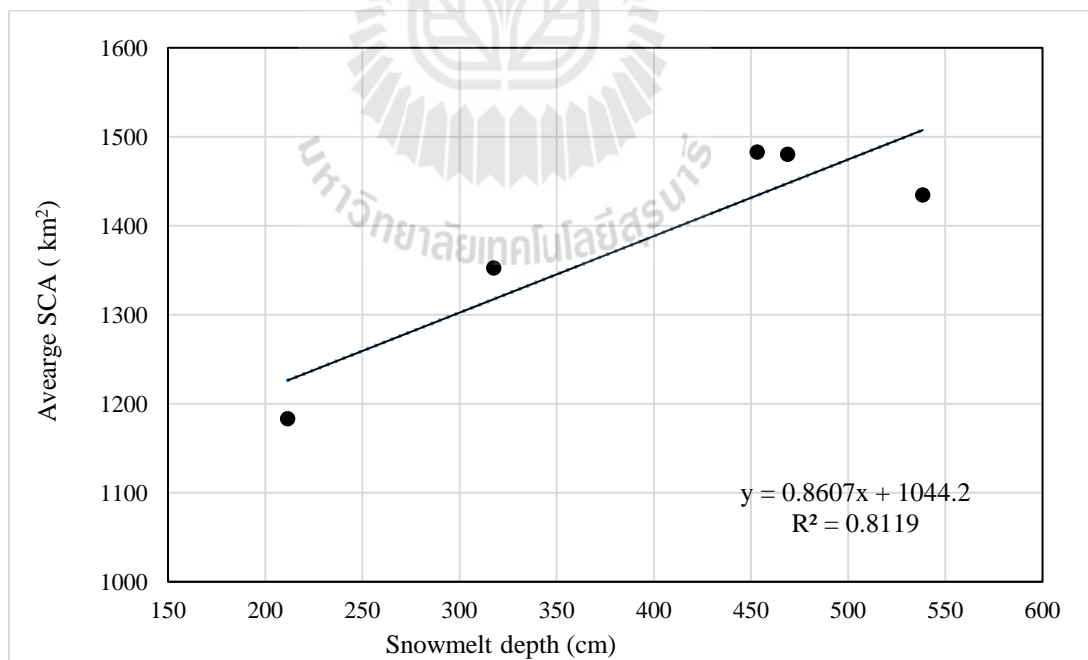


Figure 4.25 Relationship between snowmelt depth and average snow covered area.

4.2 Impact of temperature change on streamflow

To understand the effect of climate change and its interaction on snow, it is essential to create a hypothetical scenarios for better understanding. The hypothetical scenario can provide a general view on temperature impact on streamflow. The following hypothetical scenarios are set up in this study by increasing the average observed temperature during the study periods (2005-2009):

- a. Scenario 1: Observed average temperature + 1°C.
- b. Scenario 2: Observed average temperature + 2°C.
- c. Scenario 3: Observed average temperature + 3°C.

The results of the stream flow change observed from SRM simulation under the different hypothetical scenarios are separately described by hydrological year in the following section.

4.2.1 Impact of temperature change on streamflow based on 2005 simulation data

The result of the impact of temperature change on streamflow under three simulated scenarios is displayed as hydrograph in Figure 4.26 and summarized the percent increase of discharge volume in Table 4.13. It revealed that the simulated discharge volume during snowmelt period (April to August) of 2005 with value of $5,713.29 \times 10^6 \text{ m}^3$ increases by 14.73, 30.25 and 45.92% when temperature is increased by 1, 2 and 3°C, respectively.

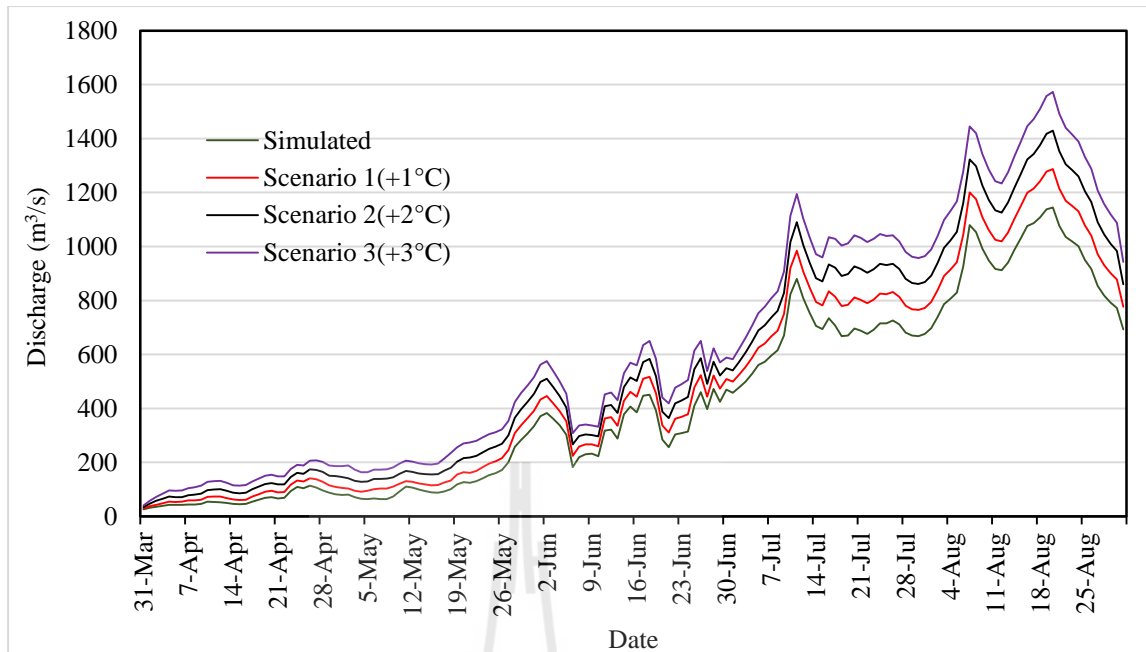


Figure 4.26 Comparison of simulated streamflow in each scenario based on simulation data of 2005.

Table 4.13 Discharge volume change and percent increase of streamflow based on simulation data of 2005.

Scenario	Peak Discharge (m³/s)	Runoff volume (10⁶ m³)	% Increase of streamflow
Simulated	1,144.1	5,713.29	
Scenario 1 (+1°C)	1,286.9	6,554.82	14.73
Scenario 2 (+2°C)	1,429.8	7,441.37	30.25
Scenario 3 (+3°C)	1,572.9	8,337.06	45.92

4.2.2 Impact of temperature change on streamflow based on 2006 simulation data

The result of the impact of temperature change on streamflow under three simulated scenarios is displayed as hydrograph in Figure 4.27 and summarized as the percent increase of discharge volume in Table 4.14. It was found that the simulated discharge volume during snowmelt period of 2006 with value of $5,719.19 \times 10^6$ m³ increases by 14.65, 30.32 and 46.98% when temperature is increased by 1, 2 and 3°C, respectively.

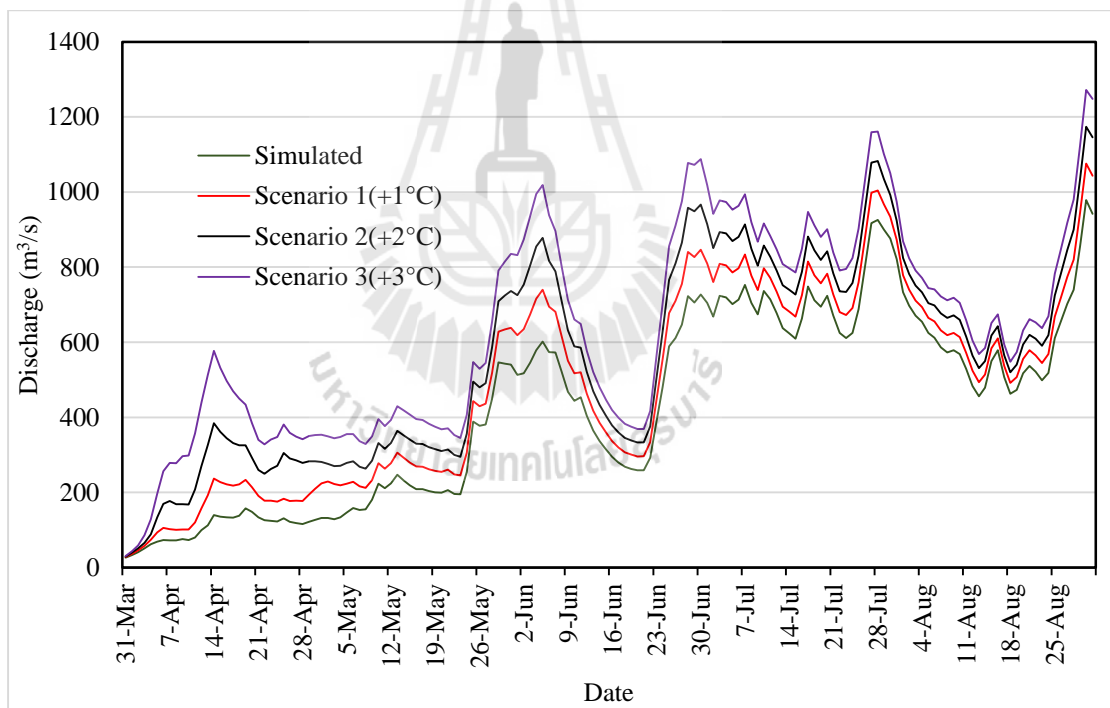


Figure 4.27 Comparison of simulated streamflow in each scenario based on simulation data of 2006.

Table 4.14 Discharge volume change and percent increase of streamflow based on simulation data of 2006.

Scenario	Peak Discharge (m³ /s)	Runoff volume (10⁶ m³)	% Increase of streamflow
Simulated	978.5	5,719.19	
Scenario 1 (+1°C)	1,076.0	6,557.17	14.65
Scenario 2 (+2°C)	1,173.9	7,452.98	30.32
Scenario 3 (+3°C)	1,272.1	8,406.13	46.98

4.2.3 Impact of temperature change on streamflow based on 2007 simulation data

The result of the impact of temperature change on streamflow in three simulated scenarios is presented as hydrograph in Figure 4.28 and summarized as the percent increase of discharge volume in Table 4.15. It showed that the normal average discharge during snowmelt period of 2007 with value of $5,750.92 \times 10^6 \text{ m}^3$ increases by 15.41, 30.91 and 46.41% when temperature is increased by 1, 2 and 3°C, respectively.

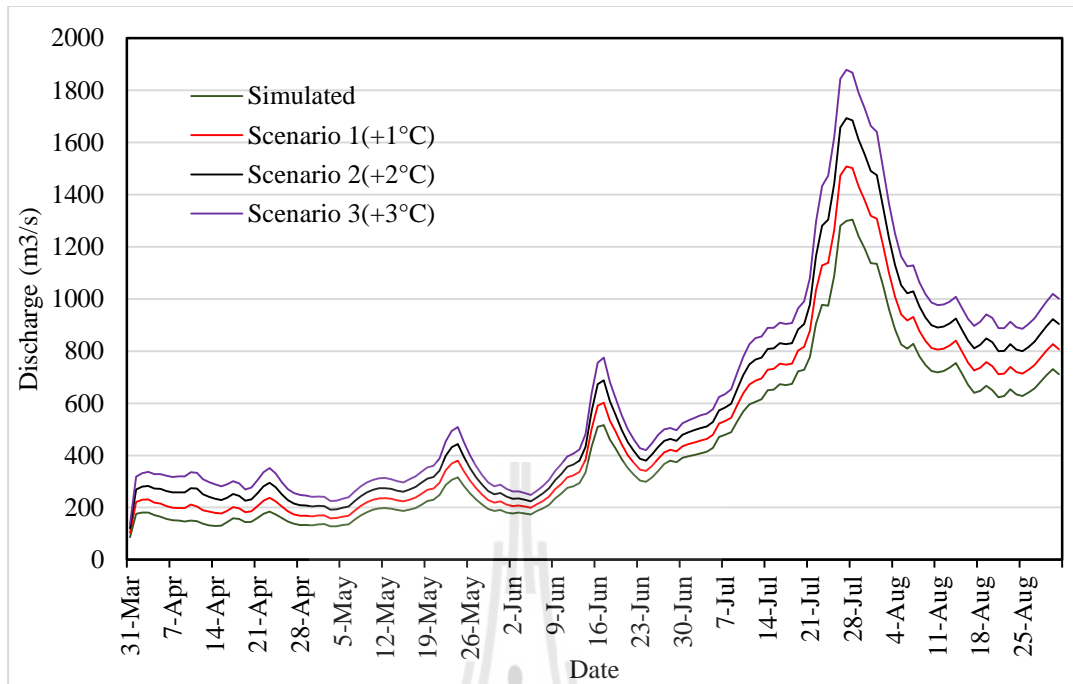


Figure 4.28 Comparison of simulated streamflow in each scenario based on simulation data of 2007.

Table 4.15 Discharge volume change and percent increase of streamflow based on simulation data of 2007.

Scenario	Peak Discharge (m³ /s)	Runoff volume (10⁶ m³)	% Increase of streamflow
Simulated	1,303.6	5,750.92	
Scenario 1 (+1°C)	1,507.3	6,637.17	15.41
Scenario 2 (+2°C)	1,692.6	7,528.50	30.91
Scenario 3 (+3°C)	1,878.5	8,419.91	46.41

4.2.4 Impact of temperature change on streamflow based on 2008 simulation data

The result of the impact of temperature change on streamflow in three simulated scenarios is presented in Figure 4.29 and summarized as the percent increase of discharge volume in Table 4.16. It revealed that the simulated discharge volume during snowmelt period of 2008 with value of $6,516.85 \times 10^6 \text{ m}^3$ increases by 13.15, 26.40 and 39.86% when temperature is increased by 1, 2 and 3°C , respectively.

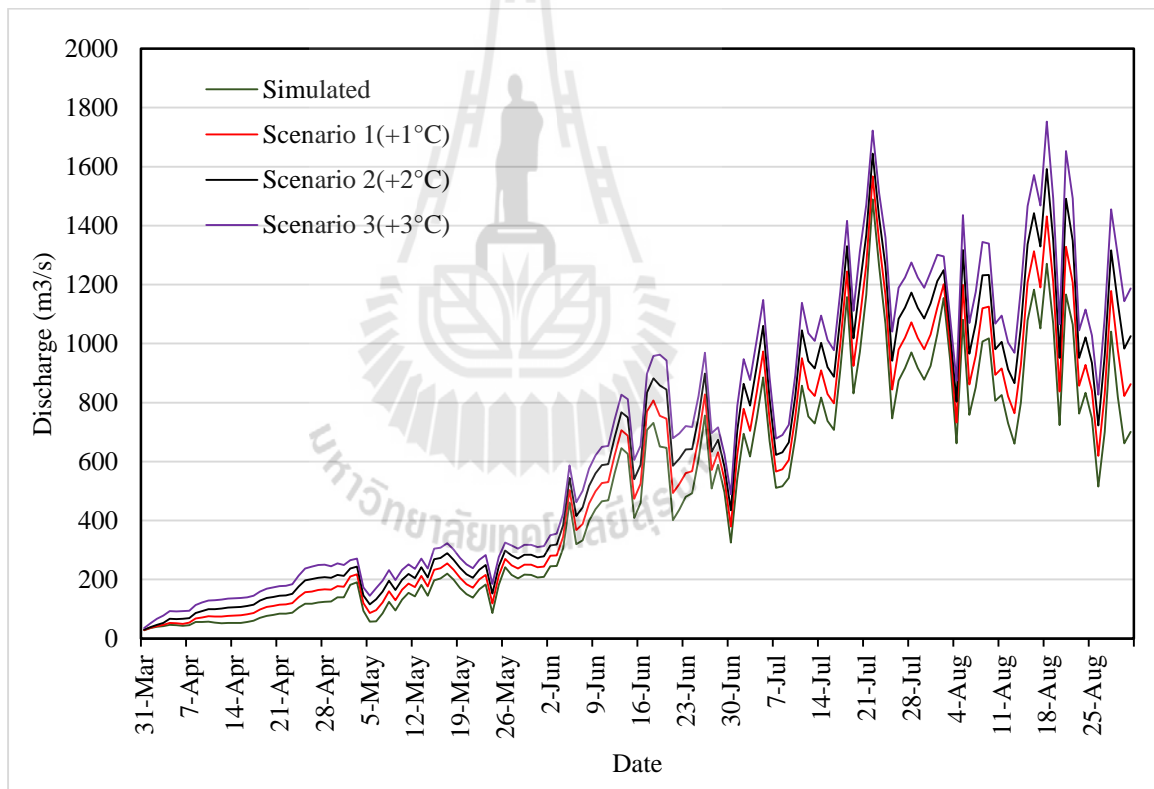


Figure 4.29 Comparison of simulated streamflow in each scenario based on simulation data of 2008.

Table 4.16 Discharge volume change and percent increase of streamflow based on simulation data of 2008.

Scenario	Peak Discharge (m³ /s)	Runoff volume (10⁶ m³)	% Increase of streamflow
Simulated	1,489.1	6,516.85	
Scenario 1 (+1°C)	1,566.7	7,373.94	13.15
Scenario 2 (+2°C)	1,644.3	8,237.60	26.40
Scenario 3 (+3°C)	1,752.3	9,114.29	39.86

4.2.5 Impact of temperature change on streamflow based on 2009 simulation data

The result of the impact of temperature change on streamflow in three simulated scenarios is demonstrated as hydrograph in Figure 4.30 and summarized the percent increase of discharge volume in Table 4.17. It showed that the simulated discharge volume during snowmelt period of 2009 with value $5,400.42 \times 10^6 \text{ m}^3$ increases by 11.84, 23.97 and 36.17% when temperature is increased by 1, 2 and 3°C, respectively.

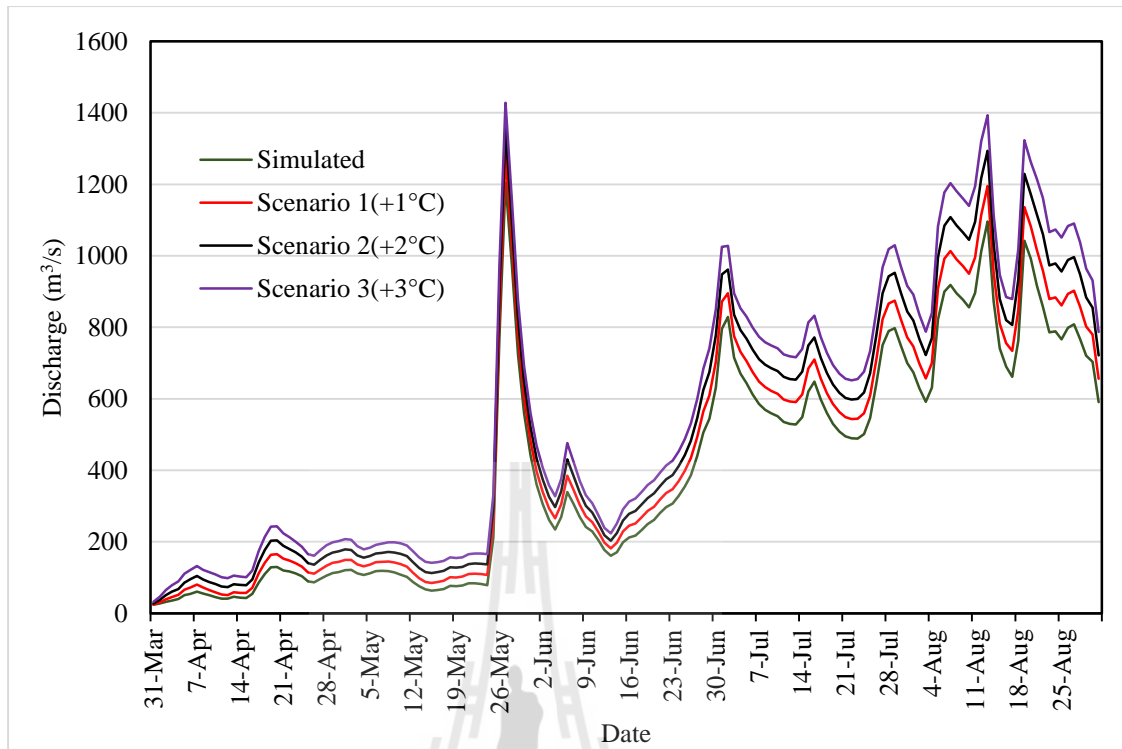


Figure 4.30 Comparison of simulated streamflow in each scenario based on simulation data of 2009.

Table 4.17 Discharge volume change and percent increase of streamflow based on simulation data of 2009.

Scenario	Peak Discharge (m³ /s)	Runoff volume (10⁶ m³)	% Increase of streamflow
Simulated	1,204.9	5,400.42	
Scenario 1 (+1°C)	1,281.6	6,040.00	11.84
Scenario 2 (+2°C)	1,355.9	6,694.76	23.97
Scenario 3 (+3°C)	1,427.9	7,353.64	36.17

4.2.6 Synthesis of impact of temperature change on streamflow during 2005-2009 simulation data

After compiling individual records of hydrological year 2005-2009 in Table 4.18, there is evident increase in snowmelt runoff of approximately 13.96, 28.37 and 43.07% under a hypothetical scenarios by increasing temperature by 1, 2 and 3°C respectively. Hereby, it is observed an increase of average temperature by 1°C, the streamflow is expected to rise approximately by 11.84-16.67% from the simulated runoff. Therefore, an average percent increase of streamflow from 5 hydrological years is here used to synthesis and compared with relevant studies under this section.

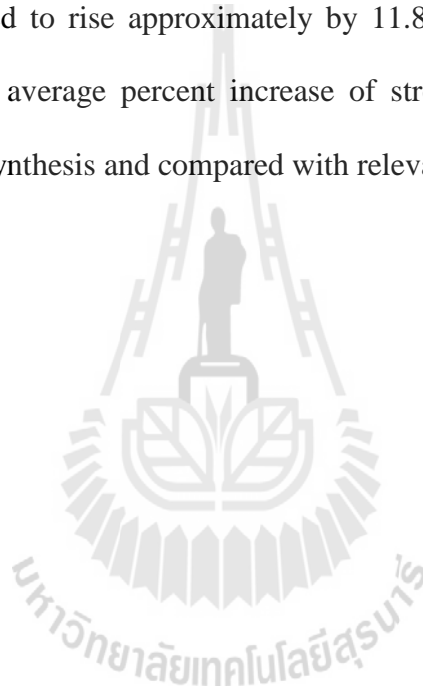


Table 4.18 Comparison of average streamflow, percent increase and average percent increase of streamflow under the hypothetical scenarios of year 2005-2009.

Year	Hydrological statistics	Simulated	Scenario 1 (+1°C)	Scenario 2 (+2°C)	Scenario 3 (+3°C)
2005	Runoff volume (10 ⁶ m ³)	5,713.29	6,554.82	7,441.37	8,337.06
	% Increase of streamflow		14.73	30.25	45.92
2006	Runoff volume (10 ⁶ m ³)	5,719.19	6,557.17	7,452.98	8,406.13
	% Increase of streamflow		14.65	30.32	46.98
2007	Runoff volume (10 ⁶ m ³)	5,750.92	6,637.17	7,528.50	8,419.91
	% Increase of streamflow		15.41	30.91	46.41
2008	Runoff volume (×10 ⁶ m ³)	6,516.85	7,373.94	8,237.60	9,114.29
	% Increase of streamflow		13.15	26.40	39.86
2009	Runoff volume (10 ⁶ m ³)	5,400.42	6,040.00	6,694.76	7,353.64
	% Increase of streamflow		11.84	23.97	36.17
Average			13.96	28.37	43.07

In 1990, Rango and van Katwijk applied SRM model to study climate change effect in Western North America Mountain basins by increasing the mean temperature by 1, 3 and 5°C. Evidently there was an increase runoff during snowmelt

season in Rio Grande basin by 2.7, 8.3 and 14.3%, respectively. Similarly, there was increase in snowmelt season runoff in Illecillewaet basin by 4.5, 11.1 and 16.3%, respectively.

Likewise, Tahir et al. (2011) studied about the temperature change impact on snow runoff in Hunza river basin, northern Pakistan and concluded with a finding that there is increase of 33% of summer discharge resulted from increase of 1°C and 64% from 2°C.

Silwal (2014) studied about the climate change in Dudhkoshi River basin, Nepal and concluded that a rise in 1°C in the mean temperature resulted in a 0.37% increase in annual runoff volume. Regmi (2011) studied on the impact of climate change by varying temperature from mean measured temperature and observed there is rise in runoff approximately at rate of 2% in winter, 5% in summer and 4% annually under the projected temperature rise of 1°C.

Unlike, Archer (2003) who applied a linear regression analysis for climate variable and streamflow indicated that a 1°C rise in the mean summer temperature resulted in a 16% increase runoff into the Hunza and Shyok River due to accelerated glacier melt. Singh and Kumar (1997) carried out an analytical studies using UBC watershed model representing temperature increase of 1-3°C in the western Himalayan region suggest an increase in glacial melt runoff by 16-50%.

For Upper Punatshang Chu basin, an increase in temperature by 1°C resulted in 14.36% increase of snowmelt runoff approximately. Thus, the results of impact of temperature change on snowmelt associated with the basin contradicted with the above studies. The discrepancy between the results obtained by different studies may be possible due to the methods, hypothesis and limitations. Moreover,

these results may be specific to a particular region because the catchment response to the climate warming may not be the same in other catchments as explained by Tahir et al. (2011).

4.3 Sensitivity analysis

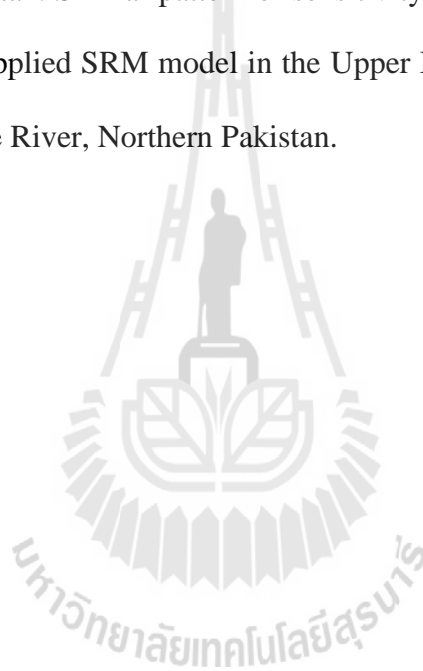
Sensitivity analysis of the SRM simulation for the Upper Punatshang Chu basin, Bhutan is carried out to check the sensitivity of its parameters. For this purpose, all the SRM parameters were varied by $\pm 10\%$ of its calibrated value used in the SRM runoff simulation of year 2007 (NSE = 90.82% and $D_v = -3.0937$).

Table 4.19 Sensitivity analysis result for the SRM simulation year 2007.

No	SRM Parameters	Simulated NSE (%)	Sensitivity test NSE (%)	NSE Difference
1	+10% of Lapse rate (γ)	90.82	71.50	19.32
	-10% of Lapse rate (γ)	90.82	64.25	26.57
2	+10% of T_{CRIT}	90.82	90.82	0.00
	-10% of T_{CRIT}	90.82	90.82	0.00
3	+ 10% of Degree day factor (α)	90.82	87.63	3.19
	- 10% of Degree day factor (α)	90.82	90.45	0.37
4	+10% of Lag time (L)	90.82	90.73	0.09
	-10% of Lag time (L)	90.82	90.90	-0.08
5	+10% of C_S	90.82	87.53	3.29
	-10% of C_S	90.82	90.51	0.31
	+10% of C_R	90.82	90.12	0.70
	-10% of C_R	90.82	90.98	-0.16
6	RCA = 1	90.82	90.82	0.00
	RCA = 0	90.82	90.79	0.03

It is clearly evident that γ is most sensitive parameter followed by α , C_S , and C_R . On other hand, parameters include T_{CRIT} , RCA and L are least sensitive parameters (Table 4.19). The pattern of NSE difference of α and C_S are identical as these parameters are strongly related to snowmelt.

In addition, this finding was similar to the previous work of Haq (2008), who applied SRM model for flood forecast and water resource management of River Swat in Kalam Basin, Pakistan. Similar pattern of sensitivity test was observed in the work of Bilal (2010) who applied SRM model in the Upper Indus Basin for water resource management of Astore River, Northern Pakistan.



CHAPTER V

CONCLUSIONS AND RECOMMENDATIONS

Under this chapter, two main results of the study include (1) snowmelt runoff simulation and (2) assessment of impact of temperature change on stream flow are here separately concluded and some recommendations are suggested for future research and development.

5.1 Conclusions

Decades ago, the snowmelt runoff research had come into focus due mainly to its capability to study about the global climate change and global warming, other than forecasting water resource availability and programming water usage and management which has improved in predicting floods driven by snow and glacier melt. In line to this, the SRM model is one kind of model which is applicable in mountainous watersheds with hydro-meteorological data-scarce to forecast and evaluate the climate change on runoff.

This research was carried out in rugged and inhospitable terrain of eastern Himalayan region i.e. Upper Punatshang Chu basin, to simulate runoff for melt season (April-August) of hydrological year 2005-2009 using temperature index model called Snowmelt Runoff Model with input data consisting of meteorological data and remote sensing data.

5.1.1 Snowmelt runoff simulation by SRM model

SRM model with its ability to simulate runoff with very less input data has gained much popularity in a mountainous region where climatological data are sparse, and the peculiarity of model is that it takes snow covered area as input data, instead of snow depth, which can be extracted using remote sensing data. Snow cover has wide application from the determination of the snow reserves to the modeling of snowmelt for prevention of flood and water management. It is found that quick and accurate information about the snow coverage is very crucial for operational forecasting and simulating the water resources applications. In this research, the 8-day snow products, MOD10A2 and MYD10A2 extracted based on NDSI algorithm with spatial resolution of 500 m of year 2005-2009 are used for mapping the extent of snow cover area of the study area.

The model was applied for melt season period for hydrological year 2005-2009 whereby year 2005 and 2006 used for calibrating the model and the remaining years for validating the model. For the calibration period, NSE and D_V values are 85.34 and -0.63% for year 2005 and 79.53 and 0.36% for year 2006. For validation period, NSE values are 90.82, 86.65 and 70.56% and D_V values are -3.09, 1.16 and 3.04% for hydrological year 2007, 2008 and 2009, respectively.

Parameters, namely, recession coefficient and time lag, are calculated from historical discharge and basin size, while the remaining parameters: α , C_R , C_S , T_{CRIT} and RCA are reviewed from literatures. The optimum range of local parameters for melt season: $\alpha = 0.4-2.4 \text{ cm}^\circ\text{C}^{-1}\text{d}^{-1}$, $C_R = 0.15-0.90$ and $C_S = 0.17-0.90$. It was observed that γ , α , C_S , and C_R are more sensitive parameters when compared to T_{CRIT} , RCA and L .

5.1.2 Impact of temperature change on streamflow

Impact of temperature change on streamflow originated from snowmelt is popularly used for studying the impact of climate change by setting up a hypothetical scenario and its interaction on snow covered area. Mostly, such situation are built to simulate the impact of climate change by assuming that if there temperature rise 1°C by then end of 2025 or 2050, then what would be the expected pattern of hydrology cycle. With similar hypothetical scenario induced in Upper Punatshang Chu basin, it is observed that by a rise of 1°C an average discharge is expected to increase by 14.36% approximately. This change apparently results from the increasing temperature, which will increase the volume of the streamflow in the region. With this information, the future hydro project dam can be built with a storage capacity to hold all the melt and thus, increase the power generation. And more over the flood mitigation program should consider the rise of 14.36% when preparing to meet future flood. Finally, the information on the impact of temperature change on streamflow can be used in the water resources planning and management purposes.

In conclusion, the results achieved by SRM model for the basin is considerable displayed good agreement when compared to results obtained in different parts of the world. The model proved to be a good tool to simulate snowmelt runoff and study impact of temperature change on stream flow requiring very less and very much available input data. With the model's ability to simulate runoff under a hypothetical scenario, thus, this research work could be treated as a miniature guide book for management of water resources, designing hydraulic system downstream and to address the mitigation strategies to combat climate change effect on mountainous region.

5.2 Recommendations

Following are the recommendation for accurate and effective future research work using SRM model:

(1) High recommend to apply SRM model to remaining basin to simulate the runoff and to gather overall information on impact of climate change in Bhutan.

(2) It is highly recommend to apply to model for the same basin to simulate for whole year round runoff.

(3) Temperature index models such as HBV and HEC-1 can be applied to estimate the snowmelt runoff for this basin and the results can be compared with this research.

(4) To achieve more accuracy in SCA mapping, a ground verification should be conducted.

(5) The temperature increase scenario should be set up according to the predicted temperature reported by IPCC.

(6) Better DEM resolution will represent terrain more accurately, hence more accurate mean hypsometric elevation can be determined.

(7) Future research can be done using rainfall data from Asian Precipitation – Highly-Resolved Observation Data Integration Toward Evaluation of Water Resources (APHRODITE) and Tropical Rainfall Measuring Mission (TRMM).

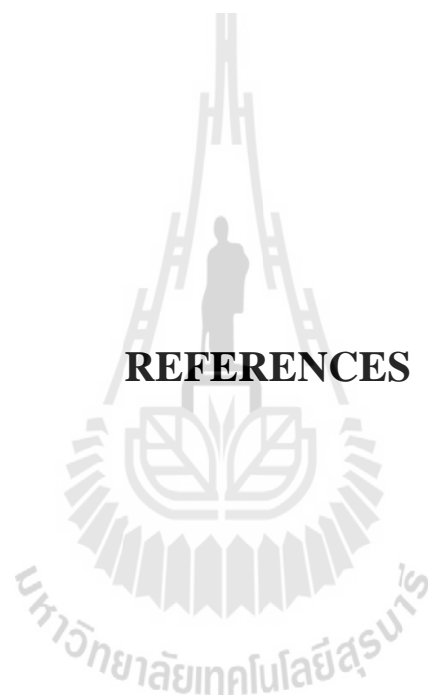
(8) Extensive research can be carried out for determining the value of runoff coefficient and degree day factor in the future.

(9) Disadvantages of trial and error method for calibration are (1) adjusting parameters is done one at a time which requires a great deal of time, (2) this method cannot achieve the global optimum because least is known about the effect of the

parameter-interactions and (3), it is difficult to know exactly when the process should be terminated because it is difficult to know whether the optimal values of the parameters have been obtained. To overcome these problems, there is options like auto –calibration using Monte Carlo Markov Chain (MCMC), design of experiment (DOE) and SCE –UA (Shuffled Complex Evolution – University of Arizona) techniques which are applied in different model. Such future research work can be carried out to apply such techniques to SRM model.

(10) The temperature index model is based on the temperature which being the main index to measure the melt of the snow, and this model fails to cover complete mechanism of energy budget. Thus, it is recommended to apply energy budget model, which includes factors such as radiation, wind and humidity, to comprehend the complete melt mechanism.





REFERENCES

REFERENCES

- Abudu, S, Cui, C., Saydi, M., and King, J.P. (2012). Application of snowmelt runoff (SRM) in mountainous watersheds: A review. **Water Science and Engineering**. 5(2): 123-136.
- Aggarwal, S.P., Thakur, P.K., Nikam, B.R., and Garg, V. (2014). Integrated approach for snowmelt runoff estimation using temperature index model, remote sensing and GIS. **Current Science**. 106(3): 397-407.
- Alam, A., Romshoo, S.A., and Bhat, S. (2011). Estimation of snowmelt runoff using snowmelt runoff model (SRM) in a Himalayan watershed. **World Journal of Science and Technology**. 1(9): 37-42.
- Archer, D.R. (2003). Contrasting hydrological regimes in the upper Indus Basin. **Journal of Hydrology**. 274:198–210.
- Arya, D.S., Gautam, A.K., and Murukar, A.R. (2014). Snowmelt modelling of Dhauligang River using snowmelt runoff model. **11th International Conference on Hydroinformatics**. HIC 2014, New York City, USA.
- Bilal, M. (2010). **Application of snowmelt runoff model (SRM) on Indus Basin in Northern Pakistan**. Master Thesis. COMSATS Institute of Information Technology, Islamabad, Pakistan.

- Butt, M.J., and Bilal, M. (2011). Application of snowmelt runoff model for water resource management. **Hydrological Processes**. 25:3735-3747.
- Chettri, N, Sharma, E., Shakya, B., Thapa, R., Bajracharya, B., Uddin, K., Oli, K.P., and Choudhury, D. (2010). **Biodiversity in the Eastern Himalayas; Status, Trends and Vulnerability to Climate Change: Climate Change Impact and Vulnerability in the Eastern Himalayas**. ICIMOD Technical Report 2. Kathmandu, Nepal.
- Dai, A. (2008). Temperature and pressure dependence of the rain-snow phase transition over land and ocean. **Geophysical Research Letter**. 35:L12802, doi:10.1029/2008GL033295.
- DeWalle, D.R., and Rango, A. (2008). **Principal of Snow Hydrology**. Cambridge University Press.
- Duran-Ballen, S.A., Shrestha, M., Wang, L., Yoshimura, K., and Koike, T. (2012). Snow cover modelling at the Puna Tsang river basin in Bhutan with corrected JRA-25 temperature. **Journal of Japan Society of Civil Engineers**. 68(4): I_235-I_240.
- Eigdir, A.N. (2003). **Investigation of the snowmelt runoff in the Orumiyeh region, using modelling, GIS and RS techniques**. Master Thesis, International Institute for Geo-Information Science and Earth Observation, the Netherlands.
- ESRI, 2015. ArcGIS Desktop Help 10.2 An overview of the hydrology toolset. [Online] available: http://resources.arcgis.com/en/help/main/10.2/index.html#/An_overview_of_the_Hydrology_tools/009z0000004w000000/.

- Ferguson, R.I. (1999). Snowmelt runoff models. **Progress in Physical Geography**. 23(2): 205-227.
- Forkuor, G., and Maathuis, B. (2012). Comparison of SRTM and ASTER derived Digital Elevation Models over two regions in Ghana – Implication for Hydrological and Environmental Modeling, Studies on Environmental and Applied Geomorphology, Dr. Tommaso Placentin(Ed.), ISBN: 978-935-51-0361-5, [Online] Available: <http://www.intechopen.com/books/studies-on-environmental-and-appliedgeomorphology/comparison-of-srtm-and-aster-derived-digital-elevation-models-over-two-regions-in-ghana>.
- Fuladipanah, M., and Jorabloo, M. (2012). The Estimation of Snowmelt Runoff Using SRM Case Study (Gharasoo Basin, Iran). **World Applied Sciences Journal**. 17(4): 433-438.
- Gafurov, A., and Bardossy, A. (2009). Cloud removal methodology from MODIS snow cover product. **Hydrology and Earth System Sciences**. 14(7): 1361-1373.
- Gitay, H., Suarez A., Watson, R.T., and Dokken, D.J. (2002). **Climate change and biodiversity**. Intergovernmental Panel on Climate Change Technical paper V.
- Gómez- Landesa, E., and Rango, A. (2002). Operational snowmelt runoff forecasting in the Spanish Pyrenees using the snowmelt runoff model. **Hydrological Process**. 16: 1583-1591.

- Gurung, D.R., Kulkarni, A.N., Giriraj, A., Aung, K.S., and Shretha, B. (2011). Monitoring of seasonal snow cover in Bhutan using remote sensing technique. **Current Science**. 101(10): 1364-1370.
- Hall, D.K., Riggs G.A., and Salomonson, V.V. (1995). Development of methods of mapping global snow cover using moderate resolution imaging spectroradiometer data. **Remote Sensing of Environment**. 54:127-140.
- Hall, D.K., Riggs, G.A., and Salomonson, V.V. (2001). Algorithm Theoretical Basis Document (ATBD) for the MODIS snow and sea ice – mapping algorithms. [Online] Available: http://modis.gsfc.nasa.gov/data/atbd/atbd_mod10.pdf.
- Hall, D.K., Riggs, G.A., Salomonson, V.V., DiGirolamo, N.E., and Bayr, K.J. (2002). MODIS Snow cover products. **Remote Sensing of Environment**. 83:181-194.
- Haq, M. (2008). **Snowmelt runoff investigation in river swat upper basin using snowmelt runoff model, remote sensing and GIS techniques**. Master Thesis. International Institute for Geo-Information Science and Earth Observation, the Netherlands.
- Harlow, R.C., Burke, E.J., Scott, R.L., Shuttleworth, W.J., Brown, C.M., and Petti, J.R. (2004). Derivation of temperature lapse rate in semi-arid south-eastern Arizona. **Hydrology and Earth System Sciences**. 8(6):1179-1185.
- He, Z.H., Parajka, J., Tian, F.Q., and Blöschl, G. (2014). Estimating degree-day factors from MODIS for snowmelt runoff modeling. **Hydrology and Earth System Sciences**. 18:477-4789.

- Hock, R. (2003). Temperature index melt modelling in mountain areas. **Journal of Hydrology**. 282:104-115.
- Immerzeel, W.W, Droogers, P., de Jong, S.M., and Bierkens, M.F.P. (2010). Satellite derived snow and runoff dynamics in the Upper Indus River basin. **Grazer Schriften der Geographie und Raumforschung**. 45: 303-312.
- IPCC (2007). "Summary for Policymakers". In **Climate Change 2007: Impacts, Adaptation and Vulnerability. Contribution of Working Group II to the Fourth Assessment Report of the Intergovernmental Panel on Climate Change**. (M.L. Parry, O.F. Canziani, J.P. Palutikof, P.J. van der Linden and C.E. Hanson, eds), p.7-22. Cambridge: Intergovernmental Panel on Climate Change and Cambridge University Press.
- Jain, S.K., Goswami, A., and Saraf, A.K. (2010). Snowmelt runoff modelling in a Himalayan basin with the aid of satellite data. **International Journal of Remote Sensing**. 31(24):6603-6618.
- Jain, S.K., Lohani, A.K., and Singh, R.D. (2012). Snowmelt runoff modeling in a basin located in Bhutan Himalaya. India Water Week 2012- **Water, Energy and Food Security: Call for Solution**: 1-13.
- Kult, J., Choi, W., and Choi, J. (2014). Sensitivity of the snowmelt runoff model to snow covered area and temperature inputs. **Applied Geography**. 55: 30-38.
- Li, X., and Williams, M.W. (2008). Snowmelt runoff modelling in an arid mountain watershed. Tarim Basin, China. **Hydrological Processes**. doi10.1002/hyp.

- Liu, J., and Rasul, G. (2007). Climate Change, the Himalayan Mountains, and ICIMOD. **Sustainable Mountain Development**. 53: 11-14.
- Ma, H., and Cheng, G. (2003). A test of snowmelt runoff model (SRM) for the Gongnaisi River basin in the western Tianshan Mountains, China. **Chinese Science Bulletin**. 48(20): 2253-2259.
- Martinec, J., and Rango, A. (1986). Parameter values for snowmelt runoff modelling. **Journal of Hydrology**. 84: 197-219.
- Martinec, J., and Rango, A. (1989). Merits of Statistical criteria for the performance of hydrological models. **Water Resource Bulletin**. 25(2): 421-432.
- Martinec, J., Rango, A., and Major, E. (1983). The Snowmelt-Runoff Model (SRM) User's Manual. NASA Reference Publication 1100.
- Martinec, J., Rango, A., and Roberts, R. (2007). **Snowmelt Runoff Model (SRM) User's Manual Version 1.11**. p 172.
- Mays, L.W. (2011). **Ground and Surface Water Hydrology**. John Wiley & Sons, Inc.
- Minder, J.R., Mote, P.W., and Lundquist, J.D. (2010). Surface temperature lapse rates over complex terrain: Lessons from the Cascade Mountains. **Journal of Geophysical Research**. 115, D14122, doi:10.1029/20009JD013493.
- Moriasi, D.N., Arnold, J.G., Van Liew, M.W., Bingner, R.L., Harmel, R.D., and Veith, T.L. (2007). Model evaluation guidelines for systematic quantification

of accuracy in watershed simulations. **American Society of Agricultural and Biological Engineers**. 50(3):885-900.

Nabi, G., Latif, M., Rehmna, H.U., and Azhar, A.H. (2011). The role of environmental parameter (degree day) of snowmelt runoff simulation. **Soil Environment**. 30(1): 82-87.

Pandy, P.K., Williams, C.A., Frey, K.E., and Brown, M.E. (2013). Application and evaluation of a snowmelt runoff model in the Tamor River basin, Eastern Himalaya using Markove Chain Monte Carlo (MCMC) data assimilation approach. **Hydrological Processes**. doi: 10.1002/hyp.10005.

Prasad, V.H., and Roy, P.S. (2005). Estimation of Snowmelt Runoff in Beas Basin, India. **Geocarto International**. 20(2): 41-47.

Ramamoorthi, A.S. (1987). Snow cover area (SCA) is the main factor in forecasting snowmelt runoff from major river basins. Large scale effects of seasonal snow cover: **Proceedings of the Vancouver Symposium**. 166: 187-198.

Rango, A., and van Katwijk, V. (1990). Development and testing of a Snowmelt Runoff Forecasting Technique. **Water Resources Bulletin**. 26(1): 135-144.

Siderius, C, Biemans, H., Wiltshire, A., Rao, S., Franssen, W.H.P, Kumar, P., Gosain, A.K., van Vliet, M.T.H., and Collins, D.N. (2013). Snowmelt contributions to discharge of the Ganges. **Science of the Total Environment**. 468-469(2013) S93-S101.

- Regmi, D. (2011). **Impact of climate change on water resources in view of contribution of snowmelt in stream flow: A case study from Langtang Basin Nepal**. PhD Dissertation. Tribhuvan University, Kirtipur, Kathmandu, Nepal.
- Riggs, G.A., Hall, D.K., and Salomonson, V.V. (2006). **MODIS Snow Products User Guide to Collection 5**. [Online] Available: http://nsidc.org/data/docs/daac/modis_v5/dorothy_snow_doc.pdf.
- Shahabi, H., Khezri, S., Ahmad, B.B., and Musa, T.A. (2014). Application of moderate resolution spectroradiometer snow cover maps in modeling snowmelt runoff process in the central Zab basin, Iran. **Journal of Applied Remote Sensing**. 8: 0844699 (1-19).
- Shawcroft, N.E. (1985). **Applying the snowmelt runoff model in Utah**. Master Thesis. Department of Civil Engineering. Brigham Young University.
- Shrestha, A.B., and Devkota, L.P. (2010). **Climate change in the eastern Himalayas: Observed trends and model projections; Climate change impact and vulnerability in the Eastern Himalayas**. ICIMOD Technical Report 1. Kathmandu, Nepal.
- Silwal, G. (2014). **Modelling snow and icemelt runoff in the context of climate change: A case study of Dudhkoshi river basin, Nepal**. Master Thesis. Tribhuvan University, Kirtipur, Kathmandu, Nepal.

- Singh, P., and Jain, S.K. (2003). Modelling of stream flow and its components for large Himalayan basin with predominant snowmelts yields. **Hydrological Sciences Journal**. 48(2): 257-276.
- Singh, P., and Kumar, N. (1997). Impact assessment of climate change on the hydrological response of a snow and glacier melt runoff dominated Himalayan river. **Journal of Hydrology**. 193: 316-350.
- Tahir, A.A., Chevallier, P., Arnaud, Y., Neppel, L., and Ahmand, B. (2011). Modeling snowmelt runoff under climate scenarios in the Hunza River basin, Karakoram Ranger, Morthern Pakistan. **Journal of Hydrology**. 409: 104-117.
- Tekeli, A.E., Akyurek, Z. Sorman, A.A., Sensoy, A., and Sorman, A. (2005). Using MODIS snow cover maps in modeling snowmelt runoff process in the eastern part of Turkey. **Remote Sensing of Environment**. 97: 216-230.
- Tenzing Lamsang (2009, 27 May). Flood kills 4. **Kuensel**. [Online] Available: http://www.bhutan-switzerland.org/pdf/Kuensel_27-05-09.pdf Accessed date May 5, 2015.
- Tiwari, S., Kar, S.C., and Bhatla, R. (2015). Examination of snowmelt over Western Himalayan using remote sensing data. **Theoretical and Applied Climatology**. doi 10.1007/s00704-15-1506-y.
- Tse-ring, K., Sharma, S., Chettri, N., and Shrestha, A. (2010). **Climate Change Vulnerability of Mountain Ecosystems in the Eastern Himalayas; Climate Change impact and Vulnerability in the Eastern Himalayas ICIMOD Synthesis Report**. Kathmandu, Nepal.

University of Illinois. (2014) Weather World 2010 Project. [Online] Available:

<http://ww2010.atmos.uiuc.edu/%28Gh%29/guides/mtr/fcst/prcp/rs.rxml>.

Accessed date November 1, 2014.

USACE (1956). **Snow Hydrology: Summary report of snow investigations**,

Washington D.C.: U.S. Department of Commerce Office of Technical

Services PB 151660.

USACE (1998). Engineering and Design Runoff from snowmelt. [Online] available:

<http://www.usace.army.mil/publications/eng-manuals/em1110-2-1406/toc.htm>.

Accessed date May 5, 2014.

USDA NRCS. (2004). National Engineering Handbook. [Online] available:

[http://www.nrcs.usda.gov/wps/portal/nrcs/detailfull/national/home/?cid=stelpr](http://www.nrcs.usda.gov/wps/portal/nrcs/detailfull/national/home/?cid=stelprdb1043063)

[db1043063](http://www.nrcs.usda.gov/wps/portal/nrcs/detailfull/national/home/?cid=stelprdb1043063). Accessed date November 21, 2014.

WMO (World Meteorological Organization) (1986). **Results of an intercomparison**

of models of snowmelt runoff. World Meteorological Organization, CP No.

5, 1211 Geneva, Switzerland.

Zhang, G., Xie, H., Yao, T., Li, H., and Duan, S. (2014). Quantitative water resources

assessment of Qinghai Lake basin using snowmelt runoff model (SRM).

Journal of Hydrology. 519: 976-987.

Zhang, Y., Li, B., Bao, A., Zhou, C., Chen, X., and Zhang, X. (2007). Study of

snowmelt runoff simulation in the Kaidu River basin. **Science in China Ser D**

- Earth Sciences. 50(1): 26-35.

Zhang, Y., Liu, S., and Ding, Y. (2006). Observed degree-day factors and their spatial variation on glaciers in western China. **Annals of Glaciology**. 43: 301-306.



CURRICULUM VITAE

Name: Jigme Tenzin

Date of Birth: 20 December, 1983

Place of Birth: Thimphu, Bhutan.

Education:

2005 Bachelor of Science. Sherubtse College (Affiliated to Delhi University, India), Tashigang, Eastern Bhutan.

2007 Post Graduation Diploma in Surveying and Mapping (Course 500 Survey Engineering). Indian Institute of Surveying and Mapping (IIMS), Survey of India. Uppal, Hyderabad, India.

Grants and Fellowships:

Government of India scholarship.

Thailand International Cooperation Agency scholarship.

Position and Place of Work:

Survey Engineer under Cadastral Information Division, National Land Commission, Thimphu, Bhutan -00975.